2015

Base Flow Recession Analysis for Streamflow and Spring Flow

Debapi Ghosh
University of Central Florida

BASE FLOW RECESSION ANALYSIS FOR STREAMFLOW AND SPRING FLOW

by

DEBAPI KUMAR GHOSH
B. Sc Bangladesh University of Engineering and Technology, 2009
M. Eng. Asian Institute of Technology, 2012

A dissertation submitted for the partial fulfillment of the requirements
of the degree of Doctor of Philosophy
in the Department of Civil, Environmental, and Construction Engineering
in the College of Engineering and Computer Science
at the University of Central Florida
Orlando, Florida

Fall Term
2015

Major Professor: Dingbao Wang

ABSTRACT

Base flow recession curve during a dry period is a distinct hydrologic signature of a watershed. The base flow recession analysis for both streamflow and spring flow has been extensively studied in the literature. Studies have shown that the recession behaviors during the early stage and the late stage are different in many watersheds. However, research on the transition from early stage to late stage is limited and the hydrologic control on the transition is not completely understood.

In this dissertation, a novel cumulative regression analysis method is developed to identify the transition flow objectively for individual recession events in the well-studied Panola Mountain Research Watershed in Georgia, USA. The streamflow at the watershed outlet is identified when the streamflow at the perennial stream head approaches zero, i.e., flowing streams contract to perennial streams. The identified transition flows are then compared with observed flows when the flowing stream contracts to the perennial stream head. As evidenced by a correlation coefficient of 0.90, these two characteristics of streamflow are found to be highly correlated, suggesting a fundamental linkage between the transition of base flow recession from early to late stages and the drying up of ephemeral streams. At the early stage, the contraction of ephemeral streams mostly controls the recession behavior. At the late stage, perennial streams dominate the flowing streams and groundwater hydraulics governs the recession behavior.

The ephemeral stream densities vary from arid regions to humid regions. Therefore, the characteristics of transition flow across the climate gradients are also tested in 40 watersheds. It is found that climate, which is represented by climate aridity index, is the dominant controlling factor on transition flows from early to late recession stages. Transition flows and long-term average base flows are highly correlated with a correlation coefficient of 0.82. Long-term average

iii

base flow and the transition flow of recession are base flow characteristics at two temporal scales, i.e., the long-term scale and the event scale during a recession period. This is a signature of the co-evolution of climate, vegetation, soil, and topography at the watershed scale.

The characteristics of early and late recession are applied for quantifying human impacts on streamflow in agricultural watersheds with extensive groundwater pumping for irrigation. A recession model is developed to incorporate the impacts of human activities (such as groundwater pumping) and climate variability (such as evapotranspiration) on base flow recession. Groundwater pumping is estimated based on the change of observed base flow recession in watersheds in the High Plains Aquifer. The estimated groundwater pumping rate is found consistent compared with the observed data of groundwater uses for irrigation.

Besides streamflow recession analysis, this dissertation also presents a novel spring recession model for Silver Springs in Florida by incorporating groundwater head, spring pool altitude, and net recharge into the existing Torricelli model. The results show that the effective springshed area has continuously declined since 1988. The net recharge has declined since the 1970s with a significant drop in 2002. Subsequent to 2002, the net recharge increased modestly but not to the levels prior to the 1990s. The decreases in effective springshed area and net recharge caused by changes in hydroclimatic conditions including rainfall and temperature, along with groundwater withdrawals, contribute to the declined spring flow.

ACKNOWLEDGMENTS

TABLE OF CONTENTS

LIST OF FIGURES

ix

LIST OF TABLES

CHAPTER 1: INTRODUCTION

1.1 <u>Base Flow Recession</u>

Base flow recession is the lower part of the falling limb of a hydrograph. The base flow recession during a dry period provides insightful hydrologic information about the watersheds, helps the water resources managers for making decisions on water supply, irrigation, hydropower production and water quality controls. Base flow recessions have been widely studied and various models for recession curves have been developed based on the observed recession characteristics [*Tallaksen*, 1995]. The first attempt to fit the recession curve was taken by *Boussinesq* [1904] and later *Maillet* [1905] assuming discharge as a simple exponential decay function of time, and most of the hydrograph recession partially and fully follow the exponential form of the recession curve [*Horton*, 1933; *Barnes*, 1939; *Werner and Sundquist*, 1951]. Besides, *Horton* [1933] and [*Werner and Sundquist* [1951] also introduced the double exponential and hyperbola equation to improve the recession equation. In addition, many other functional forms have been tested to achieve a better fit of recession curves [e.g., *Wicht*, 1943].

To eliminate time as a reference in the recession curve analysis, *Brutsaert and Nieber* [1977] proposed a classical method to analyze the time rate of change in discharge as a function of discharge itself (i.e., *-dQ/dt=f(Q)*). This method has been called recession slope curve analysis [*Rupp and Selker*, 2006]. The data points of ln(-dQ/dt) versus ln(Q) from the observations of real watersheds are usually approximately linear, suggesting a power relationship [*Brutsaert and Nieber*, 1977; *Zecharias and Brutsaert*, 1988]:

$$-\frac{dQ}{dt} = aQ^b \tag{1.1}$$

1

Based on analytical solutions of the Boussinesq equation for a horizontal aquifer with a fully penetrating stream channel, the value of *b* equals to 3 at the early stage of recession, and the value of *b* is 1 for linearized solution and 1.5 for nonlinearized solution at the late stage of recession [*Brutsaert and Nieber*, 1977]. Various forms of analytical solutions based on the Boussinesq equation for a sloping aquifer were summarized in *Rupp and Selker* [2006]. The analytical solutions involved assumptions of geometric similarity of hillslope groundwater if applied to catchments [*Brutsaert and Lopez*, 1998]. Combining the analytical solutions for the early and late recessions, aquifer parameters (e.g., saturated hydraulic conductivity, drainable porosity or aquifer thickness) at the watershed scale are estimated based on the intersection of early and late recession slope curves [*Troch et al.*, 1993; *Brutsaert and Lopez*, 1998; *Szilagyi et al.*, 1998; *Parlange et al.*, 2001].

Moving from the classical approach, *Biswal and Marani* [2010] proposed a conceptual model with a focus on the river network morphology based on the following assumptions: 1) the recession flow is assumed as a succession of steady flows, varying slowly on time in the network; 2) discharge per unit stream length *(q)* drained by the active drainage network (ADN) is assumed spatially constant and the total drainage *Q(t)* can be expressed by

$$Q(t) = q\,(t) \cdot L(t) \tag{1.2}$$

L(t) is the length of the total drainage network; 3) all saturated link of ADN are assumed to recede at the same speed in space and time. The slope of the recession is computed by differentiating the equation (1.2) in time:

$$\frac{dQ}{dt} = q\frac{dL}{dt} + L\frac{dq}{dt} \tag{1.3}$$

The first term at right hand side of the equation is controlled by stream contraction and the second term represents the aquifer depletion of stream networks; and 4) the variation of time in ADN is

assumed to be much larger than the variation in discharge per unit length in sloping aquifer. Therefore, the second term can be neglected and the recession flows carry only the geomorphologic signatures of the contributing river basin. The result of that conceptual model is found appreciable for practical homogeneous [*Mutzner et al.*, 2013] and heterogeneous region [*Biswal and Kumar*, 2013]. A transition of decreasing recession exponent from early to late recession has been observed in many other studies [e.g., *Parlange et al.*, 2001; *Rupp et al.*, 2009; *Palmroth et al.*, 2010; *Krakauer and Temimi*, 2011]. However, a transition of increasing recession exponents from early to late recession has also been observed from Cascade streams in Oregon due to two distinct geologic provinces [*Tague and Grant*, 2004]. *Clark et al.* [2009], *Harman et al.* [2009] and *Wang* [2011] also reported the transition of increasing recession exponents due to the contribution of groundwater to ephemeral and perennial stream riparian zones using Panola Mountain River Watershed (PMRW) data. Additionally, no distinct transition of the recession exponent was noticed in some watersheds [e.g., *Kirchner*, 2009].

Acceptance of the stream network as a dynamic characteristic of drainage basin directs the attention towards two aspects of the network. The perennial stream (or basic network) flows for much of the year is governed by groundwater flows, and depends upon local climatology and basin characteristics. The ephemeral stream (or expanded network) flows discontinuously as a response of individual rainfall events [*Gregory*, 1976]. As a result, the ephemeral stream becomes dry gradually during recession periods. The flowing stream length and discharge were highly correlated, and power-law relationships between flowing channel length and streamflow were usually identified [*Gregory and Walling*, 1968; *Godsey and Kirchner*, 2014]. Therefore, the contraction rate of flowing stream network decreases with time during a recession event. At the early stage of recession, the contraction rate of ephemeral streams is significant; however, at the

late stage of recession when all ephemeral streams dry up and perennial streams are the only sources for flowing streams, the contraction rate of perennial streams is negligible [*Blyth and Rodda*, 1973; *Day*, 1978; *Wigington et al.*, 2005].

Along with the physical control on base flow recession, the climate control on base flow recession is also assessed by several studies [*Wang and Wu*, 2013]. *Wang and Wu* [2013] computed the perennial stream densities for 185 watersheds based on the high resolution National Hydrography Dataset (NHD) and found that the perennial stream density declines monotonically with the increases of climate aridity index. *Wang and Wu* [2013] also assessed the similarity of climate control on long-term average base flow and perennial stream density. Since the base flow during a dry season is mostly responsible for the flowing of perennial streams networks, it is reasonable to assume that the long term average base flow is also controlled by the long-term mean climate. However, transition of recession from early to late stage and long-term average base flow are the characteristics of base flow at two temporal scale. The transition of recession from early to late stage is associated with the event scale while average base flow is associated with the long-term scale. Therefore, the connection between the transitions of recession from early to late stage can be established through the perennial streams if the transition of recession from early to late stage is controlled by the climate aridity index.

The characteristics of recession has been extensively used for many purpose, mostly applied in base flow separation [*Wittenberg*, 1999], evapotranspiration estimation [*Szilagyi et al.*, 2007], aquifer parameter estimation [*Brutsaert and Lopez*, 1998; *Troch et al.*, 1993] and quantifying of groundwater pumping [*Wang and Cai*, 2009]. The recession behaviors during early stage and late stage are different in many watersheds and research on the transition from early stage to late stage is limited. Therefore, the hydrologic control on the transition is not completely

understood. As discussed earlier that *Maillet* [1905] developed the exponential function of $Q_t = Q_0 \exp(-t/k)$ to describe the recession of base flow, where Q_t is the streamflow at time t, Q_0 is the initial streamflow, k (day) is the retention constant to represent average response time in storage. The characteristic of retention constant is different throughout the recession curve. For example: the early stage of recession has lower retention constant most likely due to the major contribution of younger groundwater while the late stage of recession exhibits higher retention constant due to the significant contribution of older groundwater during the recession. The younger groundwater normally shows shorter residence time compared to the older groundwater. The early stage of recession can be connected with the younger groundwater, and the late stage of recession can be connected with the older groundwater.

Spring recession is also another potential field of hydrology which provides perspective information on recharge, groundwater movement and storage characteristics of the aquifer [*Padilla et al.*, 1994; *Amit et al.*, 2002]. In hydrology, a spring is the natural location where groundwater naturally flows to the land surface or into a body of surface. A karst spring is the part of the karst aquifer system and contains dissolution generated conduits that permit rapid transport of groundwater to the land surface [*Huntoon*, 1995]. It often has a large magnitude of flow, provide significant contribution to water supply and tourism sector [*Goldscheider*, 2012]. The porosity of karst aquifers vary from intergranular to fracture, and to large cavernous conduits [*White*, 2002]. As a result, spring flows vary from simple Darcian to complex non-Darcian flow depending on the flow path through the matrix, fractures, conduits, or a combination of these [*Halihan and Wicks*, 1998]. In addition, the majority of water transport in a karst aquifer occurs in large dissolution conduits and is therefore often turbulent [*Atkinson*, 1977]. Several conceptual models have been developed incorporating the geometric and hydraulic characteristics of aquifers

for spring hydrograph recession [*Kresic*, 2006]. Particularly, Darcy, Poiseuille and Torricelli models have been developed for recession curves for karst springs [*Fiorillo*, 2011; *Fiorillo et al.*, 2012]. In the Darcy model, the groundwater drains freely from a tank reservoir to the spring pool through a sand filled conduit system. In the Poiseuille model, groundwater flows through a small conduit system where the effects of viscosity is neglected. In the Torricelli model, groundwater drains through a large conduit system with negligible frictional head loss through the conduit. In all of these models, the effects of spring pool altitude and net recharge (difference between recharge and groundwater pumping) on spring flow are neglected.

1.2   Research Objectives

The overarching goal of the research is to understand the base flow recession for streamflow and spring flow. In many watersheds, the recession behaviors during the early stage and late stage are different which are eventually identified by the transition of recession flows. Therefore, the dissertation focuses on the transition of recession from early stage to late stage. Scientific questions of the study include: 1) What is the dominant physical control of temporal and perennial streams on base flow recession from early stage to late stage (Chapter 1)? 2) What is the dominant climatic control of the temporal and perennial streams on base flow recession from early stage to late stage (Chapter 2)? 3) How do human interferences affect the early and late stage of recession in agricultural watershed (Chapter 3)? 4) How do the characteristics of aquifer affect the recession of spring flow (Chapter 4)? The hypotheses in this study are: 1) The transition from early to late stage of recessions occurs when flowing streams contract to perennial stream heads. 2) A similarity exists between transition of recession from early stage to late stage and long-term average base

flow. 3) The early stage of recession is hydraulically connected with younger groundwater and late stage of recession is hydraulically connected with older groundwater.

With these proposed scientific and applied questions, the objectives of this study are to: 1) Developing a systematic approach to identify the transition flow from early to late stage of recession for individual recession events, and quantifying the dominant physical control on base flow recession (Chapter 1). 2) Developing the methodology to identify the transition flows of lower envelopes of recession slope curve with an ensemble of watersheds, and quantifying the climatic control on base flow recession across climate gradients (Chapter 2). 3) Developing a recession model to quantify the groundwater depletion by analyzing the changes in recession slope (Chapter 3). 4) Developing a simple spring recession model incorporating of spring pool altitude and the net recharge to estimate the effective springshed area and the net recharge based on the changes in recession slope of spring flow (Chapter 4).

1.3 <u>Dissertation Organization</u>

The organization of dissertation from the aspect of research objectives is shown in Figure 1.1. The Figure 1.1 shows that the dissertation focus on two topics: 1) the base flow recession for streamflow and 2) the base flow recession for spring flow. The analysis of base flow recession for streamflow has been accomplished through three different studies as shown from chapter 2 to chapter 4. Chapter 2 focuses on the physical role of temporal streams and perennial streams on the transition of base flow recession from early to late stage in Panola Mountain Research Watershed (PMRW). Chapter 3 focuses on the linkage of the long term climate to the transition of base flow recession from early to late stage in 40 watersheds across climate gradients. Chapter 4 focuses on the quantification of shallow and deep groundwater depletion in the High Plains

Aquifer (HPA) by recession analysis. Chapter 5 focuses on the quantification of changes in springshed area and net recharge through recession analysis of spring flow.

```
                        ┌─────────────────────┐
                        │  Base flow Recession │
                        └─────────────────────┘
              ┌──────────────────┴──────────────────────┐
              ▼                                          ▼
    ┌──────────────────┐                      ┌──────────────────┐
    │   Streamflow     │                      │   Spring flow    │
    │    Recession     │                      │    Recession     │
    └──────────────────┘                      └──────────────────┘
              │                                          │
              ▼                                          ▼
    ┌──────────────────┐                      ┌──────────────────┐
    │  Transition of   │                      │  Transition of   │
    │ early to late    │                      │ early to late    │
    │ stage of         │                      │ stage of         │
    │ recession        │                      │ recession        │
    └──────────────────┘                      └──────────────────┘
```
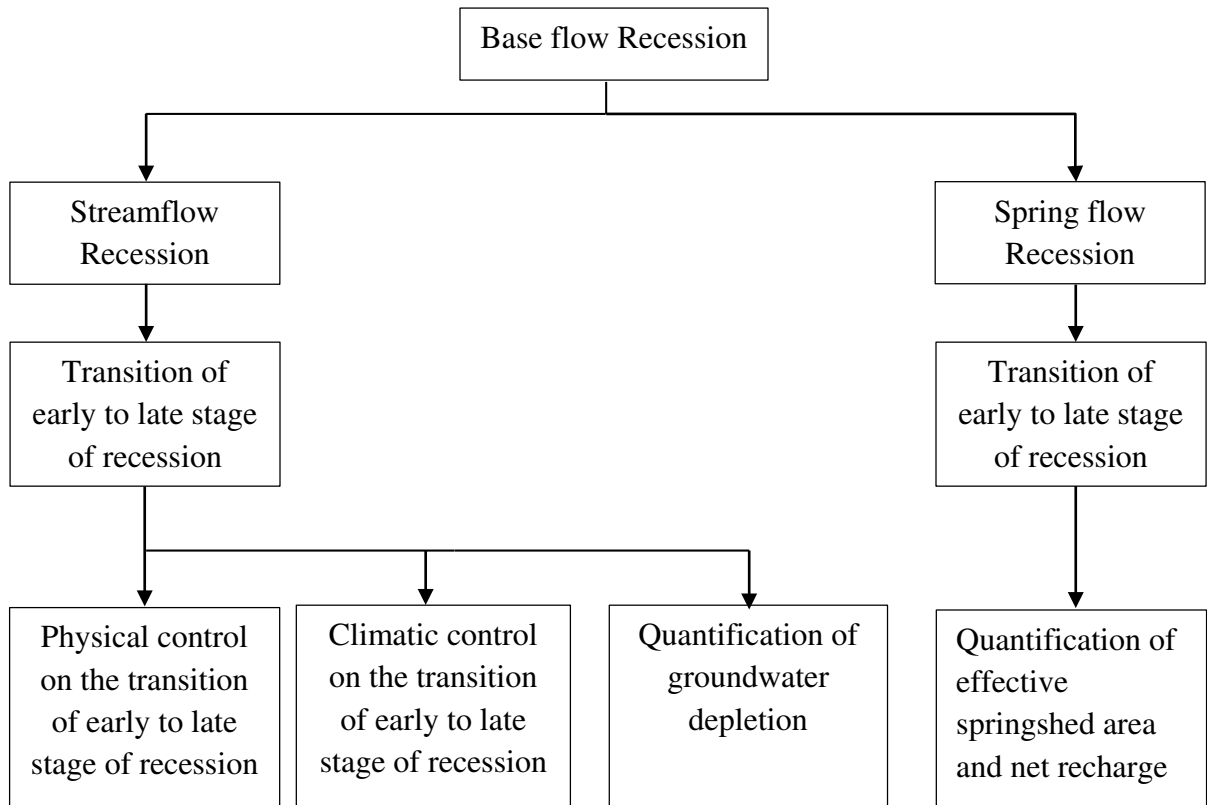
Figure 1.1. Outline of Thesis Testing

Boxes:

- Physical control on the transition of early to late stage of recession
- Climatic control on the transition of early to late stage of recession
- Quantification of groundwater depletion
- Quantification of effective springshed area and net recharge

1.4   <u>References</u>

Amit, H., V. Lyakhovsky, A. Katz, A. Starinsky, and A. Burg (2002), Interpretation of spring recession curves, *Groundwater*, *40*(5), 543-551.

Atkinson, T. (1977), Diffuse flow and conduit flow in limestone terrain in the Mendip Hills, Somerset (Great Britain), *Journal of hydrology*, *35*(1), 93-110.

Barnes, B. S. (1939), The structure of discharge-recession curves, *Eos, Transactions American Geophysical Union*, *20*(4), 721-725.

Biswal, B., and M. Marani (2010), Geomorphological origin of recession curves, *Geophysical Research Letters*, *37*, L24403, doi:10.1029/2010GL045415.

Biswal, B., and D. N. Kumar (2013), A general geomorphological recession flow model for river basins, *Water Resources Research*, *49*(8), 4900-4906.

Blyth, K., and J. C. Rodda (1973), A stream length study, *Water Resources Research*, *9*(5), 1454-1461.

Boussinesq, J. (1904), Recherches théoriques sur l'écoulement des nappes d'eau infiltrées dans le sol et sur le débit des sources, *Journal de mathématiques pures et appliquées*, 5-78.

Brutsaert, W., and J. L. Nieber (1977), Regionalized drought flow hydrographs from a mature glaciated plateau, *Water Resources Research*, *13*(3), 637-643.

Brutsaert, W., and J. P. Lopez (1998), Basin-scale geohydrologic drought flow features of riparian aquifers in the Southern Great Plains, *Water Resources Research*, *34*(2), 233-240.

Clark, M. P., D. E. Rupp, R. A. Woods, H. J. Tromp-van Meerveld, N. E. Peters, and J. E. Freer (2009), Consistency between hydrological models and field observations: linking

processes at the hillslope scale to hydrological responses at the watershed scale, *Hydrological Processes*, *23*(2), 311-319.

Fiorillo, F. (2011), Tank-reservoir drainage as a simulation of the recession limb of karst spring hydrographs, *Hydrogeology Journal*, *19*(5), 1009-1019.

Fiorillo, F., P. Revellino, and G. Ventafridda (2012), Karst aquifer draining during dry periods, *Journal of Cave and Karst Studies*, *74*(2), 148-156.

Godsey, S. E., and J. W. Kirchner (2014), Dynamic, discontinuous stream networks: hydrologically driven variations in active drainage density, flowing channels and stream order, *Hydrological Processes*, *28*(23), 5791-5803.

Goldscheider, N. (2012), A holistic approach to groundwater protection and ecosystem services in karst terrains, *AQUA mundi*, *3*, 117-124.

Gregory, K., and D. Walling (1968), The variation of drainage density within a catchment, *Hydrological Sciences Journal*, *13*(2), 61-68.

Gregory, K. J. (1976), Drainage networks and climate, *Geomorphology and climate*, 289-315.

Halihan, T., and C. M. Wicks (1998), Modeling of storm responses in conduit flow aquifers with reservoirs, *Journal of Hydrology*, *208*(1), 82-91.

Harman, C. J., M. Sivapalan, and P. Kumar (2009), Power law catchment-scale recessions arising from heterogeneous linear small-scale dynamics, *Water Resources Research*, *45*, W09404, doi*:*10.1029/2008WR007392*.*

Horton, R. E. (1933), The Role of infiltration in the hydrologic cycle, *Eos, Transactions American Geophysical Union*, *14*(1), 446-460.

Huntoon, P. W. (1995), Is it appropriate to apply porous media groundwater circulation models to karstic aquifers, *Groundwater models for resources analysis and management*, 339-358.

Kirchner, J. W. (2009), Catchments as simple dynamical systems: Catchment characterization, rainfall-runoff modeling, and doing hydrology backward, *Water Resources Research*, *45*, W02429, doi:10.1029/2008WR006912.

Krakauer, N.Y., and M. Temimi (2011). Stream recession curves and storage variability in small watersheds. *Hydrology and Earth System Sciences*, 15(7), 2377-2389.

Kresic, N. (2006), *Hydrogeology and groundwater modeling*, CRC press.

Maillet, E. T. (1905), *Essais d'hydraulique souterraine & fluviale*, A. Hermann.

Mutzner, R., E. Bertuzzo, P. Tarolli, S. V. Weijs, L. Nicotina, S. Ceola, N. Tomasic, I. Rodriguez-Iturbe, M. B. Parlange, and A. Rinaldo (2013), Geomorphic signatures on Brutsaert base flow recession analysis, *Water Resources Research*, *49*(9), 5462-5472.

Padilla, A., A. Pulido-Bosch, and A. Mangin (1994), Relative Importance of Baseflow and Quickflow from Hydrographs of Karst Spring, *Ground Water*, *32*(2), 267-277.

Palmroth, S., G. G. Katul, D. Hui, H. R. McCarthy, R. B. Jackson, and R. Oren (2010), Estimation of long-term basin scale evapotranspiration from streamflow time series, *Water Resources Research*, *46*(10), W10512, doi:10.1029/2009WR008838.

Parlange, J. Y., F. Stagnitti, A. Heilig, J. Szilagyi, M. B. Parlange, T. S. Steenhuis, W. L. Hogarth, D. A. Barry, and L. Li (2001), Sudden drawdown and drainage of a horizontal aquifer, *Water Resources Research*, *37*(8), 2097-2101.

Rupp, D. E., and J. S. Selker (2006), On the use of the Boussinesq equation for interpreting recession hydrographs from sloping aquifers, *Water Resources Research*, *42*(12), W12421, doi:10.1029/2006WR005080.

Rupp, D. E., J. Schmidt, R. A. Woods, and V. J. Bidwell (2009), Analytical assessment and parameter estimation of a low-dimensional groundwater model, *Journal of hydrology*, *377*(1), 143-154.

Szilagyi, J., M. B. Parlange, and J. D. Albertson (1998), Recession flow analysis for aquifer parameter determination, *Water Resources Research*, *34*(7), 1851-1857.

Szilagyi, J., Z. Gribovszki, and P. Kalicz (2007), Estimation of catchment-scale evapotranspiration from baseflow recession data: Numerical model and practical application results, *Journal of Hydrology*, *336*(1–2), 206-217.

Tague, C., and G. E. Grant (2004), A geological framework for interpreting the low-flow regimes of Cascade streams, Willamette River Basin, Oregon, *Water Resources Research*, *40*(4).

Tallaksen, L. M. (1995), A review of baseflow recession analysis, *Journal of Hydrology*, *165*(1–4), 349-370.

Troch, P. A., F. P. De Troch, and W. Brutsaert (1993), Effective water table depth to describe initial conditions prior to storm rainfall in humid regions, *Water Resources Research*, *29*(2), 427-434.

Wang, D. (2011), On the base flow recession at the Panola Mountain Research Watershed, Georgia, United States, *Water Resources Research*, *47*, W03527, doi:10.1029/2010WR009910

Wang, D., and X. Cai (2009), Detecting human interferences to low flows through base flow recession analysis, *Water Resources Research*, *45*, W07426, doi:10.1029/2009WR007819.

Wang, D., and L. Wu (2013), Similarity of climate control on base flow and perennial stream density in the Budyko framework, *Hydrology and Earth System Sciences*, *17*(1), 315-324.

Werner, P. W., and K. Sundquist (1951), On the groundwater recession curve for large watersheds, *IASH General Assembly, Brussels, IAHS Publication*, *33*, 202-212.

White, W. B. (2002), Karst hydrology: recent developments and open questions, *Engineering geology*, *65*(2), 85-105.

Wicht, C. L. (1943), Determination of the effects of watershed-management on mountain streams, *Eos, Transactions American Geophysical Union*, *24*(2), 594-608.

Wigington, P. J., T. J. Moser, and D. R. Lindeman (2005), Stream network expansion: a riparian water quality factor, *Hydrological Processes*, *19*(8), 1715-1721.

Wittenberg, H. (1999), Baseflow recession and recharge as nonlinear storage processes, *Hydrological Processes*, *13*(5), 715-726.

Zecharias, Y. B., and W. Brutsaert (1988), Recession characteristics of groundwater outflow and base flow from mountainous watersheds, *Water Resources Research*, *24*(10), 1651-1658.

CHAPTER 2: ON THE TRANSITION OF BASE FLOW RECESSION FROM EARLY STAGE TO LATE STAGE

2.1   Introduction

Base flow recession curve in the dry period are a distinct hydrologic signature of a watershed. It provides important information to water managers for making decision on water supply, irrigation, and management of water quality [*McGuire et al.*, 2014] and aquatic ecosystem services [*Stanley et al.*, 1997]. Base flow recession has been extensively studied in the last few decades. By eliminating post-rainfall event time reference in hydrograph recession analysis, *Brutsaert and Nieber* [1977] proposed a classical method to analyze the time rate of change in discharge as a function of discharge itself (i.e., *-dQ/dt=f(Q)*). Logarithmic graphs of ln(-d*Q*/d*t*) versus ln(*Q*) based on observed discharge demonstrate approximately linear relationships, suggesting the following power relationship [*Brutsaert and Nieber*, 1977]:

$$-\frac{dQ}{dt} = aQ^b \qquad (2.1)$$

The value of exponent *b* estimated using observed discharge differs considerably between early stage of recession with high discharge and late stage of recession with low discharge. A sharp change of the exponent value from early recession to late recession has been observed in many watersheds (e.g., [*Zecharias and Brutsaert*, 1988; *Parlange et al.*, 2001; *Palmroth et al.*, 2010; *Krakauer and Temimi*, 2011].

The controlling factors of recession exponent are complex, including groundwater hydraulics [*Brutsaert and Nieber*, 1977], the interconnection of groundwater flow systems [*Tóth*, 1963], spatial heterogeneity of watershed properties [*Harman et al.*, 2009], stream contraction [*Biswal and Marani*, 2010; *Biswal and Kumar*, 2013; *Biswal and Kumar*, 2015], and evapotranspiration [*Shaw et al.*, 2013]. In those studies which focused on the role of groundwater

hydraulics on recession behavior, the total length of stream contributing to base flow is assumed to be constant [*Troch et al.*, 1993; *Brutsaert and Lopez*, 1998]. Based on the analytical solutions of the Boussinesq equation for a horizontal aquifer with a fully penetrating stream channel, the value of b equals 3 during early recession, and it is 1 for a linearized solution and 1.5 for a non-linearized solution during late recession [*Brutsaert and Nieber*, 1977]. Aquifer parameters at the watershed scale, including saturated hydraulic conductivity, drainable porosity and aquifer depth were estimated based on analytical solutions for early and late recession [*Brutsaert and Nieber*, 1977; *Brutsaert and Lopez*, 1998; *Szilagyi et al.*, 1998; *Rupp et al.*, 2009].

The role of flowing stream contraction on recession behavior has been investigated in recent years [*Biswal and Marani*, 2010; *Mutzner et al.*, 2013]. The contraction of flowing stream networks is a result of geomorphological characteristics [*Marani et al.*, 2001]. Perennial streams are active for most of the year, depending upon local climatology and basin characteristics. Ephemeral streams are intermittently active, in response to individual rainfall events [*Blyth and Rodda*, 1973; *Gregory*, 1976; *Wang and Wu*, 2013], and gradually dry up during the recession period [*Day*, 1978; *Wigington et al.*, 2005]. The length of active channel network is highly correlated with streamflow, and power-law relationships between flowing channel length and streamflow are usually identified [*Gregory and Walling*, 1968; *Godsey and Kirchner*, 2014]. However, the linkage between drying up of ephemeral streams and ceasing of early recession has not been fully explored in the existing literature.

The contraction rate of ephemeral streams is significant at the early stage of recession; however, at the late stage of recession when all ephemeral streams have dried up and perennial streams are the only sources for flowing streams, the contraction rate of perennial streams is negligible [*Blyth and Rodda*, 1973; *Day*, 1978; *Wigington et al.*, 2005]. The objective of this study

was to identify the transition of base flow from early recession stage to late recession stage for individual recession events, and investigate the potential linkage between the transition of base flow recession and the contraction of ephemeral streams.

2.2   Panola Mountain Research Watershed and Data

To investigate the linkage between the transition of base flow recession from early to late stage and the contraction of ephemeral streams, at the minimum, streamflow data should be simultaneously recorded at both the outlet and the perennial stream heads of a watershed. Such streamflow observations are rather rare since streamflow gauges are usually located on perennial streams. Fortunately, streamflow observations are available at both the perennial stream head (84°10'24"W, 33°37'47"N) and the watershed outlet (84°10'20"W, 33°37'53"N) for the Panola Mountain Research Watershed (PMRW) [*Peters and Aulenbach*, 2011]. Therefore, the PMRW has been chosen to analyze the transitions of base flow recession from early stage to late stage.

PMRW has a drainage area of 0.41 km^2, and is located about 25 km southeast of Atlanta in the State of Georgia. It has an aridity index of 0.94, a mean annual temperature of 15.4°C, and mean annual precipitation of 1237 mm. As shown in Figure 2.1, 93% of the drainage area of PMRW is covered by forest and the rest are bedrock outcrops[*Freer et al.*, 2002]. Bedrock outcrops and riparian zones consist of about 7% and 15% of the watershed area, respectively, and hillslopes comprise the rest of it [*Inamdar and Mitchell*, 2007]. Historically, this watershed has been the subject of much research on a varity of topics, such as the control of bedrock topography over storm runoff generation at the hillslope scale [*Tromp-van Meerveld and McDonnell*, 2006a and 2006b; *Tromp-van Meerveld et al.*, 2007] and hydrologic modeling [*Peters et al.*, 2003].

Rainfall and streamflow observations exist for the period from October 1, 1985 to September 30, 2007 [*Peters and Aulenbach*, 2011]. Rainfall data were recorded at a one-minute time intervals at several tipping bucket gauges within or adjacent to PMRW, and were recorded weekly at several standard Tenite rain gauges. Comparing the weekly rainfall totals at tipping bucket gauges with those at several standard Tenite rain gauges, the tipping bucket rainfall series in the week that best reproduced the totals from the standard gauges were combined to generate the rainfall data by average [*Peters et al.*, 2003]. Streamflow data of PMRW were computed with a stage-discharge rating curve and, the stage record was obtained from a data logger at 5-minute intervals except during rainstorms when data was collected at 1-minute intervals [*Peters et al.*, 2003]. Streamflow data were available at two gauge stations as shown in Figure 2.1. One gauge station is located at the outlet of the watershed, of which the streamflow is denoted as Q_p. The other gauge, with a drainage area of 0.1 km^2, is located in the transition zone between the ephemeral and perennial riparian aquifers, approximately at the perennial stream head as shown in Figure 2.1 [*Clark et al.*, 2009]; and its streamflow is denoted as Q_e. In this study, the 5-minute streamflow series at both gauges at the outlet and the perennial stream head in PMRW were aggregated to an hourly time series. To be consistent with other studies, these hourly discharge data were converted to mm/day [e.g., *Wang*, 2011]. In a recession, the outlet discharge Q_p, that occurred at the moment when discharge at the perennial stream head Q_e diminishes to zero, is denoted as Q_{p0}.
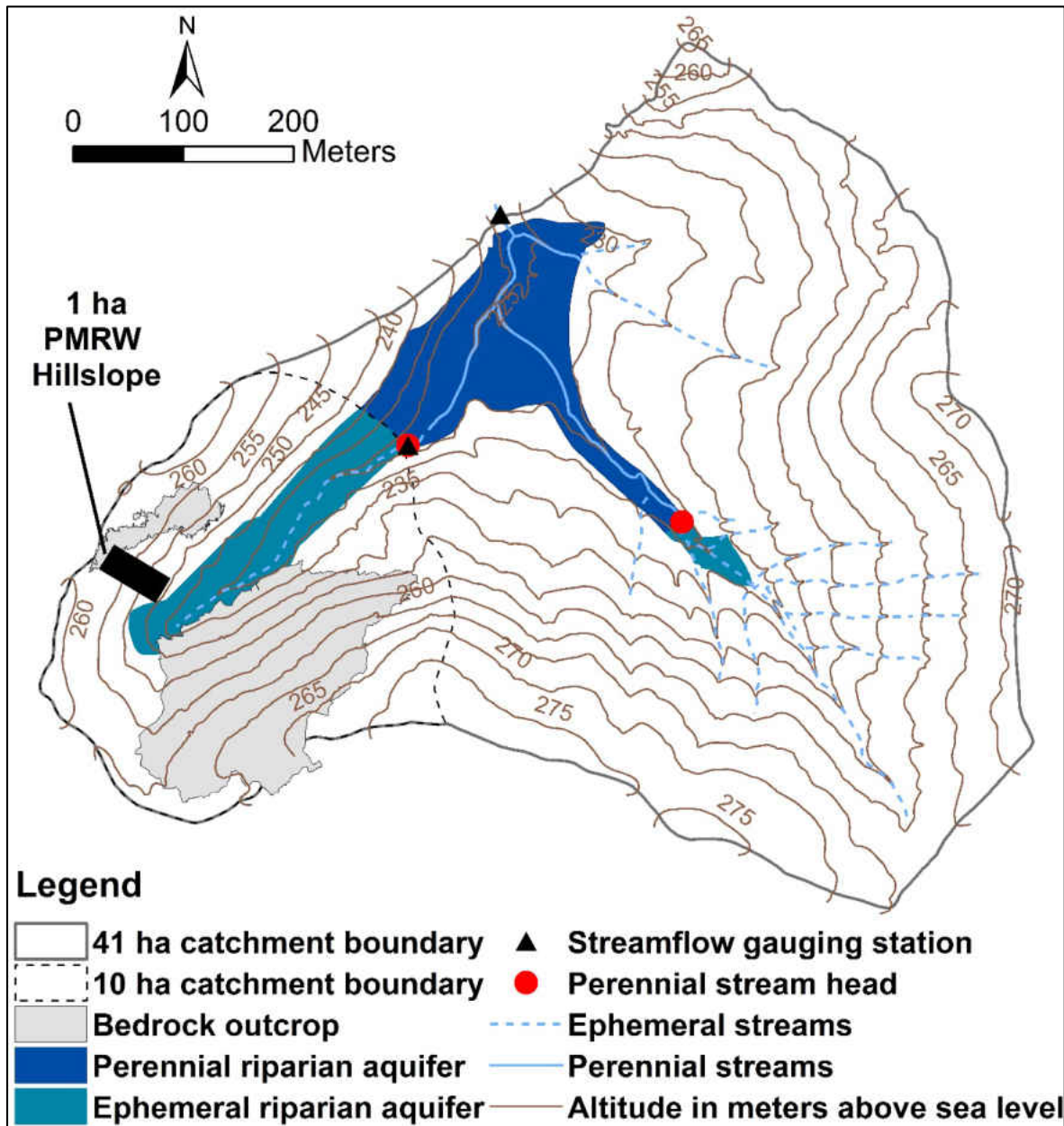
Figure 2.1. Spatial distribution of perennial and ephemeral streams, two streamflow gauge stations, and two major perennial stream heads at the PMRW (adopted from Clark et al., 2009).

2.3 **Methodology**

2.3.1 *Contraction of flowing stream to perennial stream head*

The streamflow observations at the upstream gauge in the PMRW provide an opportunity to identify the time when flowing stream contracts to the perennial stream head. Using discharge time series of the upstream gauge, the moment when the ephemeral streams dry up ($Q_e \rightarrow 0$) and the corresponding discharge at the outlet Q_{p0} was identified. Another major ephemeral tributary is located in the southern side of the watershed. The drainage areas for both perennial stream heads were about 0.1 km^2. The topographic index [*Beven and Kirkby*, 1979] for the gauged perennial stream head was 14.2, which was approximately equal to the topographic index at the other perennial stream head, 13.8. Therefore, it is reasonable to assume that the two tributaries contracted to their perennial stream heads at approximately the same time.

2.3.2 *Identifying the transition of base flow recession from early to late stages*

The first step for identifying the transition point of base flow recession was to select base flow recession events from streamflow time series, and to determine the starting time of the recession analysis. The starting time of recession is typically determined according to rainfall events or the peak discharge after a rainfall event. In order to eliminate quick flows in the recession analysis, *Brutsaert and Nieber* [1977] selected recession data that were collected at least 5 days after rainfall events. *Brutsaert and Lopez* [1998] found that the early recession analysis was sensitive to the number of days after storms. To determine the earliest onset of base flow, uninterrupted recession flow data starting from the second day after the cessation of rainfall were selected for analysis in some studies [*Troch et al.*, 1993; *Brutsaert and Lopez*, 1998; *Parlange et al.*, 2001].

In this study, the following criteria were applied to determine base flow recession segments from the hourly discharge data: 1) recession segments after rainfall events with precipitation depth greater than 55 mm are selected for recession analysis [*Clark et al.*, 2009], as 55 mm rainfall is typically required to fill the depressions in the bedrock of PMRW [*Tromp-van Meerveld and McDonnell*, 2006a and 2006b]; 2) no rainfall events occur during the recession period; 3) the first six hours of discharge data following a peak discharge should be discarded; 4) with all the above three criteria being met, discharge at the perennial stream head must be larger than zero at the starting time of recession analysis; and 5) in order to capture the late recession behavior, the discharge at the outlet should keep decreasing for at least three hours after the discharge at the perennial stream head diminishes to zero.

For each selected recession event, the data pairs of $-dQ/dt = (Q_{i+1}-Q_i)/\Delta t$ and $Q=(Q_i+Q_{i+1})/2$ were. On a recession curve, the flow rate is denoted as Q_i, where i=1, 2, 3,…N, in descending order, with Q_1 and Q_N being the largest and smallest flow rates, respectively. With respect to the first two data points (Q_1 and Q_2), the computed slope is denoted as S_1. The slope S_i was computed by cumulative regression analysis over the data points of $Q_1, Q_2, …, Q_{i+1}$, with its goodness-of-fit denoted as R^2_i. The last slope (S_{N-1}) was computed by applying cumulative regression to all the data points of the individual recession slope curve. The transition point (i^*) of base flow recession from early to late stages was identified by the change of regression slope and goodness-of-fit: 1) for $i \geq i^*$, S_i increases continuously; and 2) goodness-of-fit declines significantly from $R^2_{i^*}$ to $R^2_{i^*+1}$.

2.4   Results and Discussion

2.4.1   *Flow at the outlet when the ephemeral stream dries up*

As shown in Table 2.1, twenty three recession events during the 1985-2007 period were selected for analysis. For instant, Figure 2.2 shows the observed hydrographs at the outlet and the perennial stream head during the recession of January, 2007. After 57 mm of rainfall, the peak discharge at the outlet reached 5.85 mm day^{-1}; while the peak flow at the perennial stream head was 7.53 mm day^{-1}. The discharge in volume at the outlet was higher than that at the perennial stream head. The discharge at the perennial stream head (Q_e) gradually declined to zero; meanwhile, the discharge at the outlet declined to 0.85 mm day^{-1} (Q_{p0}). After the ephemeral stream dried up, base flow at the outlet continued to decline to 0.75 mm day^{-1} until another rainfall event occurred. Before the ephemeral stream dried up, base flow at the outlet was a result of contributions from both the ephemeral stream riparian aquifer and perennial stream riparian aquifer; whereas perennial stream discharge was maintained by the return flow through the underlying bedrock [*Clark et al.*, 2009].

The average value of Q_{p0} over the twenty-three recession events, denoted as $\overline{Q}_{p0}$, was 0.95 mm day^{-1}. The standard deviation of Q_{p0} for these events was 0.24 mm day^{-1}. In those events, it took from 13 hours to 178 hours after the peak discharge for the ephemeral streams to dry up, with an average of 71 hours. The duration of ephemeral flows depend on storm size, initial soil moisture condition, and evaporation during the recession period. The contraction of ephemeral streams is a function of variable soil depths, landforms, and hydraulic conductivity from upstream to downstream [*Clark et al.*, 2009]. Therefore, before the discharge at the perennial stream head decreases to zero, both spatial heterogeneity and groundwater hydraulics control recession behavior observed at the watershed outlet. After the ephemeral stream dries up, only the perennial

stream riparian aquifer contributes to the base flow observed at the outlet. The effect of stream

contraction is not significant when base flow is less than Q_{p0}.

Table 2.1. Characteristic values and estimated recession parameters for the twenty-three recession events

R (mm)	T_R (day)	t_p (mm/dd/yy hh)	t_r (mm/dd/yy hh)	t_{p0} (mm/dd/yy hh)	Q_{p0} (mm day^{-1})	Q_0 (mm day^{-1})	a_1 (mm$^{1-b_1}$ day$^{b_1-2}$)	b_1 (-)	b_2 (-)
65	4	01/20/88 02	01/20/88 08	01/24/88 01	0.53	0.55	2.5	2.5	12.8
60	3	02/04/88 07	02/04/88 13	02/09/88 10	0.74	0.74	2.8	2.8	6.3
59	4	10/03/88 18	10/04/88 00	10/05/88 00	0.51	0.52	2.2	2.2	6.0
123	4	10/01/89 19	10/02/89 01	10/05/89 06	0.93	0.60	2.3	2.3	12.2
57	3	12/09/89 15	12/09/89 21	12/10/89 12	1.14	0.94	3.4	3.4	12.7
56	5	01/08/90 01	01/08/90 07	01/12/90 16	1.05	0.96	2.7	2.7	8.7
78	2	03/29/91 14	03/29/91 20	04/03/91 06	1.19	1.04	2.8	2.8	29.4
61	4	08/23/92 02	08/23/92 08	08/23/92 15	1.11	1.20	0.7	2.1	9.1
67	2	11/04/92 13	11/04/92 19	11/07/92 06	1.10	0.84	2.3	3.0	8.8
192	3	10/04/95 22	10/05/95 04	10/10/95 08	0.92	0.95	2.3	2.3	14.3
64	2	10/14/95 12	10/14/95 18	10/19/95 22	0.98	0.98	3.2	3.2	4.5
168	3	10/26/97 04	10/26/97 10	10/28/97 16	1.07	1.20	1.6	1.7	5.3
91	3	05/07/99 06	05/07/99 12	05/08/99 00	1.39	1.36	1.1	2.6	10.4
56	1	07/24/99 17	07/24/99 23	07/25/99 16	0.86	0.82	1.7	1.7	4.9
59	2	02/06/02 17	02/06/02 23	02/11/02 00	0.63	0.60	2.3	2.3	11.0
67	2	03/30/02 21	03/31/02 03	04/07/02 07	0.70	0.68	2.6	3.0	5.5
86	2	10/15/02 17	10/15/02 23	10/17/02 12	0.57	0.55	1.8	1.8	7.1
104	2	09/16/04 17	09/16/04 23	09/18/04 14	1.11	1.14	0.2	2.0	7.8
64	1	09/27/04 15	09/27/04 21	09/28/04 22	1.16	1.23	2.0	2.1	6.6
73	3	11/04/04 09	11/04/04 15	11/05/04 15	1.14	1.11	3.3	3.3	10.6
77	2	11/16/06 01	11/16/06 07	11/17/06 03	1.21	1.27	2.4	2.4	6.6
55	3	12/31/06 23	01/01/07 05	01/03/07 09	1.02	1.01	2.7	2.7	4.3
57	4	01/08/07 00	01/08/07 06	01/12/07 16	0.85	0.87	2.5	2.5	13.4
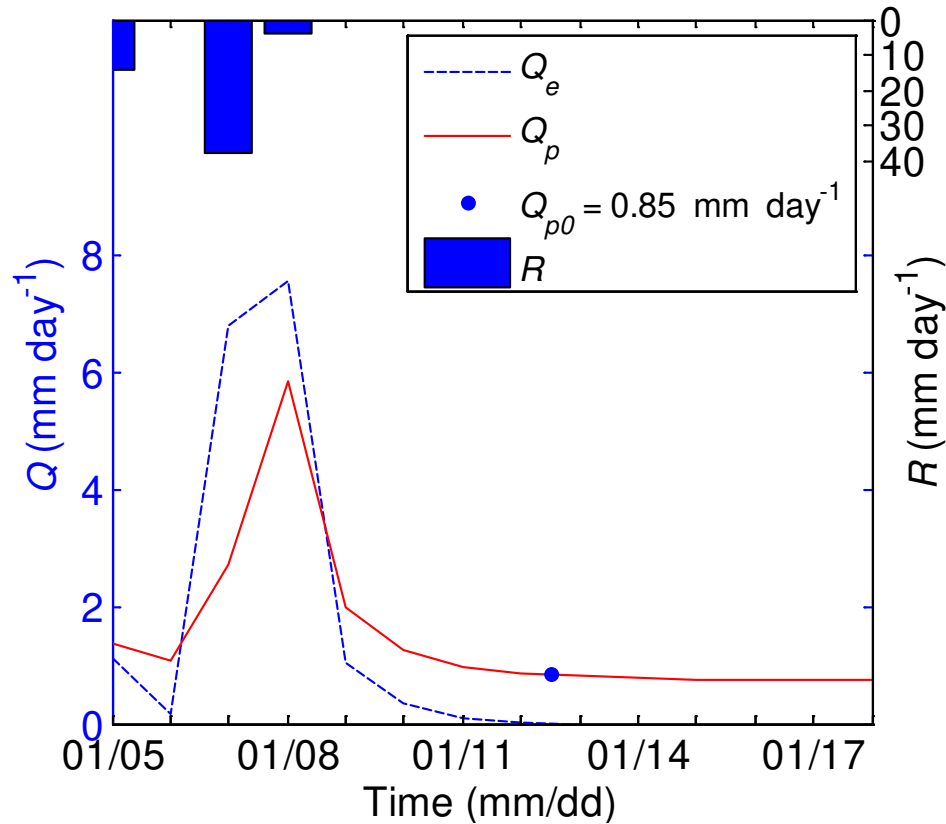
Figure 2.2. Rainfall and streamflow at the perennial stream head (Q_e) and watershed outlet (Q_p) during the recession event starting at 6 AM on 01/08/2007.

2.4.2 _Transition flow from early to late recessions_

The base flow observed at the outlet during the transition from early recession to late recession (i.e., Q_0) was identified through the cumulative regression method described above, for each recession event. The identified base flow value occurred at transition is denoted as Q_0, to distinguish from Q_{p0} which is identified with the timing of ephemeral streams contracting to perennial stream heads. The constructed pairs of recession slope data for two recession events are presented in Figure 2.3. In Figure 2.3a and 2.3c, the data points for large values of discharge (Q_p) followed approximately a straight line; and the slope increased with the decreasing discharge. The identified transition flow is plotted as solid red line in Figure 2.3a. When the discharge at the perennial stream head decreased to zero, the outlet discharge was 0.53 mm day^{-1} as shown by the

dotted blue line in Figure 2.3a. Figure 2.3b shows the corresponding slopes and coefficients of determination (R^2) from the cumulative regression analysis of $-dQ/dt \sim Q$- arranged in descending order of discharge values. The transition from early recession to late recession is marked with a red dot in Figure 2.3b with a corresponding transition flow Q_0 of 0.55 mm day^{-1}. The transition point was determined when the regression slope increased and R^2 decreased significantly with the decrease in discharge. The slope of the corresponding early recession stage (b_1) was computed as 2.5 by the cumulative regression analysis.

The values of Q_0 and b varied across individual recession events. As shown in Figure 2.3c and 2.3d, Q_0 for the event shown in Figure 2.2 was identified as 0.87 mm day^{-1}, and b_1 was estimated to be 2.5. For all twenty-three selected recession events, the identified values of Q_0 ranged from 0.52 mm day^{-1} to 1.36 mm day^{-1} (Table 2.1). The average value of Q_0 was 0.92 mm day^{-1} and the standard deviation was 0.25 mm day^{-1}. As shown in Table 2.1, b_1 varied from 1.7 to 3.4 with an average value of 2.5. The values of b_1 were found to be around 2 in other watersheds based on analysis of individual recession events [*Biswal and Marani*, 2010; *Shaw and Riha*, 2012; *Mutzner et al.*, 2013]. The average value of b_2 for the PMRW watershed was up to 9.5 using data from individual recession events, because of return flow to the perennial stream aquifer from confined aquifer [*Tromp-van Meerveld et al.*, 2007; *Clark et al.*, 2009]. Considering the return flow, the upper envelope was used for estimating the value of the exponent and the corresponding value was 1.8 [*Wang*, 2011], which was within the range of theoretical values [*Rupp and Selker*, 2006].
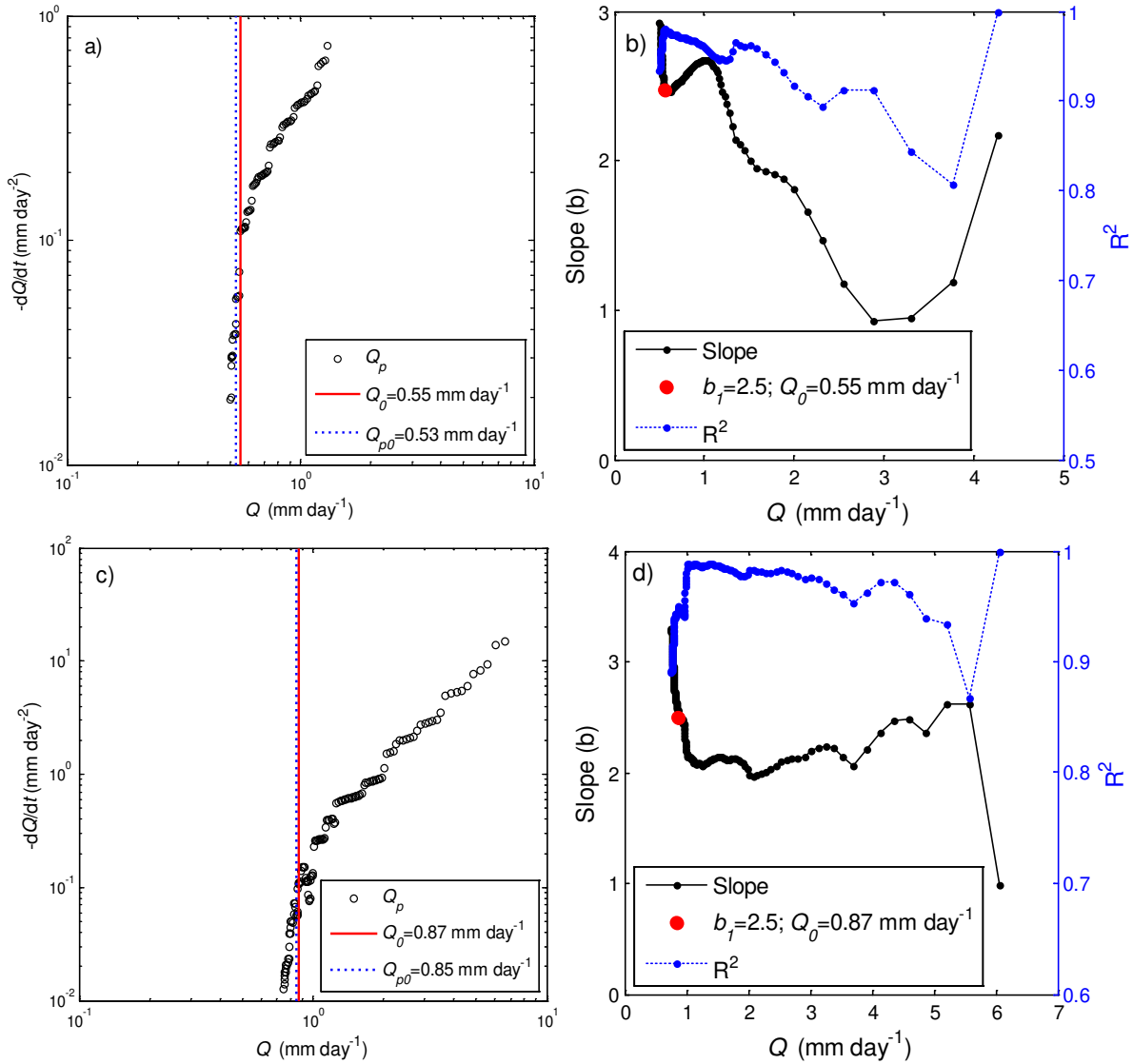
Figure 2.3. Transition of recession slope curve, the slope and R^2 of the cumulative regression analysis for recession events with peak discharge at 2 AM on 01/20/1988 (a, b) and at 0 AM on 01/08/2007 (c, d).

Table 2.1 also shows the values of recession parameter a_1 for the early stage that is dependent on the initial soil moisture conditions [*Harman and Sivapalan*, 2009; *Biswal and Marani*, 2014]. Figure 2.4 shows the scatter plot of a_1 versus peak flow (Q_h), which serves as a proxy of initial soil moisture condition. Consistent with *Biswal and Marani* [2014], the value of a_1 arguably increased with the decrease in peak discharge.
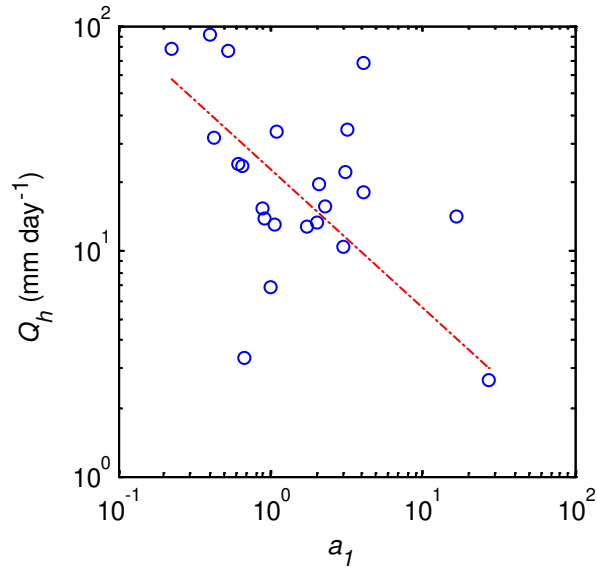
Figure 2.4. The dependence of recession coefficient a_1 on initial soil moisture condition using peak flow (Q_p) as a proxy.

2.4.3   *Comparison between Q_{p0} and Q_0*

The working hypothesis of this study was that the transition of base flow recession behavior takes place when flowing streams contract to perennial stream heads. Figure 2.5 compares the values of Q_{p0} with Q_0 for the recession events shown in Table 2.1. The correlation coefficient between Q_{p0} and Q_0 was 0.90, and the root mean square error was 0.12 mm day^{-1}. From Figure 2.5, the two characteristics streamflow, Q_{p0} and Q_0, were strongly correlated, indicating the intrinsic linkage between ending of ephemeral stream contraction and the transition of recession behavior from early stage to late stage. The data points that deviated most from the 45 degree line were associated with low values of R^2. For example, the data point deviating the most is associated with the event with peak flow occurring on October 1, 1989. The R^2 of the event is only 0.81, the lowest among all twenty-three events.
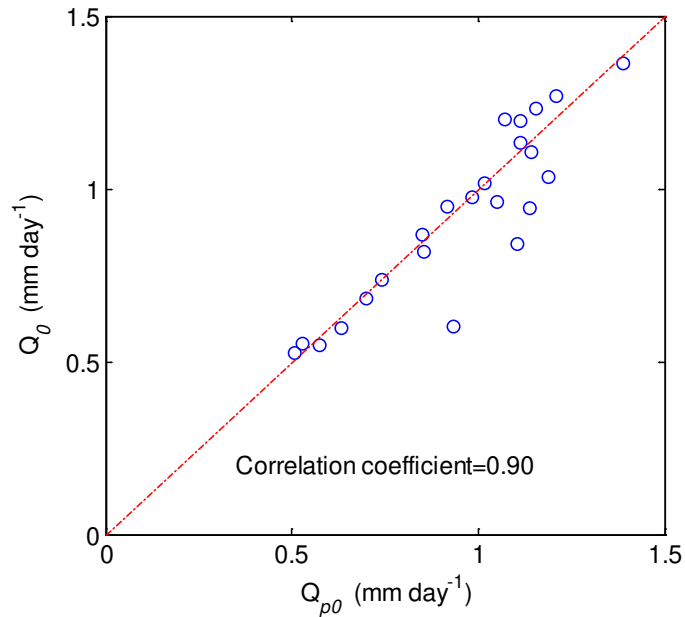
Figure 2.5. Identified values of Q_{p0} versus Q_0 for twenty-three individual recession events shown in Table 2.1.

2.5   Conclusion

This study was focused on the transition of base flow recession from early stage to late stage. A cumulative regression analysis method was proposed to identify the transition flow quantitatively for individual recession events observed in the Panola Mountain Research Watershed. The identified transition flows were then compared with the discharge rate observed when the flowing stream contracts to the perennial stream head. Results concluded that these two characteristic flows are almost identical. It was found that these two characteristics flows are strongly correlated. These findings supported the notion that the derivative of discharge in ephemeral streams is dominated by the contraction of wet channel reaches [*Biswal and Marani*, 2010], while change in discharge in perennial streams is dominated by a reduction in the discharge drained from the aquifer [*Brutsaert and Nieber*, 1977]. The contraction of ephemeral streams governs the recession rate of the early recession. At the late recession stage when perennial

28

streams provide a dominant contribution to discharge, the contraction of flowing streams is minimal and groundwater hydraulics governs the recession behavior.

Depending on the interarrival times of rainfall events, an individual recession event may only manifest an early recession stage or may last until the late recession stage emerges. Individual recession events, which include both early and late stage, are not observed frequently, particularly in relatively large watersheds. It is argued that the early stage of recession is usually observed in the high flow season (i.e., wet season); while the late recession stage is observed in the low flow season (i.e., dry season). In high flow seasons, flowing streams contract during the recession period. While in low flow seasons, perennial streams provide a dominant contribution to discharge and the contraction of flowing streams may be insignificant. Therefore, the appearance of transition flow from early recession to late recession can be viewed as a seasonal signature of base flow in the watersheds with distinct streamflow seasonality.

2.6   <u>References</u>

Beven, K., and M. Kirkby (1979), A physically based, variable contributing area model of basin hydrology/Un modèle à base physique de zone d'appel variable de l'hydrologie du bassin versant, *Hydrological Sciences Journal*, *24*(1), 43-69.

Biswal, B., and M. Marani (2010), Geomorphological origin of recession curves, *Geophysical Research Letters*, *37*, L24403, doi:10.1029/2010GL045415.

Biswal, B., and D. Nagesh Kumar (2013), A general geomorphological recession flow model for river basins, *Water Resources Research*, *49*(8), 4900-4906.

Biswal, B., and M. Marani (2014), 'Universal' recession curves and their geomorphological interpretation, *Advances in Water Resources*, *65*, 34-42.

Biswal, B., and D. N. Kumar (2015), Estimation of 'drainable' storage–A geomorphological approach, *Advances in Water Resources*, *77*, 37-43.

Blyth, K., and J. C. Rodda (1973), A stream length study, *Water Resources Research*, *9*(5), 1454-1461.

Brutsaert, W., and J. L. Nieber (1977), Regionalized drought flow hydrographs from a mature glaciated plateau, *Water Resources Research*, *13*(3), 637-643.

Brutsaert, W., and J. P. Lopez (1998), Basin-scale geohydrologic drought flow features of riparian aquifers in the Southern Great Plains, *Water Resources Research*, *34*(2), 233-240.

Clark, M. P., D. E. Rupp, R. A. Woods, H. J. Tromp-van Meerveld, N. E. Peters, and J. E. Freer (2009), Consistency between hydrological models and field observations: linking processes at the hillslope scale to hydrological responses at the watershed scale, *Hydrological Processes*, *23*(2), 311-319.

Day, D. G. (1978), Drainage density changes during rainfall, *Earth Surface Processes*, *3*(3), 319-326.

Freer, J., J. J. McDonnell, K. J. Beven, N. E. Peters, D. A. Burns, R. P. Hooper, B. Aulenbach, and C. Kendall (2002), The role of bedrock topography on subsurface storm flow, *Water Resources Research*, *38*(12), 5-1-5-16.

Godsey, S. E., and J. W. Kirchner (2014), Dynamic, discontinuous stream networks: hydrologically driven variations in active drainage density, flowing channels and stream order, *Hydrological Processes*, *28*(23), 5791-5803.

Gregory, K., and D. Walling (1968), The variation of drainage density within a catchment, *Hydrological Sciences Journal*, *13*(2), 61-68.

Gregory, K. J. (1976), Drainage networks and climate, *Geomorphology and climate*, 289-315.

Harman, C., and M. Sivapalan (2009), A similarity framework to assess controls on shallow subsurface flow dynamics in hillslopes, *Water Resources Research*, *45*, *W01417*, doi:10.1029/2008WR007067.

Harman, C. J., M. Sivapalan, and P. Kumar (2009), Power law catchment-scale recessions arising from heterogeneous linear small-scale dynamics, *Water Resources Research*, *45*, W09404, doi:10.1029/2008WR007392.

Inamdar, S. P., and M. J. Mitchell (2007), Contributions of riparian and hillslope waters to storm runoff across multiple catchments and storm events in a glaciated forested watershed, *Journal of Hydrology*, *341*(1), 116-130.

Krakauer, N. Y., and M. Temimi (2011), Stream recession curves and storage variability in small watersheds, *Hydrology and Earth System Sciences*, *15*(7), 2377-2389.

Marani, M., E. Eltahir, and A. Rinaldo (2001), Geomorphic controls on regional base flow, *Water Resources Research*, *37*(10), 2619-2630.

McGuire, L. A., J. D. Pelletier, and J. J. Roering (2014), Development of topographic asymmetry: Insights from dated cinder cones in the western United States, *Journal of Geophysical Research: Earth Surface*, *119*(8), 1725-1750.

Mutzner, R., E. Bertuzzo, P. Tarolli, S. V. Weijs, L. Nicotina, S. Ceola, N. Tomasic, I. Rodriguez-Iturbe, M. B. Parlange, and A. Rinaldo (2013), Geomorphic signatures on Brutsaert base flow recession analysis, *Water Resources Research*, *49*(9), 5462-5472.

Palmroth, S., G. G. Katul, D. Hui, H. R. McCarthy, R. B. Jackson, and R. Oren (2010), Estimation of long-term basin scale evapotranspiration from streamflow time series, *Water Resources Research*, *46*(10), W10512, doi:10.1029/2009WR008838.

Parlange, J. Y., F. Stagnitti, A. Heilig, J. Szilagyi, M. B. Parlange, T. S. Steenhuis, W. L. Hogarth, D. A. Barry, and L. Li (2001), Sudden drawdown and drainage of a horizontal aquifer, *Water Resources Research*, *37*(8), 2097-2101.

Peters, N. E., and B. T. Aulenbach (2011), Water storage at the Panola Mountain Research Watershed, Georgia, USA, *Hydrological Processes*, *25*(25), 3878-3889.

Peters, N. E., J. Freer, and B. T. Aulenbach (2003), Hydrological Dynamics of the Panola Mountain Research Watershed, Georgia, *Ground Water*, *41*(7), 973-988.

Rupp, D. E., and J. S. Selker (2006), On the use of the Boussinesq equation for interpreting recession hydrographs from sloping aquifers, *Water Resources Research*, *42*, W12421, doi:10.1029/2006WR005080.

Rupp, D. E., J. Schmidt, R. A. Woods, and V. J. Bidwell (2009), Analytical assessment and parameter estimation of a low-dimensional groundwater model, *Journal of hydrology*, *377*(1), 143-154.

Shaw, S. B., and S. J. Riha (2012), Examining individual recession events instead of a data cloud: Using a modified interpretation of dQ/dt–Q streamflow recession in glaciated watersheds to better inform models of low flow, *Journal of Hydrology*, *434–435*, 46-54.

Shaw, S. B., T. M. McHardy, and S. J. Riha (2013), Evaluating the influence of watershed moisture storage on variations in base flow recession rates during prolonged rain-free periods in medium-sized catchments in New York and Illinois, USA, *Water Resources Research*, *49*(9), 6022-6028.

Stanley, E. H., S. G. Fisher, and N. B. Grimm (1997), Ecosystem expansion and contraction in streams, *BioScience*, *47*(7), 427-435.

Szilagyi, J., M. B. Parlange, and J. D. Albertson (1998), Recession flow analysis for aquifer parameter determination, *Water Resources Research*, *34*(7), 1851-1857.

Tóth, J. (1963), A theoretical analysis of groundwater flow in small drainage basins, *Journal of Geophysical Research*, *68*(16), 4795-4812.

Troch, P. A., F. P. De Troch, and W. Brutsaert (1993), Effective water table depth to describe initial conditions prior to storm rainfall in humid regions, *Water Resources Research*, *29*(2), 427-434.

Tromp-van Meerveld, H. J., and J. J. McDonnell (2006a), Threshold relations in subsurface stormflow: 1. A 147-storm analysis of the Panola hillslope, *Water Resources Research*, *42*(2), W02410, doi:10.1029/2004WR003778.

Tromp-van Meerveld, H. J., and J. J. McDonnell (2006b), Threshold relations in subsurface stormflow: 2. The fill and spill hypothesis, *Water Resources Research*, *42*, W02411, doi:10.1029/2004WR003800.

Tromp-van Meerveld, H. J., N. E. Peters, and J. J. McDonnell (2007), Effect of bedrock permeability on subsurface stormflow and the water balance of a trenched hillslope at the Panola Mountain Research Watershed, Georgia, USA, *Hydrological Processes*, *21*(6), 750-769.

Wang, D. (2011), On the base flow recession at the Panola Mountain Research Watershed, Georgia, United States, *Water Resources Research*, *47*, W03527, doi:10.1029/2010WR009910.

Wang, D., and L. Wu (2013), Similarity of climate control on base flow and perennial stream density in the Budyko framework, *Hydrology and Earth System Science*, *17*(1), 315-324.

Wigington, P. J., T. J. Moser, and D. R. Lindeman (2005), Stream network expansion: a riparian water quality factor, *Hydrological Processes*, *19*(8), 1715-1721.

Zecharias, Y. B., and W. Brutsaert (1988), Recession characteristics of groundwater outflow and base flow from mountainous watersheds, *Water Resources Research*, *24*(10), 1651-1658.

CHAPTER 3: LINKING LONG TERM CLIMATE TO TRANSITION OF BASE FLOW RECESSION

3.1 <u>Introduction</u>

The flowing of stream networks expand during wet season as a response of rainfall events and contract during drought season [*Blyth and Rodda*, 1973; *Gregory*, 1976; *Day*, 1978]. From this perspective, the streams are categorized into ephemeral, intermittent and perennial streams. The perennial streams, the basic stream networks flow for much of the year is governed by the groundwater flow and depends upon mean annual precipitation. In temporal streams, i.e., intermittent or ephemeral streams, flows as a responses of seasonal and individual rainfall events, depends on the seasonal precipitation.

De Wit and Stankiewicz [2006] studied the relation between perennial stream density (D_P) (ratio between total perennial stream length and drainage area) and the mean annual precipitation in Africa. In that study, D_P was close to zero when precipitation was less than 400 mm yr^{-1}; increased when precipitation was between 400 mm yr^{-1} to 1000 mm yr^{-1}; then decreased when precipitation was larger than 1000 mm yr^{-1}.

However, the runoff at mean annual scale is proportionally controlled by both water and energy supply. *Budyko* [1974] demonstrated that the partitioning of precipitation into runoff and evaporation was primarily controlled by climate aridity index (E_P/P). *Wang and Wu* [2013] later found that climate aridity index (E_P/P) had a dominant control on perennial stream density (D_P) based on the high resolution National Hydrography Dataset of 185 watersheds. They also found a strong correlation between the long term average base flow *(Q_b)* and perennial stream density (D_P), which reveals the co-evolution between the water balance and perennial stream networks. This indicates that long term average base flow *(Q_b)* is controlled by the climate aridity index

(E_P/P) through perennial stream networks. However, both the transition from early to late recession (Q_0) and long-term average base flow (Q_b) are the characteristics of base flows; Q_0 is associated with the event scale while Q_b is associated with the long-term scale. If the transition from early to late recession occurs when flowing streams contract to perennial stream heads, the flow at the transition from early to late recessions (Q_0) will be, via first order, controlled by long-term mean climate (E_p/P). The connection between Q_0 and Q_b can be established through the perennial streams. The major objective of this study was to quantify the transition flows of an ensemble of watersheds with a gradient of climate aridity indices, and to compare the transition flow with the corresponding long-term average base flow.

3.2 <u>Watersheds with distinct transitions from early to late recessions</u>

If daily streamflow and rainfall data are available, the transition flow can be determined by the lower envelope of $-dQ/dt$ versus Q on log-log space. Daily streamflow and rainfall data during 1948-2003 were available for the international Model Parameter Estimation Experiment (MOPEX) watersheds [*Duan et al.*, 2006]. Therefore, recession analysis was conducted on the MOPEX watersheds and watersheds with distinct transition behavior from early to late recessions were only selected for recession analysis to minimize the uncertainty of the identification of transition flow. The background information of the 40 selected watersheds including USGS gage number, drainage area, and climate aridity index are shown in Table 3.1. The drainage area of the watersheds ranges from 173 km^2 to 9402 km^2, and the climate aridity index ranges from 0.38 to 1.09. Figure 3.1 shows the spatial distribution of the 40 watersheds.
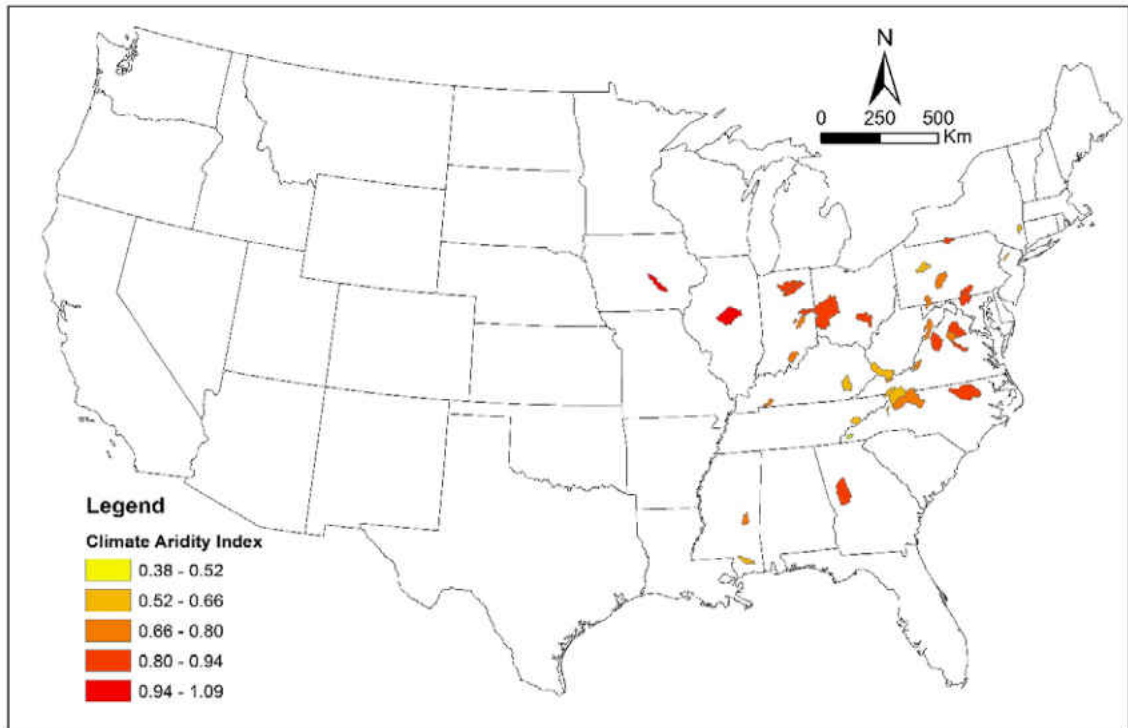
36

Figure 3.1. Spatial distribution of 40 case study watersheds.

Table 3.1. Forty case study watersheds with distinct transitions from early to late recessions

Watershed	USGS gage	Drainage area (km^2)	E_p/P	Q_b (mm/day)	Q_0 (mm/day)	Recession parameter			
						a_1	b_1	a_2	b_2
Wappinger Creek, NY	01372500	469	0.65	0.97	0.98	0.041	1.8	0.041	0.9
Pequest River, NJ	01445500	275	0.60	1.11	1.13	0.032	1.8	0.034	1.2
Cowanesque River, PA	01520000	772	0.81	0.53	0.50	0.102	1.8	0.054	0.8
Juniata River, PA	01559000	2113	0.79	0.92	0.82	0.035	2.4	0.029	1.4
West Conewago Creek, PA	01574000	1321	0.84	0.65	0.70	0.067	2.0	0.045	1.0
South Branch Potomac River, WV	01606500	1663	0.72	0.73	0.73	0.073	2.0	0.057	1.2
South Fork Shenandoah River, VA	01628500	2808	0.83	0.66	1.21	0.040	2.6	0.045	2.0
Monocacy River at Jug Bridge, MD	01643000	2116	0.82	0.69	0.67	0.062	1.8	0.051	1.3
Rappahannock River, VA	01664000	1606	0.81	0.72	1.20	0.027	2.3	0.034	0.9
Rapidan River, VA	01667500	1222	0.78	0.76	0.78	0.047	1.8	0.043	1.4
Rappahannock River, VA	01668000	4134	0.82	0.64	0.59	0.056	2.1	0.033	1.1
South Anna River, VA	01672500	1020	0.83	0.48	0.46	0.068	2.2	0.021	0.8
Craig Creek, VA	02018000	852	0.73	0.73	0.68	0.062	2.1	0.043	1.2
Tar River, NC	02083500	5654	0.85	0.64	0.55	0.087	2.7	0.024	0.5
Yadkin River, NC	02116500	5905	0.70	0.91	1.01	0.018	3.7	0.018	1.8
Linville River, NC	02138500	173	0.55	1.49	1.29	0.013	2.7	0.021	0.9
Flint River, GA	02347500	4791	0.82	0.75	0.79	0.032	2.9	0.021	1.0
Chunky River, MS	02475500	956	0.71	0.64	0.57	0.081	2.1	0.053	1.3
Red Creek, MS	02479300	1142	0.64	1.10	1.01	0.025	3.0	0.025	1.3
Redbank Creek, PA	03032500	1368	0.66	1.02	1.07	0.053	2.0	0.056	1.2
Casselman River, PA	03079000	989	0.69	1.04	1.28	0.053	1.9	0.061	1.3
Hocking River, OH	03159500	2442	0.83	0.62	0.80	0.081	2.5	0.062	1.2
New River, VA	03164000	2929	0.63	1.21	1.55	0.008	3.3	0.019	1.2
Tug Fork, WV	03214000	3077	0.65	0.85	1.01	0.067	2.0	0.068	1.3
Stillwater River, OH	03266000	1683	0.90	0.48	0.51	0.110	2.0	0.078	1.3
Great Miami River, OH	03274000	9402	0.87	0.59	0.52	0.088	2.1	0.047	1.2
South Fork Kentucky River, KY	03281500	1870	0.64	0.71	0.55	0.103	2.0	0.044	0.6

Watershed	USGS gage	Drainage area (km²)	E_p/P	Q_b (mm/day)	Q_0 (mm/day)	Recession parameter			
						a_1	b_1	a_2	b_2
Blue River, IN	03303000	1233	0.76	1.26	1.26	0.029	2.3	0.040	0.8
Eel River, IN	03328500	2043	0.91	0.61	0.63	0.049	2.4	0.028	1.2
Tippecanoe River, IN	03331500	2217	0.92	0.78	0.86	0.025	2.1	0.021	0.9
White River, IN	03348000	1052	0.86	0.58	0.64	0.058	3.0	0.027	1.2
Big Blue River, IN	03361500	1090	0.80	0.68	0.62	0.067	2.5	0.041	1.5
Sugar Creek, IN	03361650	243	0.80	0.60	0.49	0.105	2.4	0.040	1.0
Little River, KY	03438000	632	0.73	0.92	0.51	0.048	1.7	0.028	0.9
Little Pigeon River, TN	03470000	914	0.56	0.98	0.92	0.051	2.4	0.046	1.3
South Fork Holston River, VA	03473000	780	0.60	1.06	1.11	0.024	2.9	0.028	1.4
Crooked Creek, PA	03521500	355	0.69	0.82	0.87	0.055	2.3	0.047	1.2
Valley River, NC	03550000	269	0.38	1.73	1.76	0.011	2.3	0.022	1.2
North Skunk River, IA	05472500	1891	1.09	0.36	0.44	0.060	1.7	0.031	0.9
Salt Creek, IL	05582000	4672	1.00	0.49	0.57	0.046	2.2	0.021	0.8

3.3   **Methodology**

The following procedures were adopted for quantifying the transition flow from early to late recessions and were applied to the 40 study watersheds.

3.3.1   *Computing data points of –dQ/dt versus Q*

The time series of the daily streamflow hydrograph for each watershed during 1948-2003 were used for analysis. The falling limbs of the hydrographs were the input of individual recession analysis. The following criteria was used to select the data points for computing the data pairs of –dQ/dt and Q: 1) The first 3 days of falling limbs is excluded to minimize the impact of quick flow; 2) The remaining recession data include at least 3 days of recession flow so that there is more than 1 data pair of –dQ/dt and Q from each recession segment. The data pairs of –dQ/dt and Q were then computed to perform the recession analysis.

3.3.2   *Determining lower envelopes of recession slope curves*

In the literature, the lower envelope of recession slope curve is usually determined by visual exploration. To minimize the subjective effect on the identification of transition flow, the lower envelope was determined by the following steps: 1) The entire data points in the recession slope curve were sorted in a descending order by Q; 2) The sorted data points were divided into a certain number of bins; 3) The data points in each bin were sorted in a descending order by $-dQ/dt$; 4) The data points of the lower 10-30% in each bin were selected; 5) The average values of Q and $-dQ/dt$ over the selected lower data points in each bin (i) were computed and denoted as $\bar{Q}_i$ and $\overline{-dQ/dt}_i$ which constituted the lower envelope. In step 4, if a smaller percentage was used (e.g., 10%), the identified lower envelope might fluctuate. Therefore, the lower 30% of each bin were selected in this study after conducting sensitivity analysis.

The range of each bin in step 2 was determined with the following consideration. In the recession slope curve plot, the data points in the region with higher values of Q were denser compared with the region with smaller Q values. The number of data points in a bin with higher Q values was larger. For higher values of Q, the ranges of bins were determined by selecting 5% of the total number of data points in each bin initially. For lower values of Q, 2.5% of total number of data point was selected in each bin due to the low density of the data points. Furthermore, the range of Q in each bin was neither less than 1 percent nor more than 10 percent of the total range of Q (i.e., maximum Q – minimum Q). Typically 20-30 bins were selected for each watershed in the study watersheds.

3.3.3   _Identifying transition flows of lower envelopes_

Transition flows were identified based on the lower envelope represented by the data points of $(\bar{Q}_i, \overline{-dQ/dt_i})$, where $i=1,2,3,.....N$ and $\bar{Q}_i$ increases with i. $\bar{Q}_1$ is the smallest value of bin-averaged discharge, and $\bar{Q}_N$ is the largest value of bin-averaged discharge. The transition of a lower envelope was identified by the cumulated regression analysis. For a given data point $(1 < j \leq N)$ of a lower envelope, linear regression analysis was conducted based on the cumulative data points of $(\bar{Q}_i, \overline{-dQ/dt_i})$ with $i = 1,2, ... j$ in log-log space. The obtained slope and goodness-of-fit $(1 < j \leq N - 1)$ are denoted as K_j and $R^2{}_j$, respectively. For example, the slope K_1 was computed based on the regression analysis of the first two data points associated with $\bar{Q}_1$ and $\bar{Q}_2$; K_2 was also computed by regression analysis of $\bar{Q}_1$, $\bar{Q}_2$, and $\bar{Q}_3$. Since the slope of early recession was larger than that of late recession, the transition point $\bar{Q}_o$ was identified if K_j continuously increases with j following the identified transition point. In most cases, $R^2{}_j$ decreased following

the transition point, and $R^2{}_j$ was used as an auxiliary criterion when noise exists in the trend of slope.

3.3.4   *Quantifying long-term average base flow for 40 watersheds*

In this study, the long-term average base flow was computed based on the daily base flow during the period of 1948-2003. One parameter low pass filtering method with filter parameters of 0.925, was applied to separate the base flow from the surface runoff [*Sivapalan et al.*, 2011].

3.4   **Results**

3.4.1   *Base flow separation and sensitivity analysis for 40 watersheds*

Figure 3.2 shows the daily total streamflow and base flow in the period of 01/01/1948-12/31/1948 for the West Conewago Creek watershed in Pennsylvania (USGS gage 1574000). The long-term average base flow was 0.65 mm/day, and the base flow index (base flow/total streamflow) was 0.56 (Figure 3.2). The daily base flows were lower than the long-term average value during the dry seasons from July to October.
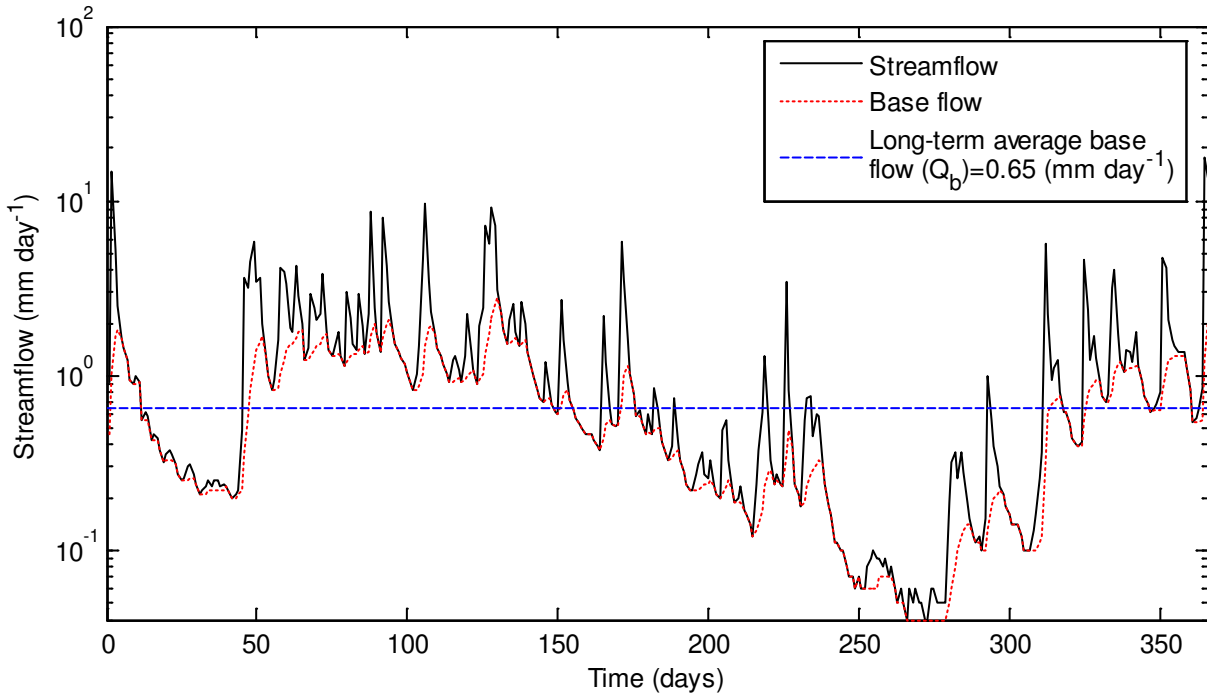
Figure 3.2. Base flow separation results from 01/01/1948 to 12/31/1948 at the West Conewago Creek in Pennsylvania (USGS gage 1574000).

3.4.2 *The transition flows at the lower envelopes of recession slope curves for 40 watersheds*

The transition flows at the lower envelopes of recession slope curves were identified by the cumulative regression method discussed in section 3.3. Figure 3.3 presents the results for three watersheds. As shown in Figure 3.3a, the lower envelope is represented by red dots (Q_L). Cumulative regression analysis was conducted over the identified points constituting the lower envelope. As shown in Figure 3.3b, when discharge was larger than 0.70 mm/day (the red dot), the slope started to increases and R^2 started to decline. Therefore, $Q_0=0.70$ mm/day was the identified transition flow which is plotted as a solid red line in Figure 3.3a. The slope at the transition point by cumulative regression analysis was 0.96. The recession parameters at the early and late recession stages were estimated by regression analysis. In order to ensure that the intersection of regression lines at the identified transition point, the regression lines were forced to

43

pass through the transition point. The recession parameters for all the study watersheds are shown in Table 3.1. The range of the transition flow was between 0.44 mm/day to 1.76 mm/day. The recession slope varied from 1.7 to 3.7 for early recessions and from 0.5 to 2.0 for late recessions. Table 3.1 also shows the values of Q_b and Q_0, as well as the recession parameters at the early and late stages for all 40 watersheds.
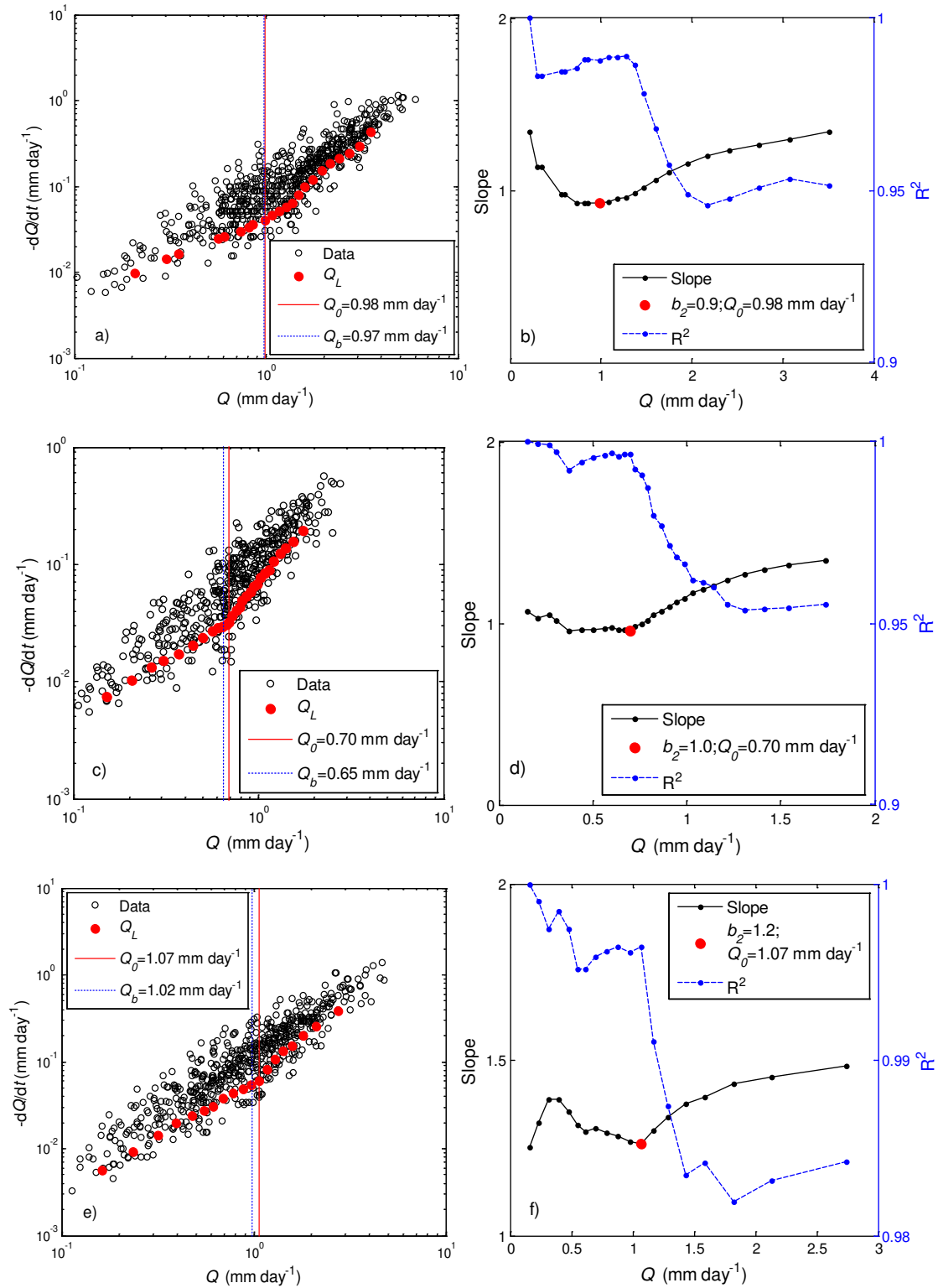
Figure 3.3. Transition of recession slope curve (Q_0) obtained from lower envelope (Q_L), long-term average base flow (Q_b), the slope and R^2 of the cumulative regression analysis for USGS gage 01372500 (a, b), USGS gage 01574000 (c, d) and USGS gage 03032500 (e, f).

3.4.3   The transition flows at the lower envelopes of recession slope curves for 40 watersheds

Figure 3.4 illustrates the dependence of transition recessions (Q_0) on long-term average climate aridity index (E_p/P) and long-term average base flow (Q_b). As expected, transition flow decreased with E_p/P as shown in Figure 3.4a. The correlation coefficient between Q_0 and E_p/P was -0.68. Since both Q_0 and Q_b were predominately controlled by long-term climate, the comparison between these two characteristic base flows is presented in Figure 3.4b. The average value of Q_0 and Q_b were 0.84 mm day^{-1} and 0.81 mm day^{-1} for 40 watersheds. The correlation coefficient and root mean square error (RMSE) between Q_0 and Q_b were 0.82 and 0.18 mm day^{-1}, respectively.
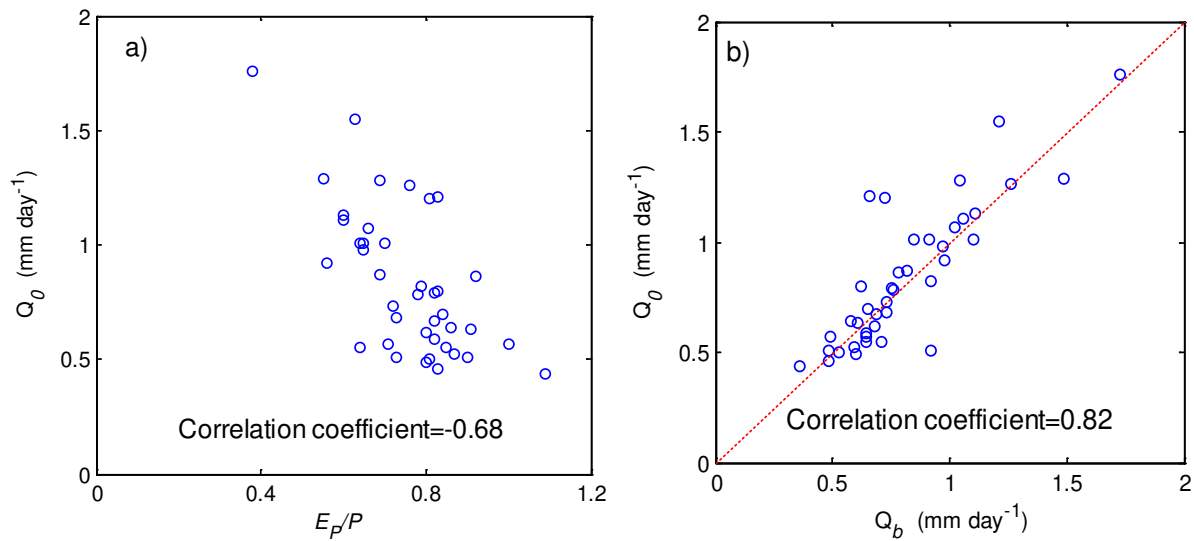
Figure 3.4. The dependence of transition from early to late recessions (Q_0) a) on long-term average climate aridity index (E_p/P) and b) long-term average base flow (Q_b).

3.5 **Summary and Conclusion**

The purpose of this study was to test the control of climate on the transition from early to late recession stages. It is found that climate, represented by climate aridity index, has a dominant control on the transition from early to late recession stages. In each watershed, the values for the transition flow and the long-term average base flow were found to be very similar. In reality, the long term average base flow and the transition of base flow from early to late recession are basically the form of base flow at two temporal scales, i.e., the long-term time scale and the event scale during a recession period. This finding manifests that the base flow characteristics at long term scale and event scale during a recession period have a connection through the recession and both are primarily controlled by climate. The water managers will be able to predict the long term base flow and climate situation after quantifying the transition flow of recession from the event scale data when long term data is not available.

3.6   <u>References</u>

Blyth, K., and J. C. Rodda (1973), A stream length study, *Water Resources Research*, *9*(5), 1454-1461.

Budyko, M. (1974), *Climate and Life*, 508 pp, Academic Press*,* New York.

Day, D. G. (1978), Drainage density changes during rainfall, *Earth Surface Processes*, *3*(3), 319-326.

De Wit, M., and J. Stankiewicz (2006), Changes in surface water supply across Africa with predicted climate change, *Science*, *311*(5769), 1917-1921.

Duan, Q., et al. (2005), Model Parameter Estimation Experiment (MOPEX): An overview of science strategy and major results from the second and third workshops, *Journal of Hydrology, 320*(1)*,* 3-17.

Gregory, K. J. (1976), Drainage networks and climate, *Geomorphology and climate*, 289-315.

Sivapalan, M., M. A. Yaeger, C. J. Harman, X. Xu, and P. A. Troch (2011), Functional model of water balance variability at the catchment scale: 1. Evidence of hydrologic similarity and space-time symmetry, *Water Resources Research*, *47*, W02522, doi:10.1029/2010WR009568.

Wang, D., and L. Wu (2013), Similarity of climate control on base flow and perennial stream density in the Budyko framework, *Hydrology and Earth System Science*, *17*(1), 315-324.

CHAPTER 4: QUANTIFYING GROUNDWATER DEPLETION IN HIGH PLAINS AQUIFER BY RECESSION ANALYSIS

4.1 <u>Introduction</u>

The irrigation sector becomes the largest water consumption sector throughout the world, account for about 70 % of global freshwater uses and 90 % of consumptive water uses [*Siebert et al.*, 2010; *Döll et al.*, 2009; *Shiklomanov*, 2000]. Since the surface water is affected by water quality and climate variability, groundwater has been replaced as the major source of water in many agricultural watersheds. It is estimated that about 600–1100 km^3 of groundwater is abstracted globally every year, between one fifth to one third of the total global freshwater withdrawals [*Döll et al.*, 2009; *Zektser and Lorne*, 2004]. Furthermore, about 20% of the global groundwater abstraction is only utilized for irrigation purpose [*Zektser and Lorne*, 2004]. In humid regions, the groundwater recharge most likely exceeds the groundwater withdrawal and eventually contributes significantly to the river flows. In arid and semi-arid regions, the agricultural sector needs more water during the long growing season. As a result, the groundwater withdrawal frequently exceeds the aquifer recharge due to the absence of other alternative sources of water, leads to the subsequent groundwater depletion [*Siebert et al.*, 2010]. It is estimated that total global groundwater depletion is equivalent to a 12.6 mm rise in sea level since the year of 1900, accounts for more than 6 % of total sea-level rise [*Konikow*, 2011].

The High Plains/Ogallala aquifer (HPA), is known as one of the largest agricultural areas in the world, covers about 450,000 km^2 in parts of eight states (South Dakota, Nebraska, Wyoming, Colorado, Kansas, Oklahoma, New Mexico, and Texas) in the central United States [*Strassberg et al.*, 2009]. The HPA has about 175,000 km^2 of cropland which is about 27 % of irrigated land in United States. In HPA, the access of surface water resources are limited to a few rivers (e.g.,

Platte, Republican, and Arkansas rivers), most likely dominated by internally drained ephemeral lakes or playas (~50,000 playas) because of its extreme flat topography [*Scanlon et al.*, 2012]. However, the groundwater is one of the potential sources of water resource due to the low ratio of precipitation and potential evapotranspiration, and about 30% of all groundwater withdrawal for irrigation in Unites States comes from the HPA [*Dennehy*, 2000]. The substantial uses of groundwater started from ~1950s for irrigation purpose [*Gutentag et al.*, 1984] and a total 330 km^3 of groundwater has been depleted in the period of ~1950s to 2007 [*Scanlon et al.*, 2012]. However, the change of groundwater depletion is not uniform throughout the HPA. If groundwater depletion were uniform, the HPA would decline only an average of ~4m of water table. In reality, the spatial depletion is very localized throughout the HPA. There is much higher depletion in the central and southern HPA, and almost no depletion in the northern part of HPA. As an example, average groundwater depletion is about 11 m in Texas, and about 0.3 m in Nebraska [*Scanlon et al.*, 2012].

There are several approaches to quantify the groundwater depletion using the changes of water level [*McGuire*, 2003; *Faunt et al.*, 2009], water budget [*Kjelstrom*, 1995], pumpage fraction [*Anderson et al.*, 1992] and volume of subsidence [*Kasmarek and Strom*, 2002; *Kasmarek et al.*, 2004]. All of the approaches require different data such as: water level data, groundwater pumping data and volume of subsidence data, which are not always available for ungaged watershed. However, the streamflow and precipitation data are available for the most of the watersheds in the world, providing the opportunity to perform the recession analysis and estimates the aquifer parameters [*Brutsaert and Lopez*, 1998; *Troch et al.*, 1993], evapotranspiration [*Szilagyi et al.*, 2007] and groundwater pumping [*Wang and Cai*, 2009] at the watershed scale.

To describe the recession characteristics of base flow, *Maillet* [1905] used the exponential function of $Q_t = Q_0 \exp(-t/k)$, where Q_t is the streamflow at time t, Q_0 is the initial streamflow,

k is the retention constant represents the average response time in storage. The characteristics of retention constant is different throughout the recession curve, separate the early and late stage of recession. The early stage of recession shows lower retention constant most likely due to the major contribution of the younger groundwater. However, the late stage of recession exhibits higher retention constant due to the significant contribution of older groundwater during the recession. This indicates that the early stage of recession is predominantly linked with the younger groundwater and the late stage of recession is mostly linked with the older groundwater.

The major focus of the study was on estimation of groundwater depletion in the heavily groundwater dependent agricultural watershed. In this study, the agricultural watershed was selected from the part of HPA, where groundwater and streamflow had been depleted extensively as a result of large scale groundwater pumping for irrigation. A conceptual recession model was developed to estimate the groundwater depletion by incorporating the direct human interference (such as groundwater pumping) as well as natural interference (such as evapotranspiration) into the recession analysis. In agricultural watersheds, the early and late recession pattern are unimpaired by the groundwater pumping and evapotranspiration during the winter. However, the early and late recession pattern of hydrograph are greatly influenced by groundwater pumping and evapotranspiration during the crop growing season. The changes of recession patterns of observed hydrographs were simulated with the conceptual model and the pumping rate of groundwater along with the evapotranspiration during the last half century were retrieving using the streamflow data.

4.2   Study and Data Collection

Beaver River Watershed (BRW) is a watershed underlying above the southern HPA, shared by the border of Oklahoma, Texas and New Mexico State as shown in Figure 4.1. It covers partly

the Union county of New Mexico; Cimarron, Texas and Beaver county of Oklahoma State; and Dallam, Sherman and Hansford county of Texas State. The water flows from the east of Union county of New Mexico to the west of Beaver county of Oklahoma and drains approximately 20,700 km^2 of area into the outlet (Latitude 36°49'20" N and 100°31'08" W) at the Beaver River. The climate is semi-arid with an approximately average annual precipitation of 449 mm and annual evapotranspiration of 406.4 mm [*Johnson and Duchon*, 1995]. More than 88% of precipitation occurs from April through September and the growing season for most of the crops falls within this period. The average monthly precipitation can be as high as 70 mm in July and as low as 10 mm in January. The elevation of the watershed varies from 724 m to 2654 m above mean sea level. More than 90% of the watershed falls below the elevation of 1435 m.

Daily streamflow for the period of 1940-2014 was obtained from U.S. Geological Survey (USGS) gage station no. 07234000, and daily precipitation data was obtained from the physical science division of Earth System Research Laboratory (ESRL) of National Oceanic and Atmospheric Administration (NOAA) (http://www.esrl.noaa.gov/psd/data/gridded/data.gpcc.html) for the period of 1948-2006. Considering the overlap of all the available data, this study was focused on the years of 1948-2006. Irrigated groundwater use data were obtained in county level from U.S. Geological Survey (USGS) in every five years for the period of 1985-2005.
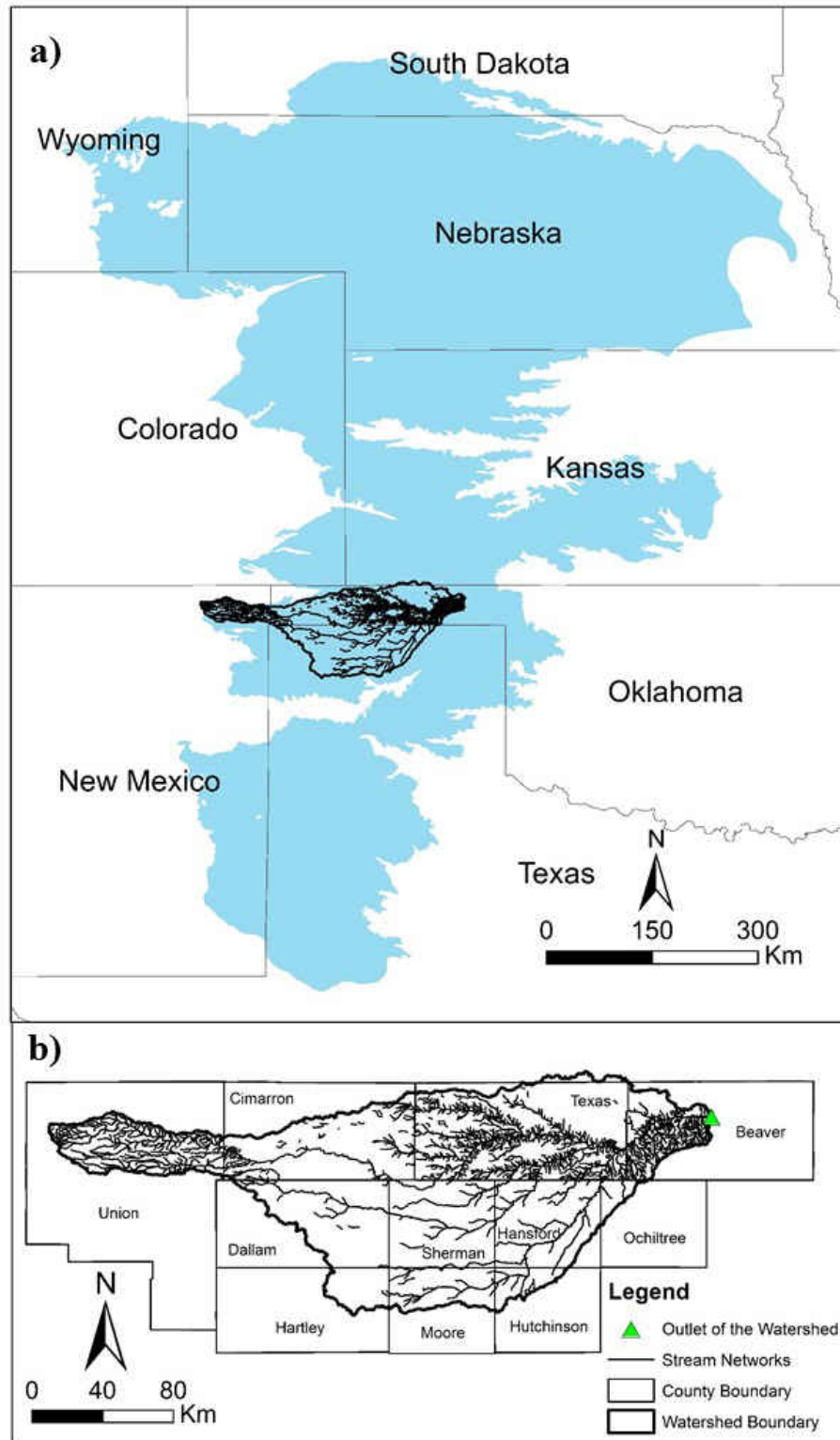
Figure 4.1. The study area a) High Plain Aquifer (HPA) b) Beaver River Watershed (BRW).

4.3   Methodology

4.3.1   Identification of least irrigation and evapotranspiration period

In natural watersheds, the recession has significant seasonal variation, and is usually faster in summer season due to the high evapotranspiration rate [*Wittenberg*, 2003; *Tallaksen*, 1995; *Moore*, 1997; *Wittenberg and Sivapalan*, 1999]. In agricultural watersheds, the recession is faster in summer season because of high groundwater withdrawals in crop growing season [*Wang and Cai*, 2010]. The underlying counties of BRW used more than 90% of total groundwater for irrigation purposes during the period of 1985-2005 [*USGS*, 1985, 1990, 1995, 2000, 2005, 2010]. Therefore, BRW is reasonably considered as an agricultural watershed.   Corn and winter wheat were the major crops of BRW [*USDA*, 2007a, 2007b, 2007c; *USDA*, 2012a, 2012b, 2012c]. Corn was planted at the beginning of April and harvested by early November [*NASS*, 1997, 2010], and April to August was the peak water demand period for corn. Although winter wheat was planted at the middle of September and harvested by the middle of July [*NASS*, 1997, 2010], March to July was the key water demand period for winter wheat. Thus, September to February was considered as the least irrigation season which had trivial effects on recession. In addition, winter season (December, January and February) had also the lowest evapotranspiration effects on recession. Therefore, November to February was reasonably considered as the least irrigation and evapotranspiration period.

4.3.2   Identification of the early and late stage of base flow recession events

The first step for identifying the early and late stage of base flow recession was the least irrigation and evapotranspiration period, was to select the recession events from streamflow data. The starting time of recession is normally determined by the rainfall events or the peak streamflow

after rainfall events. To eliminate the effects of quick flow on the recession analysis, *Brutsaert and Nieber* [1977] selected the recession data at least 5 days after the rainfall events. *Brutsaert and Lopez*, [1998] also found that the early recession analysis was sensitive to the number of days after storms. To determine the earliest onset of base flow, uninterrupted recession flow data starting from the second day after the cessation of rainfall were selected for analysis [*Troch et al.*, 1993; *Brutsaert and Lopez*, 1998; *Parlange et al.*, 2001]. In this study, the recession segment after a rainfall event ≥1 mm were selected for recession analysis and two days of streamflow data after the peak discharge were discarded from the recession segment to avoid the effects of quick flow.

In order to identify the transition of recession, the streamflow (Q_i) and the corresponding time (t_i) were selected for each recession event. The streamflow in ascending order in a recession curve is denoted as Q_i, where i=1, 2, 3,…N, with Q_1 and Q_N being the smallest and largest flow rates, respectively. With respect to the first two data points (Q_1 and Q_2), the computed slope is denoted as S_1. The slope S_i was computed by cumulative regression analysis over the data points of Q_1, Q_2, …… Q_{i+1}. The corresponding goodness-of-fit is denoted as R^2_i. The last slope (S_{N-1}) was computed by regression over all the data points of the individual recession curve. The transition point (i^*) of recession from early to late stages was identified by the trend of slope and goodness-of-fit: 1) for $i \geq i^*$, S_i increases continuously; and 2) goodness-of-fit declines abruptly from $R^2_{i^*}$ to $R^2_{i^*+1}$.

4.3.3 *Quantification of Evapotranspiration and Groundwater Depletion*

Maillet [1905] first used the exponential decay function to describe the recession characteristics of base flow which was mainly originate from Boussinesq's nonlinear differential equation. It implies that that the aquifer behaves like a single linear reservoir with storage, S (mm), linearly proportional to outflow, Q_s (mm day^{-1}):

$$S=k. Q_s \qquad (4.1)$$

where S (mm) is the amount of groundwater storage in the aquifer, Q_s (mm day^{-1}) is the amount of groundwater hydraulically connected with the streams and k (day) is the retention constant which can be considered to represent average response time in storage.

Incorporating the groundwater pumping and evapotranspiration, the water balance equation is written as:

$$-\frac{dS}{dt} = (Q_s + Q_p + Q_{et}) \qquad (4.2)$$

where Q_{et}(mm day^{-1}) is the groundwater evapotranspiration loss, and Q_p (mm day^{-1}) is the groundwater pumping rate from the aquifer.

The total streamflow during the recession stage is the sum of the groundwater hydraulically connected with the streams, effluent discharge and the water withdrawal from the stream networks:

$$Q=Q_s + Q_e - Q_r \qquad (4.3)$$

where, Q_e (mm day^{-1}) is the effluent discharge and Q_r (mm day^{-1}) is the water withdrawal from the stream networks.

The effluent discharge is considered to be a function of the groundwater pumping

$$Q_e= (1\text{-}\beta) \, Q_p \qquad (4.4)$$

where β is the consumption rate of human water withdrawal. The value of β is normally larger in agricultural watershed and assumed close to 1.

BRW is an agricultural watershed and the surface water withdrawal from the stream networks is very trivial compared to the groundwater withdrawal [*Scanlon et al.*, 2012; *USGS*, 1985, 1990, 1995, 2000, 2005, 2010], the β is assumed to be 1 and Q_r is considered as zero.

Considering (4.3) and (4.4), substituting (4.1) into (4.2),

$$-\frac{dQ}{dt} = -\frac{dQ_s}{dt} = \frac{1}{k}(Q_s + Q_p + Q_{et}) \tag{4.5}$$

Integrating both side of equation (4.5) from t to t_0, the base flow is obtained by assuming constant pumping and evapotranspiration rates during the recession event.

$$Q_t = (Q_{t0} + Q_p + Q_{et})e^{-\frac{\Delta t}{k}} - (Q_p + Q_{et}) \tag{4.6}$$

where Q_t is the base flow at time t and Q_{t0} is the base flow at t_0. If k_1 (day) and k_2 (day) are the retention constant during the early and late stage of recession, respectively. Q_{p1}(mm day^{-1}) and Q_{p2}(mm day^{-1}) are comparatively younger and older groundwater pumping rate associated with the early and late stage of recession during the recession period. The base flow during the early stage of recession can be written as:

$$Q_t = (Q_{t0} + Q_{p1} + Q_{et})e^{-\frac{\Delta t}{k_1}} - (Q_p + Q_{et}) \tag{4.7}$$

Additionally, the base flow during the late stage of recession can be written as:

$$Q_t = (Q_{t0} + Q_{p2} + Q_{et})e^{-\frac{\Delta t}{k_1}} - (Q_p + Q_{et}) \tag{4.8}$$

As the recession curve becomes straight line for the logarithms of Q value, k_1 (day) and k_2 (day) can be determined easily as an inverse of the early and late stage of recession slope from the plot

of ln(Q) versus t, represented by m_1 (day^{-1}) and m_2 (day^{-1}), respectively. Therefore, base flow during the early stage of recession can be expressed as:

$$Q_t = \left(Q_{t0} + Q_{p1} + Q_{et}\right)e^{-m_1 \Delta t} - \left(Q_p + Q_{et}\right) \qquad (4.9)$$

The base flow during the late stage of recession can be expressed as:

$$Q_{t+\Delta t} = \left(Q_{t0} + Q_{p2} + Q_{et}\right)e^{-m_2 \Delta t} - \left(Q_p + Q_{et}\right) \qquad (4.10)$$

4.4   Results and Discussion

4.4.1   Streamflow under direct human interference

The uses of groundwater for irrigation purpose began from ~1950s which significantly changes the hydrological behaviors of the watershed by depleting the groundwater and altering the streamflow characteristics. In order to determine the temporal variation of hydrological behavior, a double mass curve is plotted between one hydrologic variable which is less affected by human interference and another variable significantly affected by human interference. The direct runoff is relatively impacted by the anthropogenic activities whereas precipitation unlike direct runoff is little affected by human activities. Considering these two variables, Figure 4.2 shows a double mass plot of cumulative precipitation and direct runoff data at the outlet of BRW during the period of 1948-2006. The slope of the double mass curve is represented by runoff ratio (R) which is the ratio of cumulative direct runoff and cumulative precipitation and the slope is 0.7 %, and 0.07%, respectively during the years of 1948-1972 and 1973-2006. Based on the ratio, the data has been reasonably split into 1948-1969 (pre-1970s) and 1970-2006 (post-1970s) to quantify the hydrological and agricultural changes over time.
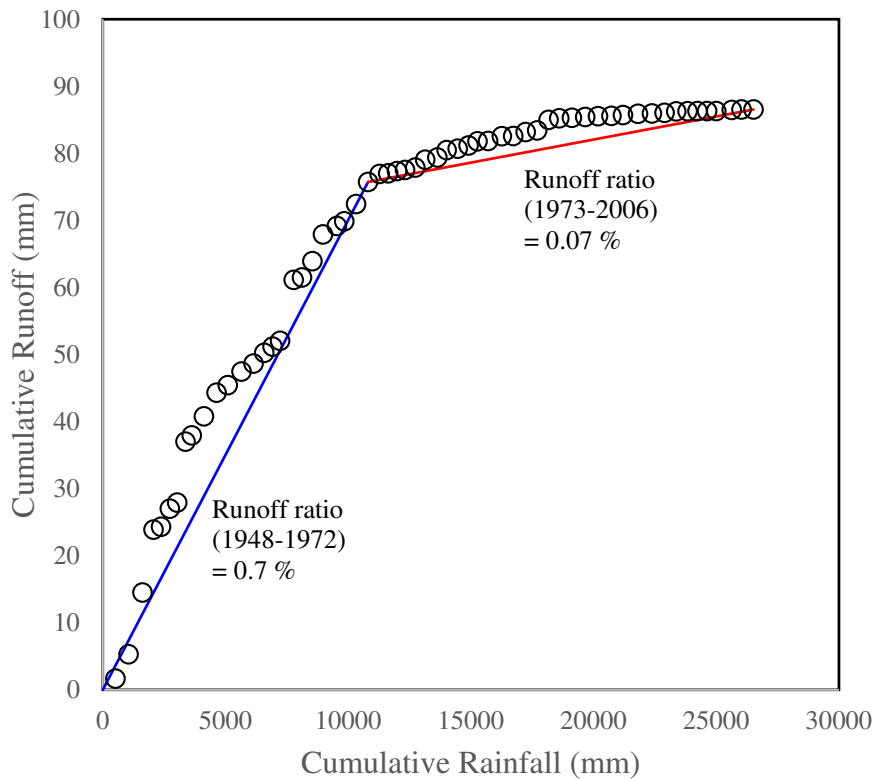
Figure 4.2. Cumulative precipitation and direct runoff for 1948-2006 for BRW.

The changes of streamflow under human interferences can be understood comprehensibly through the percentiles analysis of streamflow and flow duration curve as shown in Figure 4.3. As a demonstration, Figure 4.3a shows the 1st, 10th, 50th, 90th and 99th percentiles of the streamflow at the outlet of BRW. During the last 58 years, the high flow (Q99 and Q90) and low flow (Q10, Q1) had been decreased significantly as shown in Figure 4.3a. However, the changes of low flow (Q10, Q1) was more significant and variable due to the positioning of BRW in the temperature dry climate, characterized by high inter-annual precipitation variability and significant zero flow. In addition, the mean of the median flow (Q50) also demonstrated a similar decreasing trend of high flow with significant variability. Figure 4.3b shows the comparison of flow duration curve at the outlet of BRW during the period of pre-1970s to post-1970s. The average high flow (Q1 and Q10)

59

had declined by 88% and 76%, respectively between these two periods. However, the average

median flow (Q50) decreased more significantly from 0.001775 mm day^{-1} to 0.0000627 mm day^{-1} between pre-1970s to post-1970s, which was about 96% less than the period of pre-1970s. The

minimum nonzero flow for pre-1970s and post-1970s was 0.0000095 mm day^{-1} and 0.0000012

mm day^{-1}, respectively. In addition, nonzero flow had about 78% exceedance probability which

represents that stream networks dry out almost evenly during these two periods.
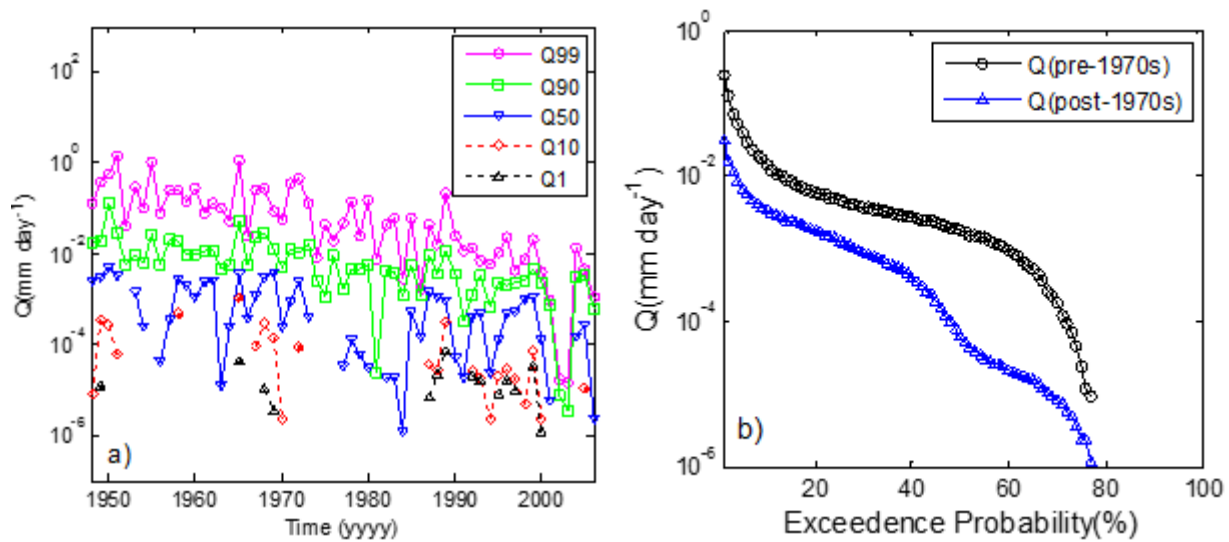
Figure 4.3. a) the 1st, 10th, 50th, 90thand 99th percentiles of the streamflow b) the flow duration curve during the period of pre-1970s and post-1970s at the outlet of BRW.

The changes of streamflow and the flow components under agricultural development is

shown in Figure 4.4. As shown in Figure 4.4a, the annual streamflow varied from 15.42 mm day^{-1} in 1950 to 0.00045 mm day^{-1} in 2003. The mean annual streamflow declined significantly from

4.83 mm day^{-1} to 0.89 mm day^{-1} from pre-1970s to post-1970s. The streamflow also become less

variable in post-1970s compared to pre-1970s. To understand the behavior of flow components

under agricultural development, the streamflow has divided into three components: the overland

flow, subsurface flow and base flow. The base flow has longer travel time, less susceptible with

climate variability. On the other hand, overland flow and subsurface flow have shorter travel time

60

and more subjected to climate variability. To separate the base flow from the streamflow, one parameter low pass filtering method with a filter parameters of 0.925 was used in this study [*Sivapalan et al.*, 2011]. The temporal changes of base flow index (BFI, ratio of the base flow and streamflow) during the period of 1948-2006 is shown in Figure 4.4. The annual BFI ranged from 0.16 in 1981 to 0.87 in 2005. The annual BFI changed from 0.38 to 0.56 in the period of pre-1970s to post-1970s. The conversion of natural grassland to irrigated cropland led to the decreases of the slow components due to the depletion of aquifer discharge by pumping.
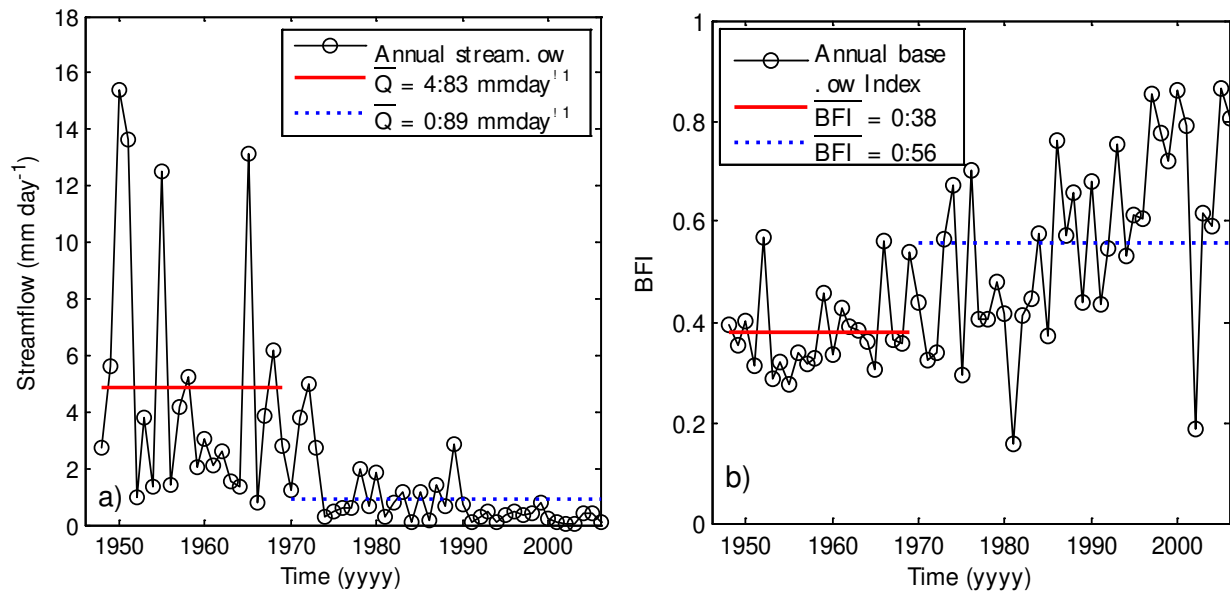
Figure 4.4. The annual changes of a) streamflow (Q) and b) base flow index (BFI) during the period of pre-1970s and post-1970s.

Along with the temporal changes of streamflow and other flow components, the seasonal variability of streamflow was also observed in BRW. Figure 4.5 shows the monthly distribution of streamflow by every decade during the period of 1950-2006, (the monthly change of streamflow in 1948 and 1949 is not considered here). The results shows that the average monthly streamflow declines more significantly in post-1970s compared to pre-1970s. The consistent and less fluctuate streamflow distribution were observed during the month of November to February in every decade

61

from 1950s to 2000s as shown in Figure 4.5, and it reasonably supported November to February as the least irrigation and evapotranspiration period. As shown in Figure 4.5, the streamflow was started to decline during the month of September to October in 1970s and similar trend was also exhibited in 1990s and 2000s, considering that 1970s was the beginning of the extensive irrigation period.
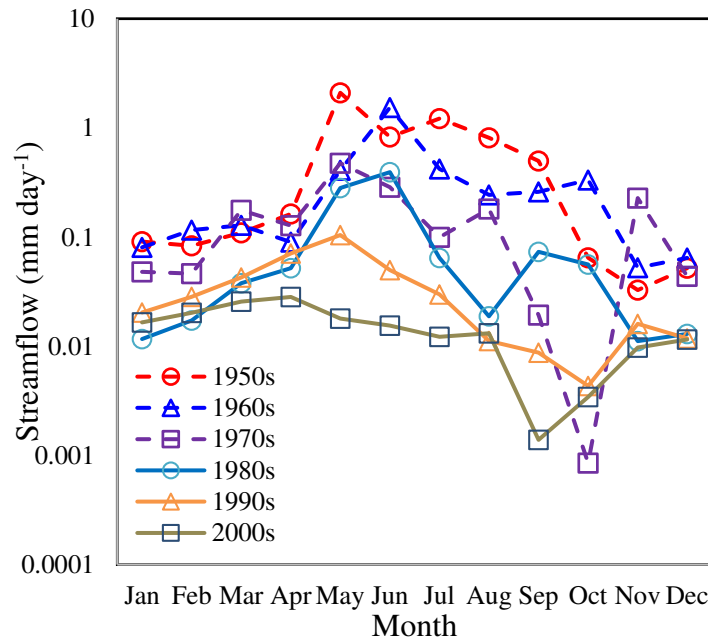
Figure 4.5. Monthly changes of streamflow averaged by decades

4.4.2   *Recession curves under least irrigation and evapotranspiration period*

Evapotranspiration, surface water withdrawal and groundwater withdrawals significantly change the recession curves. In this study, the surface water withdrawal was neglected and consider only the groundwater withdrawals (i.e., groundwater pumping) along with the evapotranspiration was considered. As discussed before, the evapotranspiration and groundwater pumping had negligible effects on recession curve during November to February. Therefore, the recession slope (both early and late stage of recession) was first calculated during November to February. In order to identify the early and late stage of recession, a total of three recession events

with a distinct transition during the period of November to February, were selected for recession

analysis as shown in Table 4.1.

Table 4.1. The start and end dates for the selected recession events along with their early and late recession slopes with distinct transition point.

Serial No	t_s (mm/dd/yyyy)	t_e (mm/dd/yy hh)	Q_0 (mm day^{-1})	m_1 (day^{-1})	m_2 (day^{-1})
1	02/18/1950	02/26/1950	0.0034	0.08	0.05
2	01/19/1951	01/26/1951	0.0066	0.19	0.03
3	12/20/1958	12/27/1958	0.0031	0.12	0.03

Note: the start time of recession analysis (t_s); the end time of recession analysis (t_e); the transition flow from early to late recessions (Q_0); the slope of the early recession stage (m_1); and the slope of the late recession stage (m_2).

The transition from early recession to late recession (Q_0) was identified by conducting a recession slope curve analysis of individual recession event. A constructive pair of recession slope data for a recession event on 01/19/1950 is shown in Figure 4.6. The data points for large and small value of streamflow follow straight line with different slope in semi log scale, separated by the identified transition flow plotted as dash line in Figure 4.6a. Figure 4.6b shows the corresponding slope and coefficient of determination (R^2) from the cumulative regression analysis of recession in ascending order of discharge value. The transition from early to late recession is marked by a red dot in Figure 4.6b with a corresponding transition of flow 0.0066 mm day^{-1} determined when the regression slope increase continuously and R^2 decreases abruptly with the increases of discharge. The slope of the late recession stage (m_2) varies from 0.03 to 0.05 as shown in Table 4.1. Therefore, the highest value of m_2 (0.05) was considered as a threshold to separate the early and late stage of recession. The recession slope greater than 0.05 day^{-1}, and less than or equal to 0.05 day^{-1} were considered as early and late recession slope, respectively. Forty four recession events were selected for analyzing the early and late recession as shown in Table 4.2.
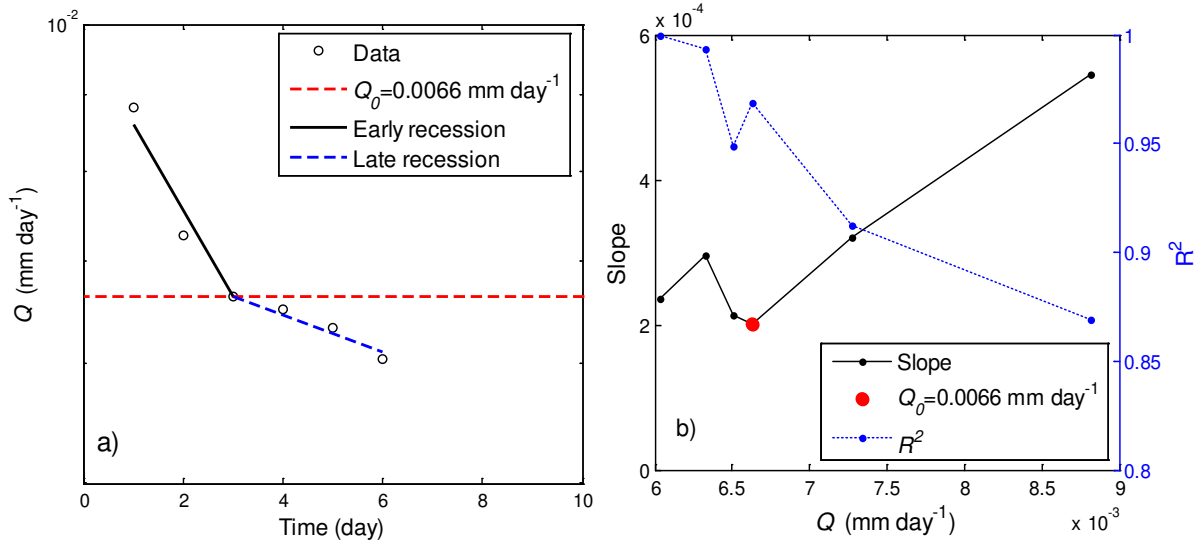
Figure 4.6. Transition of base flow recession, the slope and R^2 of the cumulative regression analysis for recession events on 03/01/1949 (a, b).

Table 4.2. Characteristic values and estimated recession parameters for the forty one recession events

Serial No	t_s (mm/dd/yyyy)	t_e (mm/dd/yyyy)	Q_{t0} (mm day^{-1})	m_1 (day^{-1})	m_2 (day^{-1})
01	01/08/1948	01/21/1948	0.0059	0.11	
02	11/04/1948	11/11/1948	0.0059	0.31	
03	12/01/1948	12/09/1948	0.0052	0.10	
04	11/08/1949	11/14/1949	0.0030	0.15	
05	11/28/1949	12/04/1949	0.0035	0.07	
06	02/19/1949	02/26/1949	0.0078		0.05
07	02/18/1950	02/22/1950	0.0049	0.08	
	02/22/1950	02/26/1950	0.0034		0.05
08	01/19/1951	01/22/1951	0.0098	0.19	
	01/22/1951	01/26/1951	0.0066		0.03
09	01/07/1953	01/17/1953	0.0059	0.26	
10	01/28/1953	02/11/1953	0.0020		0.03
11	01/31/1954	02/09/1954	0.0040		0.05
12	02/19/1958	02/26/1958	0.0066	0.33	
13	12/20/1958	12/24/1958	0.0047	0.12	
	12/24/1958	12/27/1958	0.0031		0.03
14	02/10/1959	02/21/1959	0.0059	0.08	
15	02/26/1963	03/06/1963	0.0041		0.03
16	02/19/1960	02/25/1960	0.0054	0.38	
17	11/13/1960	11/21/1960	0.0024	0.07	
18	02/10/1961	02/18/1961	0.0092	0.13	
19	01/09/1963	01/15/1963	0.0034	0.53	

Serial No	t_s (mm/dd/yyyy)	t_e (mm/dd/yyyy)	Q_{t0} (mm day^{-1})	m_1 (day^{-1})	m_2 (day^{-1})
20	01/27/1968	02/05/1968	0.0046	0.08	
21	11/24/1968	12/11/1968	0.0050		0.02
22	01/13/1969	01/22/1969	0.0054		0.02
23	11/25/1971	12/02/1971	0.0196	0.09	
24	12/15/1971	12/25/1971	0.0083		0.02
25	01/19/1972	01/27/1972	0.0060	0.07	
26	02/14/1972	02/23/1972	0.0039	0.06	
27	11/10/1981	11/20/1981	0.0000	0.09	
28	02/10/1984	02/15/1984	0.0000	0.16	
29	11/24/1985	11/30/1985	0.0008	0.08	
30	12/06/1985	12/14/1985	0.0014	0.25	
31	12/21/1985	12/26/1985	0.0006		0.04
32	10/17/1987	10/22/1987	0.0019	0.12	
33	01/26/1988	02/02/1988	0.0028		0.04
34	02/14/1988	02/21/1988	0.0025		0.05
35	01/28/1993	02/10/1993	0.0021		0.02
36	02/25/1998	03/03/1998	0.0011		0.03
37	11/13/1998	11/22/1998	0.0024	0.05	
38	02/02/1999	02/22/1999	0.0020		0.02
39	02/10/2005	02/19/2005	0.0045		0.03
40	11/28/2004	12/05/2004	0.0038		0.04
41	02/24/2005	03/15/2005	0.0035		0.01

Note: the start time of recession analysis (t_s); the end time of recession analysis (t_e); the initial streamflow (Q_{t0}); the slope of the early recession stage (m_1); and the slope of the late recession stage (m_2).

Figure 4.7a and Figure 4.7c shows the trends of m_1 and m_2, respectively in the period of 1948-2006. The m_1 was as high as 0.53 in 1963 and as low as 0.05 in 1998. The range of m_2 varied from 0.01 in 2005 to 0.05 in 1949. Figure 4.8b and 4.8d illustrates the frequency distribution of observed m_1 and m_2, respectively from November to February during the period of 1948-2006. The result shows that the highest frequency of m_1 was observed in the range of 0.050-0.1. Therefore, m_1=0.075 was selected as the best value when groundwater pumping and evapotranspiration had least effect on recession analysis. In addition, the highest frequency distribution of m_2 was observed in the range of 0.02-0.04, thus, m_2=0.03 was selected as the best

value while groundwater pumping and evapotranspiration have lowest effects on recession analysis.
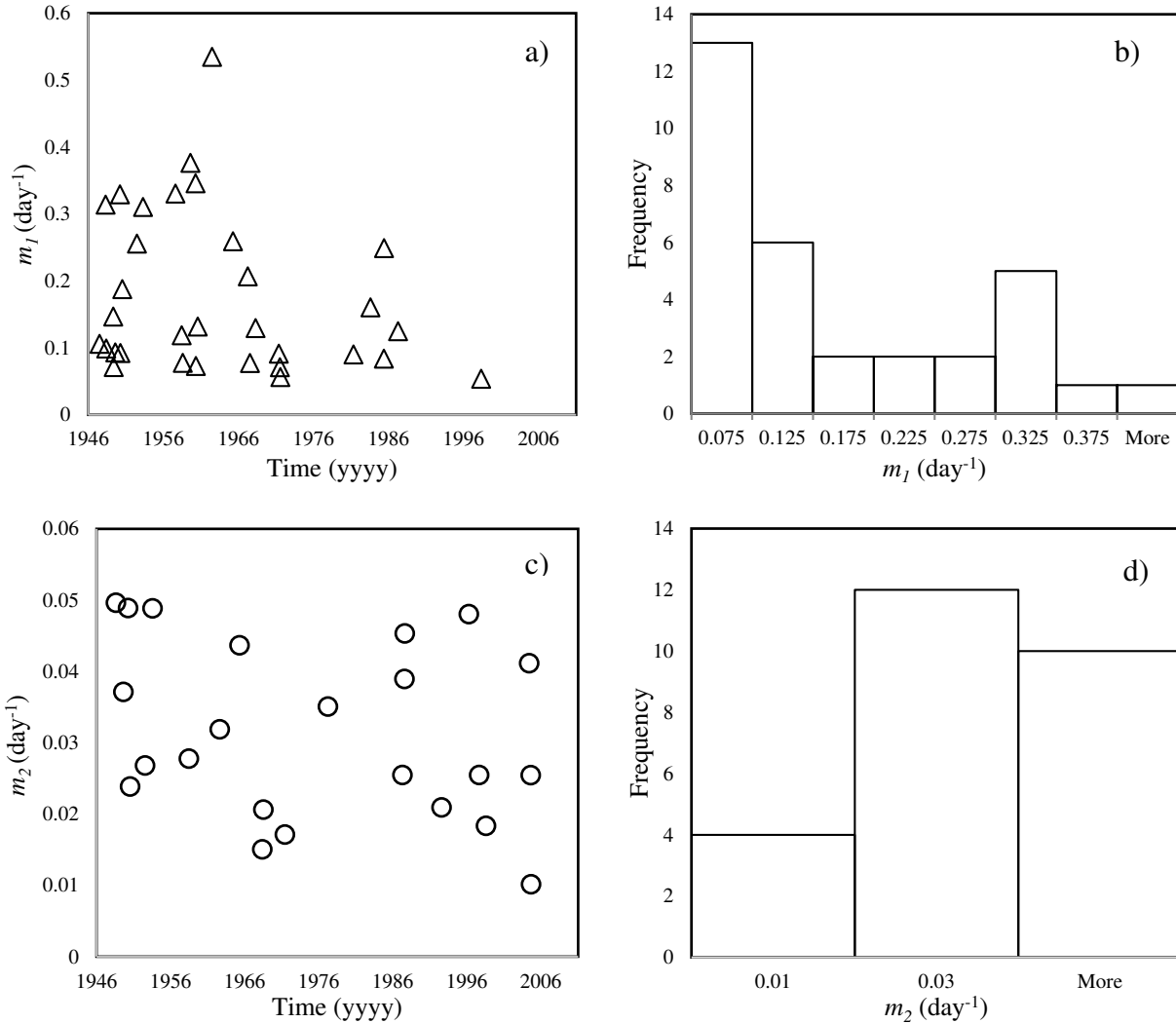
Figure 4.7. The trends of a) m_1 and c) m_2, and the frequency distribution of b) m_1 and d) m_2 from November to February during the period of 1948-2006.

4.4.3   *Estimation of human interference given streamflow recession*

As discussed before, the evapotranspiration and shallow groundwater pumping rate ($Q_{et+}Q_{p1}$) can be estimated by fitting the equation (4.9) for given initial streamflow (Q_{t0}) and slope of early recession (m_1), minimizing the root mean square error between the observed streamflow recession curve and simulated streamflow recession curve from equation (4.9). In addition, the

66

evapotranspiration and deep groundwater pumping rate ($Q_{et+Q_{p2}}$) can be also quantified by fitting the equation (4.10) for given initial streamflow (Q_{t0}) and slope of late recession (m_2). The estimated $Q_{et+Q_{p1}}$ associated with recession curve are shown in Figure 4.8a-4.8d in the selected years.

Q_{t0}=0.0025 mm day^{-1} $Q_{et+Q_{p1}}$=0.001 mm day^{-1} $\quad$ Q_{t0}= 0.0040 mm day^{-1}, $Q_{et+Q_{p1}}$=0.002 mm day^{-1}

Q_{t0}=0.0045 mm day^{-1}, $Q_{et+Q_{p1}}$=0.0045 mm day^{-1} $\quad$ Q_{t0}=0.0020 mm day^{-1}, $Q_{et+Q_{p1}}$=0.0002 mm day^{-1}
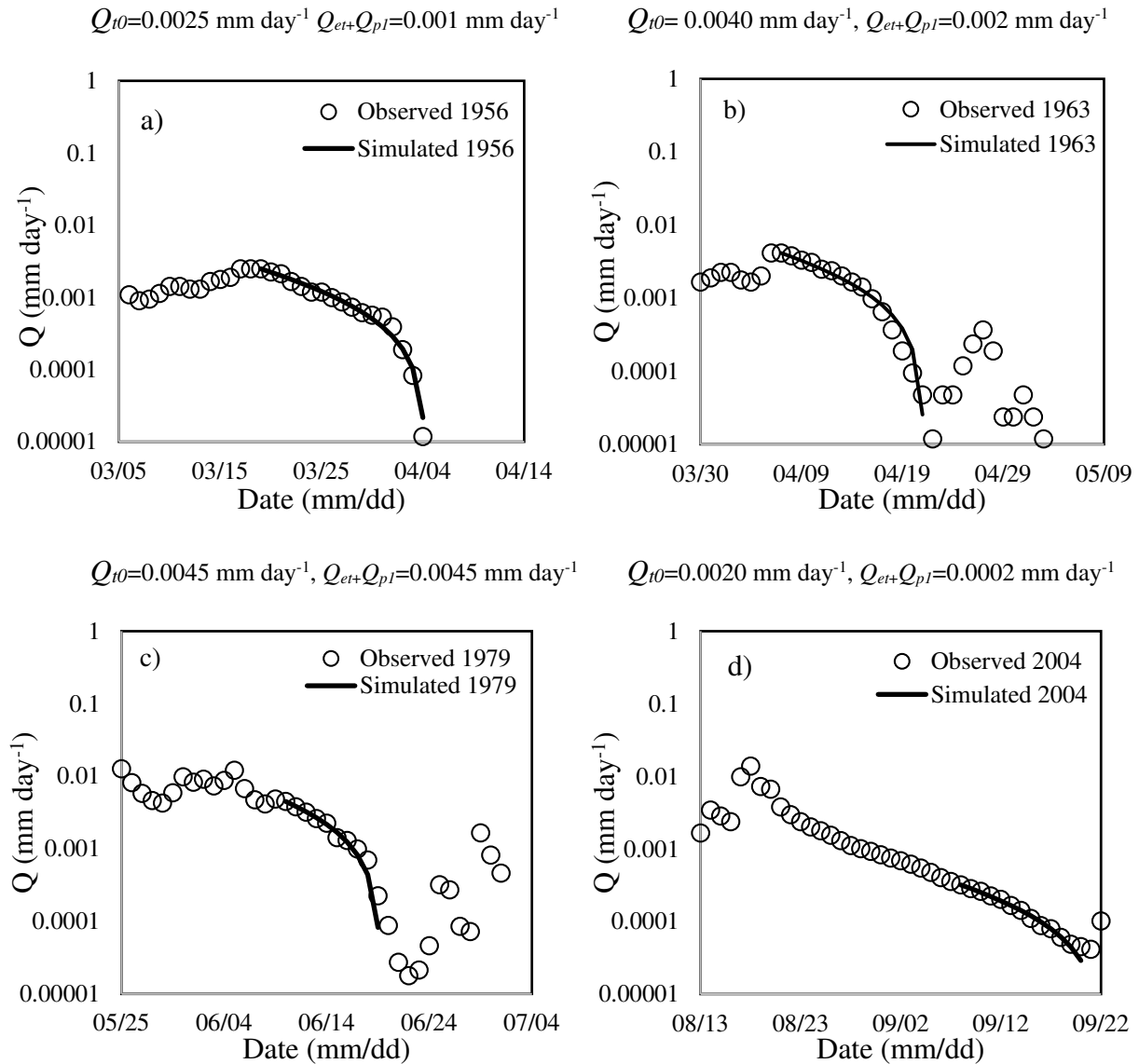
Figure 4.8. Streamflow recession during the selected year: a) 1956, b) 1963, c) 1979 and d) 2004.

The low flow (Q10, Q5) and median flow (Q50) decreased significantly during the period of 1948-2006. The initial streamflow (Q_{t0}) for different recession events could also decline significantly during the period of 1948-2006, might underestimate the value of evapotranspiration and groundwater pumping rate as shown in Figure 4.9. In Figure 4.9, an observed recession event in June, 1979 was compared with the same recession event multiplying by a factor of 0.1. Therefore, the initial streamflow for the new recession event moved from 0.0045 mm day^{-1} to 0.00045 mm day^{-1}. As a result, the value of $Q_{et}+Q_{pl}$, calculated by fitting equation (4.9), also reduced from 0.0045 mm day^{-1} to 0.00045 mm day^{-1}.
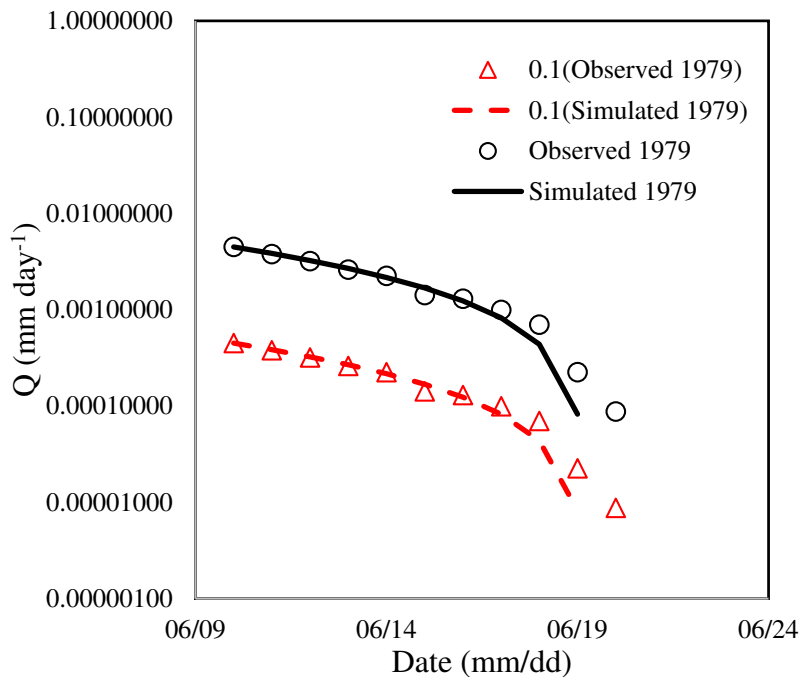
Figure 4.9. Effect of initial streamflow on the estimation of evapotranspiration and groundwater pumping rate.

In order to compare these two recession events, the recession events with same initial streamflow could be selected to perform the recession analysis. However, recession events starting with the same initial streamflow was difficult to find because of the decreasing trends of streamflow. Therefore, all of the recession were normalized with a certain initial value. The

average initial streamflow for early and late recession were 0.0137 mm day^{-1} and 0.0019 mm day^{-1}, respectively during the period of 1948-2006. All the early recession events were multiplied with the ratio of average initial streamflow and observed initial streamflow (Q_{t0}) for early recession to normalize the early recession events to a certain initial value. The similar step was also applied for late recession events. The $Q_{et}+Q_{p1}$ and $Q_{et}+Q_{p2}$ are calculated using equation (4.9) and (4.10), respectively to compare with the observed irrigated groundwater uses as shown in Figure 4.10. The Figure 4.10a shows the observed irrigated groundwater uses in the underlying counties of BRW during the period of 1985 to 2010. The $Q_{et}+Q_{p1}$ estimated from the recession analysis during the period of 1985-2006 are shown in Figure 4.10b. The irrigated groundwater uses is increased significantly from 1985, reached to peak at 1995 and started to decline again after 1995. The computed $Q_{et}+Q_{p1}$ as shown in Figure 4.10b was consistent with observed irrigated groundwater uses. However, there was not enough late recession data during 1985-2006 to compute the trend of $Q_{et}+Q_{p2.}$
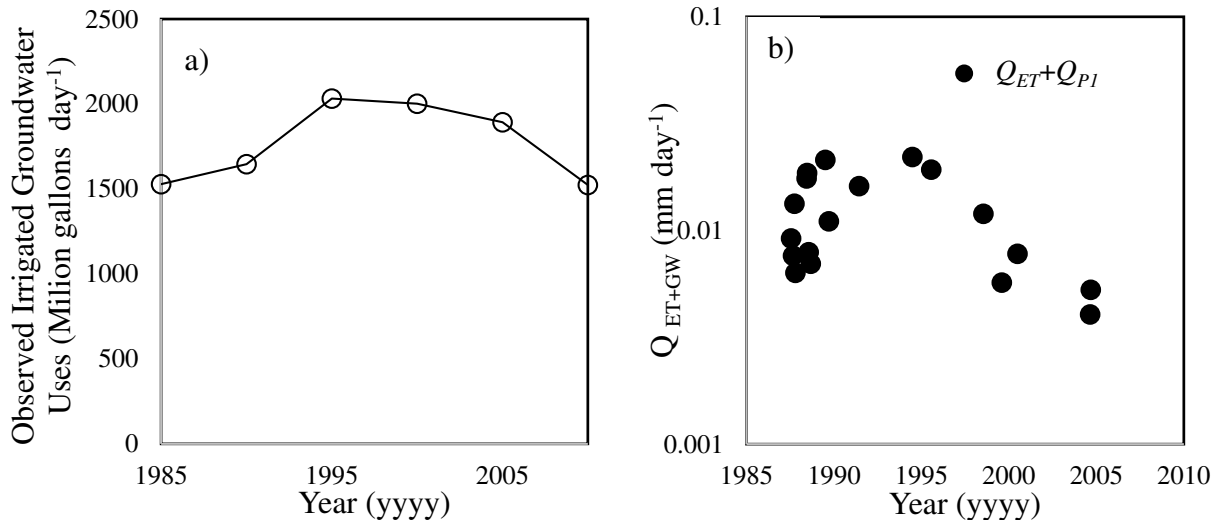
Figure 4.10. a) observed irrigated groundwater uses underlying the counties of BRW in the period of 1985-2010 b) computed groundwater pumping rate along with ET estimated from the recession analysis during the period of 1985-2006.

4.5   Summary and Conclusion

Direct human interference, especially the groundwater pumping significantly affected the flow recession process. The changes of groundwater pumping altered the dynamic of low-flow regime in an agricultural watershed. Using a case study in BRW located in well studied HPA, this study presented a method where recession analysis was extended to incorporate the human interference especially the groundwater pumping in agricultural watershed. During the period of 1948-2006, the groundwater pumping in the area caused significant decreases in low flow (Q1 and Q10) magnitude by 88% and 76%.

The groundwater pumping is usually difficult to estimate in ungagged station. The model proposed in this study can be used to estimate the groundwater pumping for given streamflow, precipitation and evapotranspiration data. However, the deep groundwater pumping is quite difficult to estimate when late stage of recession is unavailable.

It should be noted that several sources of uncertainty exists on the estimation of shallow and deep groundwater pumping. First, the identification of the starting time of the recession event can affect the recession result. Second, the average value of the initial streamflow may not be stationary, depends on the selection criteria of the recession events. Third, the human interference such as shallow and deep groundwater pumping may change day to day whereas it is considered constant during recession. Fourth, the fluctuation of streamflow during long dry period has a significant uncertainty of estimation of recession parameter.

4.6   References

Anderson, T. W., G. W. Freethey, and P. Tucci (1992), Geohydrology and water resources of alluvial basins in south-central Arizona and parts of adjacent states, US Government Printing Office, *United States Geological Survey Professional Paper 1406-B*, 77 pp.

Brutsaert, W., and J. L. Nieber (1977), Regionalized drought flow hydrographs from a mature glaciated plateau, *Water Resources Research*, *13*(3), 637-643.

Brutsaert, W., and J. P. Lopez (1998), Basin-scale geohydrologic drought flow features of riparian aquifers in the Southern Great Plains, *Water Resources Research*, *34*(2), 233-240.

Dennehy, K. (2000), High Plains Regional Ground Water Study. US Geological Survey Fact Sheet FS 091–00, *United States Geological Survey Fact Sheet FS-091-00,* 6 pp.

Döll, P., K. Fiedler, and J. Zhang (2009), Global-scale analysis of river flow alterations due to water withdrawals and reservoirs, *Hydrology and Earth System Science*, *13*(12), 2413-2432.

Faunt, C., R. Hanson, K. Belitz, W. Schmid, S. Predmore, D. Rewis, and K. McPherson (2009), Numerical Model of the Hydrologic Landscape and Groundwater Flow in California's Central Valley, in "Groundwater Availability of the Central Valley Aquifer, California," edited by Faunt, CC, *United States Geological Survey Professional Paper 1766*, 225 pp.

Gutentag, E. D., F. J. Heimes, N. C. Krothe, R. R. Luckey, and J. B. Weeks (1984), Geohydrology of the High Plains aquifer in parts of Colorado, Kansas, Nebraska, New Mexico, Oklahoma, South Dakota, Texas, and Wyoming, *United States Geological Survey Professional Paper 1400-B*, 66 pp.

Johnson, H. L., and C. E. Duchon (1995), *Atlas of Oklahoma climate*, University of Oklahoma Press Norman.

Kasmarek, M. C., and J. L. Robinson (2004), Hydrogeology and simulation of ground-water flow and land-surface subsidence in the northern part of the Gulf Coast aquifer system, Texas, *United States Geological Survey Scientific Investigations Report 2004-5102*, 111 pp.

Kasmarek, M. C., and W. Eric (2002), Hydrogeology and simulation of ground-water flow and land-surface subsidence in the Chicot and Evangeline aquifers, Houston area, Texas, *United States Geological Survey Water-Resources Investigations Report 02-4022*.

Kjelstrom, L. C. (1995), Streamflow gains and losses in the Snake River and ground-water budgets for the Snake River Plain, Idaho and eastern Oregon, *United States Geological Survey Professional Paper 1408-C*, 47 pp.

Konikow, L. F. (2011), Contribution of global groundwater depletion since 1900 to sea-level rise, *Geophysical Research Letters*, *38*, L17401*,* doi:10.1029/2011GL048604*.*

Lapworth, D. J., A. M. MacDonald, G. Krishan, M. S. Rao, D. C. Gooddy, and W. G. Darling (2015), Groundwater recharge and age-depth profiles of intensively exploited groundwater resources in northwest India, *Geophysical Research Letters*, *42,* doi:10.1002/2015GL065798.

Maillet, E. T. (1905), *Essais d'hydraulique souterraine & fluviale*, A. Hermann.

McGuire, V. L. (2003), Water-level changes in the High Plains aquifer, predevelopment to 2001, 1999 to 2000, and 2000 to 2001, *United States Geological Survey Fact Sheet 078-03*.

Moore, R. D. (1997), Storage-outflow modelling of streamflow recessions, with application to a shallow-soil forested catchment, *Journal of Hydrology*, *198*(1–4), 260-270.

NASS, U. (2010), Field Crops: Usual Planting and Harvesting Dates, *USDA National Agricultural Statistics Service, Agricultural Handbook 628*.

NASS, U. (1997), Field Crops: Usual Planting and Harvesting Dates for U.S. Field Crops, *USDA National Agricultural Statistics Service, Agricultural Handbook 628*.

Parlange, J. Y., F. Stagnitti, A. Heilig, J. Szilagyi, M. B. Parlange, T. S. Steenhuis, W. L. Hogarth, D. A. Barry, and L. Li (2001), Sudden drawdown and drainage of a horizontal aquifer, *Water Resources Research*, *37*(8), 2097-2101.

Scanlon, B. R., C. C. Faunt, L. Longuevergne, R. C. Reedy, W. M. Alley, V. L. McGuire, and P. B. McMahon (2012), Groundwater depletion and sustainability of irrigation in the US High Plains and Central Valley, *Proceedings of the national academy of sciences*, *109*(24), 9320-9325.

Shiklomanov, I. A. (2000), Appraisal and assessment of world water resources, *Water international*, *25*(1), 11-32.

Siebert, S., J. Burke, J.-M. Faures, K. Frenken, J. Hoogeveen, P. Döll, and F. T. Portmann (2010), Groundwater use for irrigation–a global inventory, *Hydrology and Earth System Sciences*, *14*(10), 1863-1880.

Sivapalan, M., M. A. Yaeger, C. J. Harman, X. Xu, and P. A. Troch (2011), Functional model of water balance variability at the catchment scale: 1. Evidence of hydrologic similarity and space-time symmetry, *Water Resources Research*, *47*, W02522, doi:10.1029/2010WR009568.

Strassberg, G., B. R. Scanlon, and D. Chambers (2009), Evaluation of groundwater storage monitoring with the GRACE satellite: Case study of the High Plains aquifer, central United States, *Water Resources Research*, *45*, W05410, doi:10.1029/2008WR006892.

Swana, K. A., J. A. Miller, A. S. Talma, T. H. Darrah, M. Butler, and K. Fifield (2015), Comparing the Residence Time of Deep vs Shallow Groundwater in the Karoo Basin, South Africa using 3H, 14C, 36Cl and 4He Isotopes, *Procedia Earth and Planetary Science*, *13*, 215-218.

Szilagyi, J., Z. Gribovszki, and P. Kalicz (2007), Estimation of catchment-scale evapotranspiration from baseflow recession data: Numerical model and practical application results, *Journal of Hydrology*, *336*(1–2), 206-217.

Tallaksen, L. M. (1995), A review of baseflow recession analysis, *Journal of Hydrology*, *165*(1–4), 349-370.

Troch, P. A., F. P. De Troch, and W. Brutsaert (1993), Effective water table depth to describe initial conditions prior to storm rainfall in humid regions, *Water Resources Research*, *29*(2), 427-434.

USDA (2007a), 2007 Census of Agriculture, New Mexico State and County Data http://www.agcensus.usda.gov/Publications/2007/Full_Report/Volume_1,_Chapter_2_Co unty_Level/New_Mexico/st35_2_001_001.pdf

USDA (2007b), 2007 Census of Agriculture, Oklahoma State and County Data http://www.agcensus.usda.gov/Publications/2007/Full_Report/Volume_1,_Chapter_2_Co unty_Level/Oklahoma/st40_2_001_001.pdf

USDA (2007c), 2007 Census of Agriculture, Texas State and County Data http://www.agcensus.usda.gov/Publications/2007/Full_Report/Volume_1,_Chapter_2_Co unty_Level/Texas/st48_2_001_001.pdf

USDA (2012a), 2012 Census of Agriculture, New Mexico State and County Data

http://www.agcensus.usda.gov/Publications/2012/Full_Report/Volume_1,_Chapter_2_Co

unty_Level/New_Mexico/st35_2_001_001.pdf

USDA (2012b), 2012 Census of Agriculture, Oklahoma State and County Data

http://www.agcensus.usda.gov/Publications/2012/Full_Report/Volume_1,_Chapter_2_Co

unty_Level/Oklahoma/st40_2_001_001.pdf

USDA (2012c), 2012 Census of Agriculture, Texas State and County Data

http://www.agcensus.usda.gov/Publications/2007/Full_Report/Volume_1,_Chapter_2_Co

unty_Level/Texas/st48_2_001_001.pdf

USGS (1985), County Level Water Use Data for New Mexico, Oklahoma and Texas State in 1985,

http://waterdata.usgs.gov/nwis/wu

USGS (1990), County Level Water Use Data for New Mexico, Oklahoma and Texas State in 1990,

http://waterdata.usgs.gov/nwis/wu

USGS (1995), County Level Water Use Data for New Mexico, Oklahoma and Texas State in 1995,

http://waterdata.usgs.gov/nwis/wu

USGS (2000), County Level Water Use Data for New Mexico, Oklahoma and Texas State in 2000,

http://waterdata.usgs.gov/nwis/wu

USGS (2005), County Level Water Use Data for New Mexico, Oklahoma and Texas State in 2005,

http://waterdata.usgs.gov/nwis/wu

USGS (2010), County Level Water Use Data for New Mexico, Oklahoma and Texas State in 2010,

http://waterdata.usgs.gov/nwis/wu

Wang, D., and X. Cai (2009), Detecting human interferences to low flows through base flow

recession analysis, *Water Resources Research*, *45*, W07426, doi:10.1029/2009WR007819.

Wang, D., and X. Cai (2010), Comparative study of climate and human impacts on seasonal baseflow in urban and agricultural watersheds, *Geophysical Research Letters*, *37*, L06406, doi:10.1029/2009GL041879.

Wittenberg, H. (1999), Baseflow recession and recharge as nonlinear storage processes, *Hydrological Processes*, *13*(5), 715-726.

Wittenberg, H. (2003), Effects of season and man-made changes on baseflow and flow recession: case studies, *Hydrological Processes*, *17*(11), 2113-2123.

Wittenberg, H., and M. Sivapalan (1999), Watershed groundwater balance estimation using streamflow recession analysis and baseflow separation, *Journal of hydrology*, *219*(1), 20-33.

Zektser, I. S., and E. Lorne (2004), Groundwater resources of the world: and their use, in *IhP Series on groundwater*, edited, Unesco.

CHAPTER 5: QUANTIFYING CHANGES OF SPRINGSHED AREA AND NET RECHARGE THROUGH RECESSION ANALYSIS OF SPRING FLOW

5.1 Introduction

A spring is any natural situation where groundwater naturally flows to the land surface or into a body of surface water. Shallow water springs can be classified based on their outlet types, such as depression springs, contact springs, artesian springs, and karst springs. A depression spring is formed when the upper surface of the saturation zone intersects the land surface. Similarly, a contact spring is formed when the accumulated water in porous rock overlying impervious material contacts the land surface. In contrast, an artesian spring is formed through a fissure in the rock of a confined aquifer and its overlying confining units. Karst aquifer systems contain conduits formed by dissolution that permit rapid transport of groundwater to the land surface [*Huntoon*, 1995]. Karst springs with large magnitudes of flow provide great environmental and economic values such as water supply and tourism [*Goldscheider*, 2012].

Spring recession analysis has been utilized for estimating aquifer characteristics [*Amit et al.*, 2002]. *Fiorillo* [2014] provided comprehensive reviews of karst spring recession focused on analytical, numerical, and physical models. Various empirical and analytical models have been proposed to fit the recession limb of spring hydrographs [*Padilla et al.*, 1994], similar to streamflow recession. *Mangin* [1975] fitted the early recession curve as a non-exponential component and the late recession curve as an exponential component for a spring. *Baedke and Krothe* [2001] divided the karst spring recession into an early stage associated with conduit flow, a late stage associated with diffused flow, and an intermediate stage which utilizes a combination of conduit and diffused flows. However, the hydrograph shape of spring recession varies with

spring systems due to the variability of hydrogeological settings and climate characteristics [*Atkinson*, 1977].

Several conceptual models incorporating the geometric and hydraulic characteristics of aquifers have been developed for spring hydrograph recession [*Kresic*, 2006]. Particularly, Darcy, Torricelli, and Poiseuille models have been developed for recession curves for karst springs [*Fiorillo*, 2011; *Fiorillo et al.*, 2012]. In the Darcy model, the groundwater drains freely from a tank reservoir to the spring pool through a sand filled conduit system. In the Torricelli model, groundwater drains freely from a tank reservoir to the spring pool through a large conduit system with negligible frictional head loss through the conduit. In this model, the effects of spring pool altitude on spring flow are neglected. In the Poiseuille model, the conduit area is considered too small to neglect the effects of viscosity. The effects of recharge on the spring flow are neglected in all of the above models.

The main objective of this study was to extend the existing Torricelli model incorporating of the impacts of net recharge and spring pool altitude. The net recharge is defined as recharge minus groundwater pumping and evapotranspiration. The structure of the study area and the methodological approach are discussed in Sections 5.2 and 5.3.

5.2   Silver Springs

Silver Springs, located about 9 km east of Ocala in Central Marion County, is one of the largest magnitude springs in central Florida with a historical flow of 21 m^3/s prior to the year 2000 [*Osburn et al.*, 2002]. Silver Springs forms the headwater of the Silver River, which is the largest tributary of the Ocklawaha River [*Rosenau et al.*, 1977]. Silver Springs is a well-known tourist attraction due to its naturally clear water, aquatic wildlife, and famous glass bottom boats [*Samek*,

2004; *King*, 2004; *Walsh et al.*, 2009]. Agriculture is the dominant land use within the springshed. Recently, the area has experienced rapid population growth and the surrounding rural area has become attractive for urban development [*Phelps*, 2004].

Silver Springs consists of several large springs including the Main Spring, the Abyss, the Blue Grotto, and numerous smaller springs. The Main Spring contains an interconnected cave system and a matrix system controlled by regional fracture. The flow system of the Silver Springs results from groundwater flow through convergent conduits in deep and shallow aquifers [*Knowles et al.*, 2010]. The spring flow is primarily supported by 300-460 m thick limestone in the Upper Floridian Aquifer (UFA).

Delineation of the groundwater basin (i.e., springshed) was mainly based on the potentiometric head of the aquifer. However, the boundary of the springshed may change seasonally due to the temporal variation of potentiometric head. The springshed shown in Figure 5.1 was delineated from a 100 year capture zone, and resulted in an area of approximately 2,240 km^2 [*SJRWMD,* 2013].

The climate in the Silver Springs region is humid and subtropical. The mean annual air temperature is 21.8 °C with average maximum and minimum temperatures of 28.7 °C and 15.0 °C, respectively. The average annual precipitation is 1290 mm. Winters are mild and dry, and summers are hot and rainy. More than 58 percent of the precipitation occurs from June through October. Monthly precipitation can be as high as 188 mm in June and as low as 54 mm in November [*NOAA*, 2010].

Daily hydroclimatic data including spring flow, spring pool altitude, groundwater head, and precipitation were obtained at the gage stations shown in Figure 5.1. Daily spring flow for the period of 1933-2012 was obtained from U.S. Geological Survey (USGS) gage station no.

02239501, and daily groundwater head in the UFA for the period of 1969-2012 was obtained from the St. Johns River Water Management District (SJRWMD) at the observation well of M-0028. Daily spring pool altitude was recorded at USGS station 02239500 from 1947-2012. The spring flow station is located 500 m from the main spring pool. The distance between the spring pool altitude gage and the observation well is 4855 m. All elevations are referenced to the North American Vertical Datum of 1988 (NAVD88).
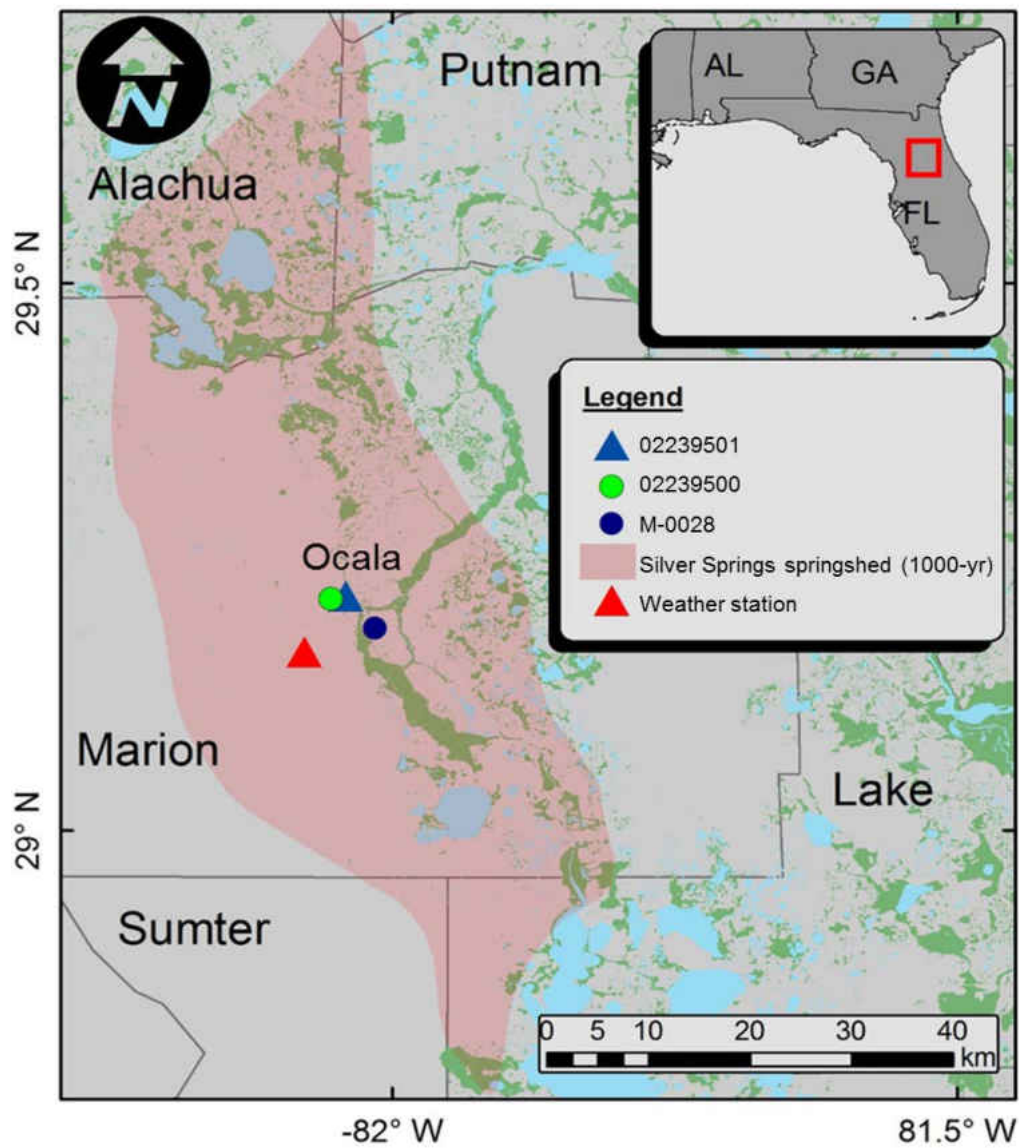
Figure 5.1. The springshed of Silver Springs, and the gage stations for spring flow, spring pool altitude, groundwater head, and weather station.

Daily precipitation data for 1965-2012 was obtained from NOAA's (National Oceanic and Atmospheric Administration) National Climatic Data Center (NCDC). Considering the overlap of all the available data, this study was focused on the years of 1970-2012. Figure 5.2 shows the mean monthly values of groundwater head, spring pool altitude, and spring flow. The peak groundwater head and peak flow occured in October with two recession periods for spring flow (October to February and April to June). An abrupt drop in flow of Silver Springs was observed near year 2000 (Figure 5.3a). The average flow for 1970-1999 was 21.5 m^3/s and declined to 14.7 m^3/s from 2000-2012. Also, after 2000, the groundwater head in the observation well dropped from 12.74 m to 12.60 m (Figure 5.3b). As shown in Figure 5.3c, the spring pool altitude increased from 11.77 m to 12.01 m post-2000 due to the growth of submerged exotic and native vegetation and backwater effects from the Silver River [*SJRWMD*, 2012]. The average difference of groundwater head and spring pool altitude declined from 0.90 m to 0.60 m as shown in Figure 5.3d, which directly caused the decline of spring flow.
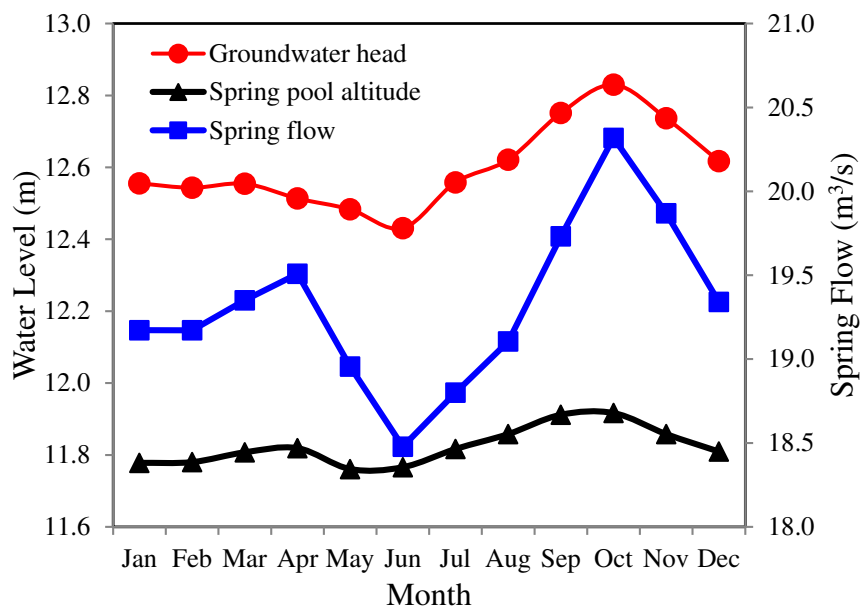
Figure 5.2. The mean monthly values of groundwater head, spring pool altitude, and spring flow during the period of 1970-2012.
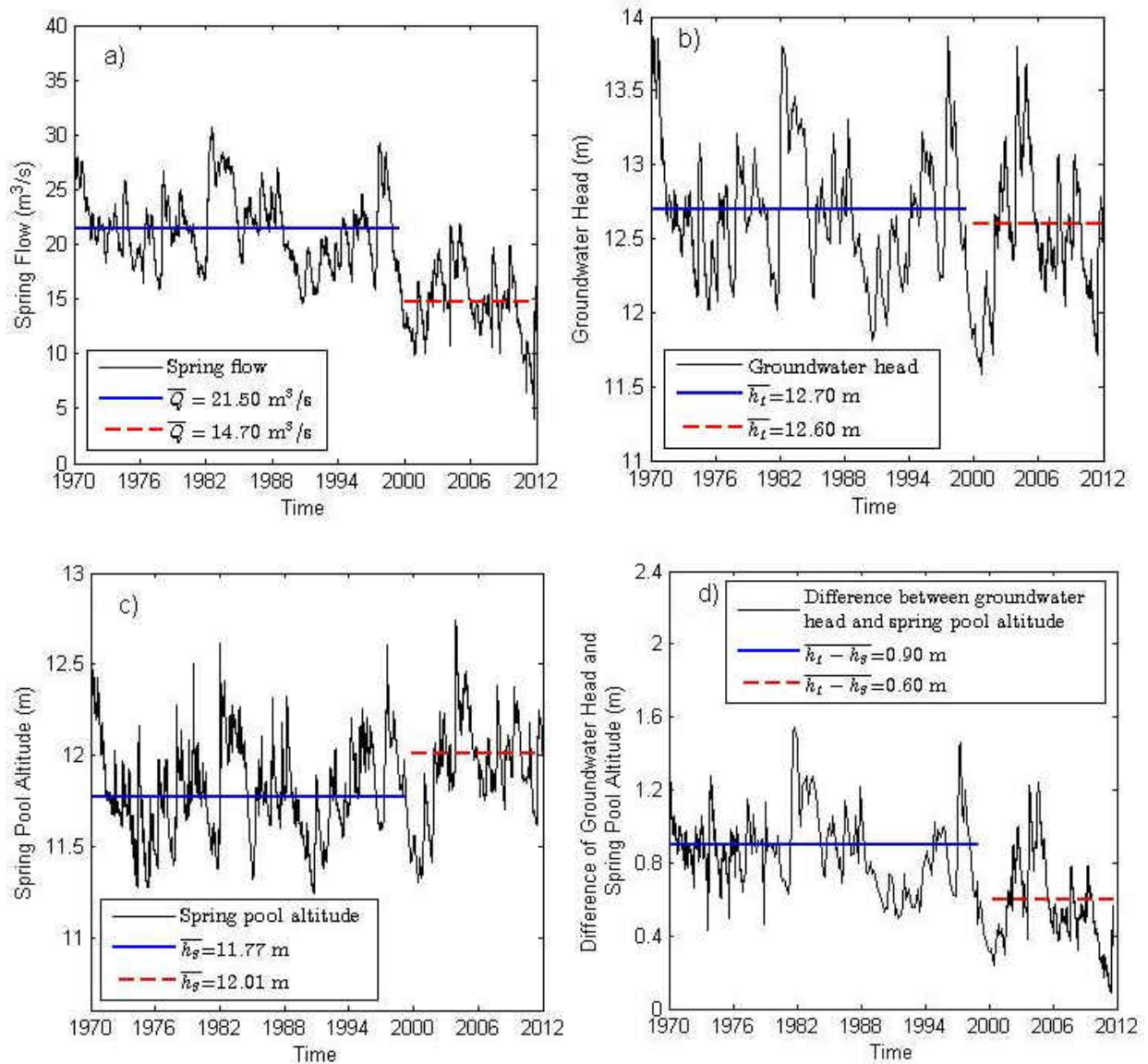
Figure 5.3. Daily a) spring flow, b) groundwater head, c) spring pool altitude, and d) groundwater head and spring pool altitude difference from Silver Springs and their average values during the periods of 1970-1999 and 2000-2012, respectively.

In this study, a spring recession model was developed incorporating of spring pool altitude

and the impacts of net recharge into the existing Torricelli model. The spring recession model was

applied to Silver Springs in order to estimate the effective springshed area and the net recharge

based on the changes in recession slope of spring flow, groundwater head, and spring pool altitude.

The results of the updated Torricelli model allow further assessment of the contributions to the declined flow of Silver Springs during recession periods.

5.3   **Methodology**

5.3.1   *Spring Recession Model*

In this study, the conceptual Torricelli model (Figure 5.4) includes a tank reservoir with area A_1, groundwater head h_1, and a conduit located at the bottom of the tank [*Fiorillo*, 2011]. The Torricelli model was extended to include the spring pool altitude, denoted as h_3, and the head (h_{nr}) from net recharge. The conduit was assumed to be filled with water. The water in the tank reservoir drained to the spring pool through a single conduit with a cross sectional area A_2. The path between the tank reservoir and the spring pool was considered constant with no other sources of recharge along the conduit section. The extended Torricelli model is a lumped conceptual representation of the complex physical system. The static head from the tank reservoir was converted to velocity and pressure heads when water flows into the conduit system and was reverted back to the static head when water enters the spring pool. The size of the spring pool was large enough to assume negligible velocity in the spring pool.
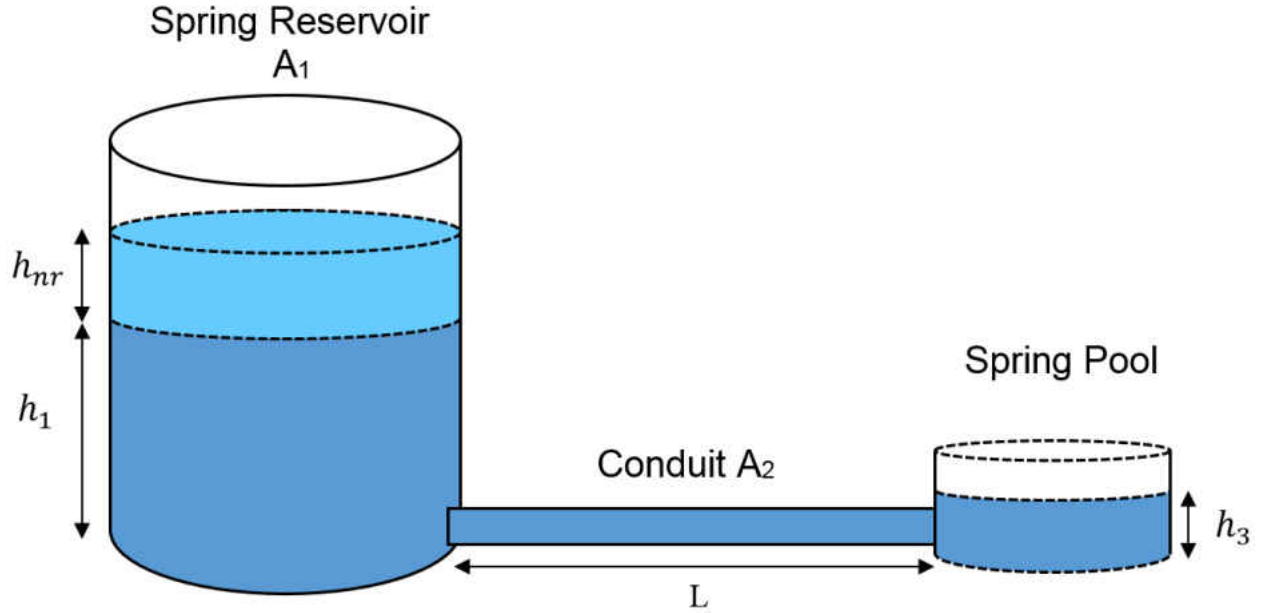
Figure 5.4. The Torricelli (linear) recession model (solid line) and the extended Torricelli (nonlinear) recession model considering spring pool altitude and the impact of net recharge (i.e., recharge minus groundwater pumping and evapotranspiration).

The energy equation between the reservoir and spring pool is written as:

$$h_1 + h_{nr} = h_3 + h_f \tag{5.1}$$

where, h_f is the head loss between the tank reservoir and spring pool. Differentiating the equation (1) in terms of time results in,

$$\frac{dh_1}{dt} + \frac{dh_{nr}}{dt} = \frac{dh_3}{dt} + \frac{dh_f}{dt} \tag{5.2}$$

where $-\frac{dh_1}{dt}$ is the recession slope of the groundwater head; $\frac{dh_{nr}}{dt}$ is the change of head due to the net recharge; and $-\frac{dh_3}{dt}$ is the recession slope of the spring pool altitude. From the principle of conservation of mass, the spring flow into the spring pool must be equal to the water storage variation in the tank reservoir. Therefore:

$$-A_1 \frac{dh_1}{dt} + Q_{nr} = Q \tag{5.3}$$

where Q is the spring flow into the spring pool (m³/d); Q_{nr} is the net recharge rate (m³/d), the difference between recharge and groundwater pumping, which can be represented by:

$$Q_{nr} = -A_1 \frac{dh_{nr}}{dt} \tag{5.4}$$

The spring flow changes from laminar to turbulent as groundwater approaches the spring pool, and the Darcy-Weisbach equation was used to account for such groundwater head loss [*Sepúlveda*, 2009]. From this, head loss in the conduit was computed as $h_f = f \frac{Lv_2^2}{2gD_2}$, where f is a dimensionless friction factor; L is the total length of flow path in the conduit system; v_2 is the velocity in the conduit; D_2 is the diameter of the conduit; and g is gravitational acceleration. Substituting $v_2 = Q/A_2$ and $D_2 = \sqrt{4A_2/\pi}$ into the head loss equation and differentiating the head loss equation in terms of time, one obtains:

$$\frac{dh_f}{dt} = f \frac{\sqrt{\pi}LQ}{2gA_2^{2.5}} \frac{dQ}{dt} \tag{5.5}$$

where $-\frac{dQ}{dt}$ is the recession slope of the spring flow. If the groundwater head and spring pool altitude decline with constant rates (i.e., $-\frac{dh_1}{dt} = C$ and $-\frac{dh_3}{dt} = D$, substituting equations (3), (4) and (5) into equation (2), one obtains:

$$A_1 = \frac{Q}{(D - f \frac{\sqrt{\pi}LQ}{2gA_2^{2.5}} \frac{dQ}{dt})} \tag{5.6}$$

After computing A_1, the net recharge can be computed as $Q_{nr} = Q - A_1 C$, from equation (3). The springshed area of Silver Springs was solved for given values of Q, D, f, L, $\frac{dQ}{dt}$ and A_2. The values of C and D were estimated from linear regression analysis based on the observed groundwater head and the spring pool altitude, respectively. The values of spring flow recession slopes were also estimated from linear regression analysis based on the observed spring flow. To predict the flow of Silver Springs, *Sepúlveda*, [2009] developed a nonlinear model based on the

85

Darcy-Weisbach equation. Groundwater head, spring pool altitude, and a constant value of D_2 (11 m) were incorporated into the model, i.e., $Q = A_2 K_e \sqrt{\frac{h_f}{L}}$, in which K_e is the effective hydraulic conductivity. The effective hydraulic conductivity (K_e) and the Reynolds number (R_e) for the conduit flow between the spring pool and the nearest groundwater observation well of CE-76 (close to M-0028) were estimated as 14.4 m/s and 2×10^6, respectively [*Sepúlveda*, 2009]. From the Darcy-Weisbach equation with the parameter f, flow was computed as $Q = A_2 \sqrt{\frac{2gD_2}{f} \cdot \frac{h_f}{L}}$. Comparing these two equations for spring flow, one obtains $f = \frac{2gD_2}{K_e^2}$; and substituting K_e and D_2 into the equation, f was computed as 1.04. The magnitude of f was comparable to other Karst springs in Mendip Hills, England [*Atkinson*, 1977] and River Rise, Florida [*Martin*, 2003].

5.4 Results and Discussion

In consideration of the seasonal variation of spring flow, recession events beginning in October were selected (Figure 5.2). A total of 22 events with varied durations between 24 to 260 days were selected for the recession analysis. The start dates and end dates for all of the recession events are shown in Table 5.1.

Table 5.1. The start and end dates for the selected recession events along with their recession slopes for groundwater head, spring pool altitude and spring flow.

Index	Start Date	End Date	Recession Slope of Groundwater Head, C (m/d)	Recession Slope of Spring Pool Altitude, D (m/d)	Recession Slope of Spring Flow (m³/s/d)
1	10/31/70	01/12/71	0.0068	0.0033	0.0473
2	10/07/74	02/15/75	0.0049	0.0026	0.0439
3	10/01/76	11/09/76	0.0037	0.0027	0.0461
	11/10/76	12/03/76	0.0033	0.0010	0.0345
4	10/01/78	12/31/78	0.0057	0.0034	0.0388
5	10/16/82	01/19/83	0.0080	0.0030	0.0459
6	10/19/83	12/11/83	0.0028	0.0020	0.0232
7	10/01/84	06/06/85	0.0040	0.0025	0.0303
8	10/01/88	06/18/89	0.0040	0.0020	0.0296
8	10/08/89	12/17/89	0.0033	0.0022	0.0190
10	10/01/90	12/25/90	0.0021	0.0015	0.0228
11	10/01/91	02/21/92	0.0034	0.0018	0.0253
12	10/20/98	01/25/99	0.0046	0.0020	0.0385
13	10/01/00	11/22/00	0.0022	0.0019	0.0232
	11/23/00	03/12/01	0.0022	0.0015	0.0119
14	10/20/02	11/13/02	0.0037	0.0028	0.0120
15	10/21/03	01/10/04	0.0046	0.0024	0.0235
	01/11/04	02/18/04	0.0030	0.0015	0.0175
16	10/22/04	03/24/05	0.0058	0.0031	0.0291
17	10/05/05	10/31/05	0.0050	0.0026	0.0389
	11/01/05	12/17/05	0.0043	0.0013	0.0314
18	10/01/06	11/05/06	0.0032	0.0019	0.0224
	11/06/06	12/08/06	0.0032	0.0019	0.0123
19	11/01/07	01/25/08	0.0037	0.0030	0.0138
20	10/10/08	02/09/09	0.0052	0.0033	0.0354
	02/10/09	05/11/09	0.0039	0.0018	0.0398
21	10/16/09	11/21/09	0.0043	0.0028	0.0287
22	10/01/10	01/02/11	0.0045	0.0027	0.0348

5.4.1 *Recession slopes of groundwater head and spring pool altitude*

The recession slope of groundwater head (C) and the slope of spring pool altitude (D) were estimated for each recession event from a linear regression based on the observed daily value of groundwater head and spring pool altitude. Recession events were identified based on the duration of a constant recession slope, dividing events into early and late stages when slopes changed. To demonstrate this, Figure 5.5 shows groundwater head and spring pool altitude for the recession event starting on 10/10/2008. The value of C was 0.0052 m/d for the early stage and 0.0039 m/d for the late stage (Figure 5.5a); and the value of D was 0.0033 m/d for the early stage and 0.0018 m/d for the late stage (Figure 5.5b). Among the 22 events, C varied from 0.0021 to 0.0080 m/d, and D ranged from 0.0010 to 0.0034 m/d (Table 5.1). C was greater than D for all of the recession events. As highlighted in Table 5.1, the values of C or D declined from early to late stages for 6 recession events; and the declining rate of D was greater than that of C. For the event starting on 10/01/1976, C declined by 11% from 0.0037 at the early stage to 0.0033 at the late stage; while D declined by 63% from 0.0027 at the early stage to 0.0010 at the late stage.
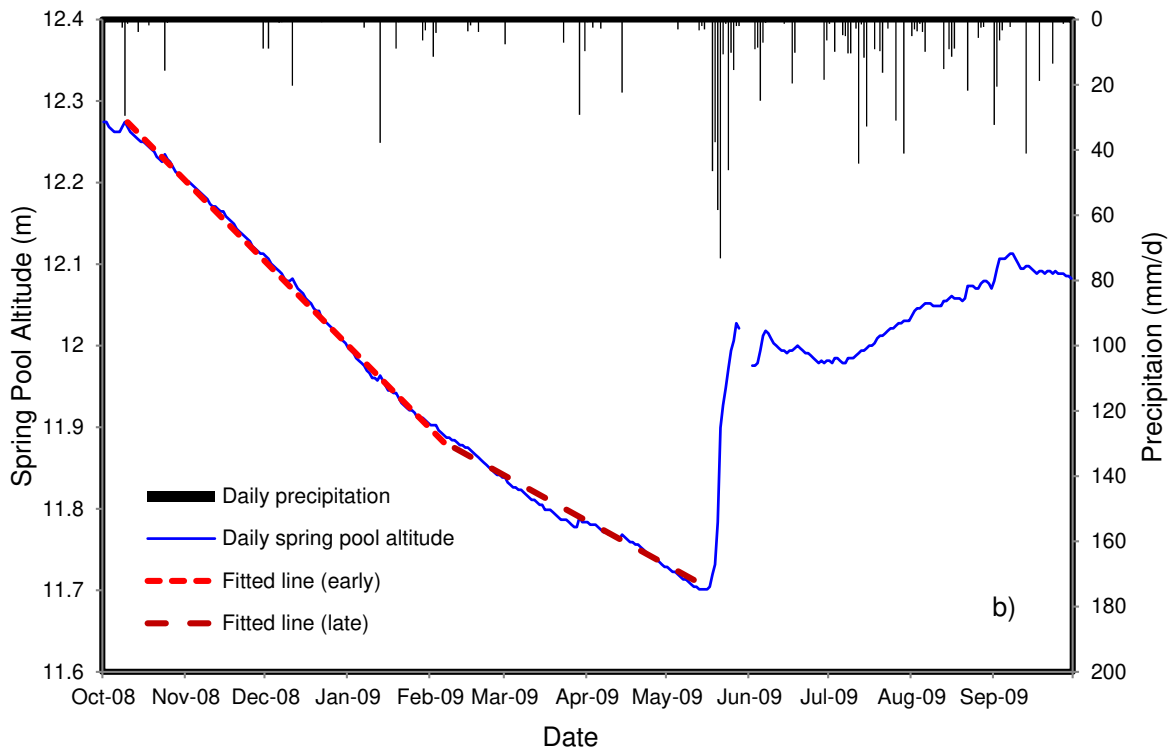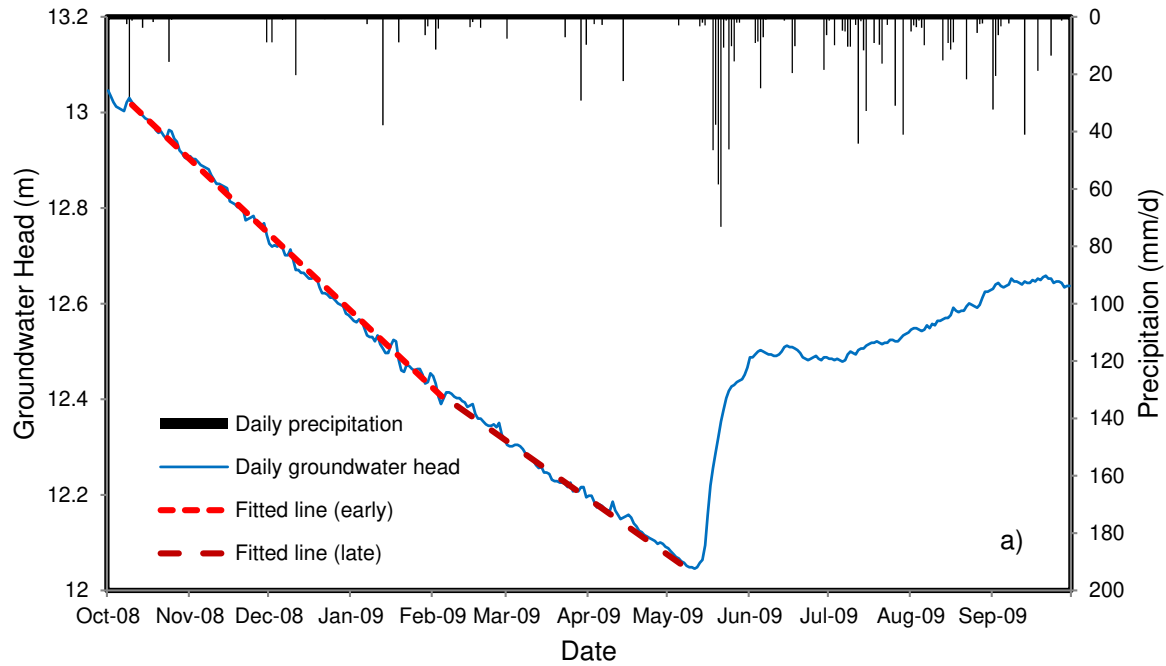
Figure 5.5. a) daily groundwater head and the estimated recession slope of groundwater head C=0.0052 m/d (early stage) and C=0.0039 m/d (late stage) and b) daily spring pool altitude and the recession slope of spring pool altitude D=0.0033 m/d (early stage) and D=0.0018 m/d (late stage) for a recession event during 10/10/2008 - 05/11/2009 as shown in Table 5.1.

The computed values of C and D for all the selected recession events during the period of 1970-2010 are plotted in Figure 5.6. C and D declined from 1970 to 1990, were stable from 1991 to 1999; and increased after 2000., C and D increased. The springshed area A_1 decreases as D increases, as equation (5.6) shows. Therefore, the increasing trend of D post-2000 contributed to the reduction of springshed area. The increase of spring pool altitude and its recession slope was predominantly influenced by the growth of submerged aquatic vegetation and the backwater effect from the Silver River [*SJRWMD*, 2012]. Since net recharge was computed from $Q - A_1 C$, reduced net recharge could contribute to the increasing trend of C post-2000.
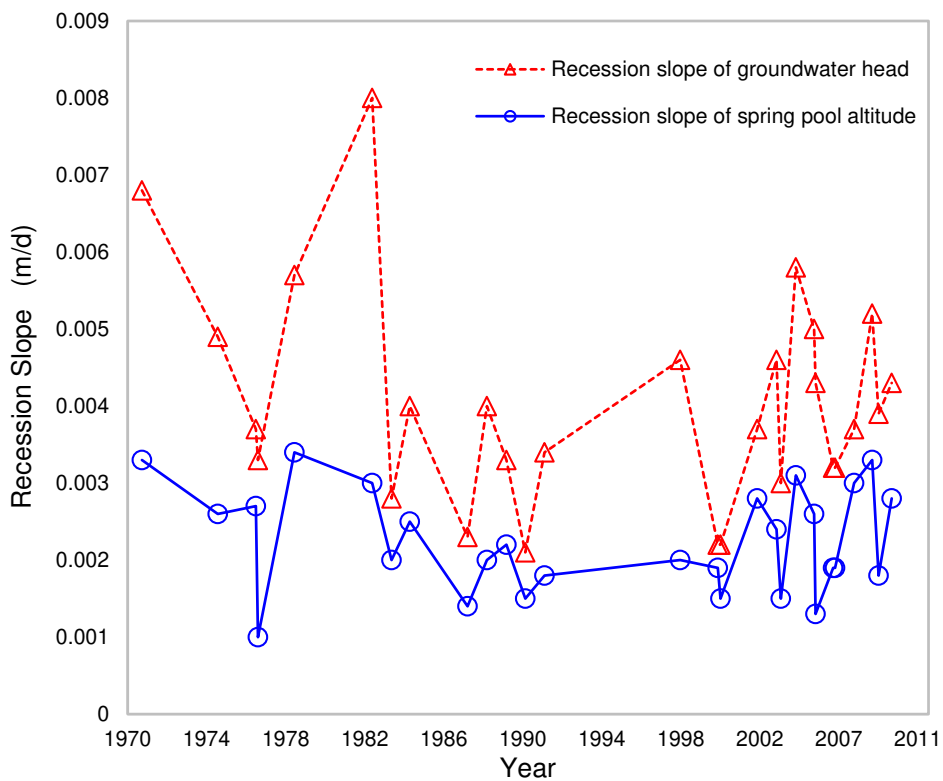
Figure 5.6. The recession slopes of groundwater head (C) and spring pool altitude (D) during the period of 1970-2012.

5.4.2   *Recession slopes of spring flow*

The recession slope of spring flow was estimated for each recession event using a linear regression from the observed daily spring flow. To demonstrate this, Figure 5.7a shows the recession event that began on 10/01/1984, where the estimated recession slope for spring flow was 0.0303 m^3/s/d. Figure 5.7b shows spring flow recession for the event starting on 10/10/2008, where the estimated recession slope was 0.0354 m^3/s/d for the early stage and 0.0398 m^3/s/d for the late stage. Table 5.1 shows the recession slope of spring flow for all events.
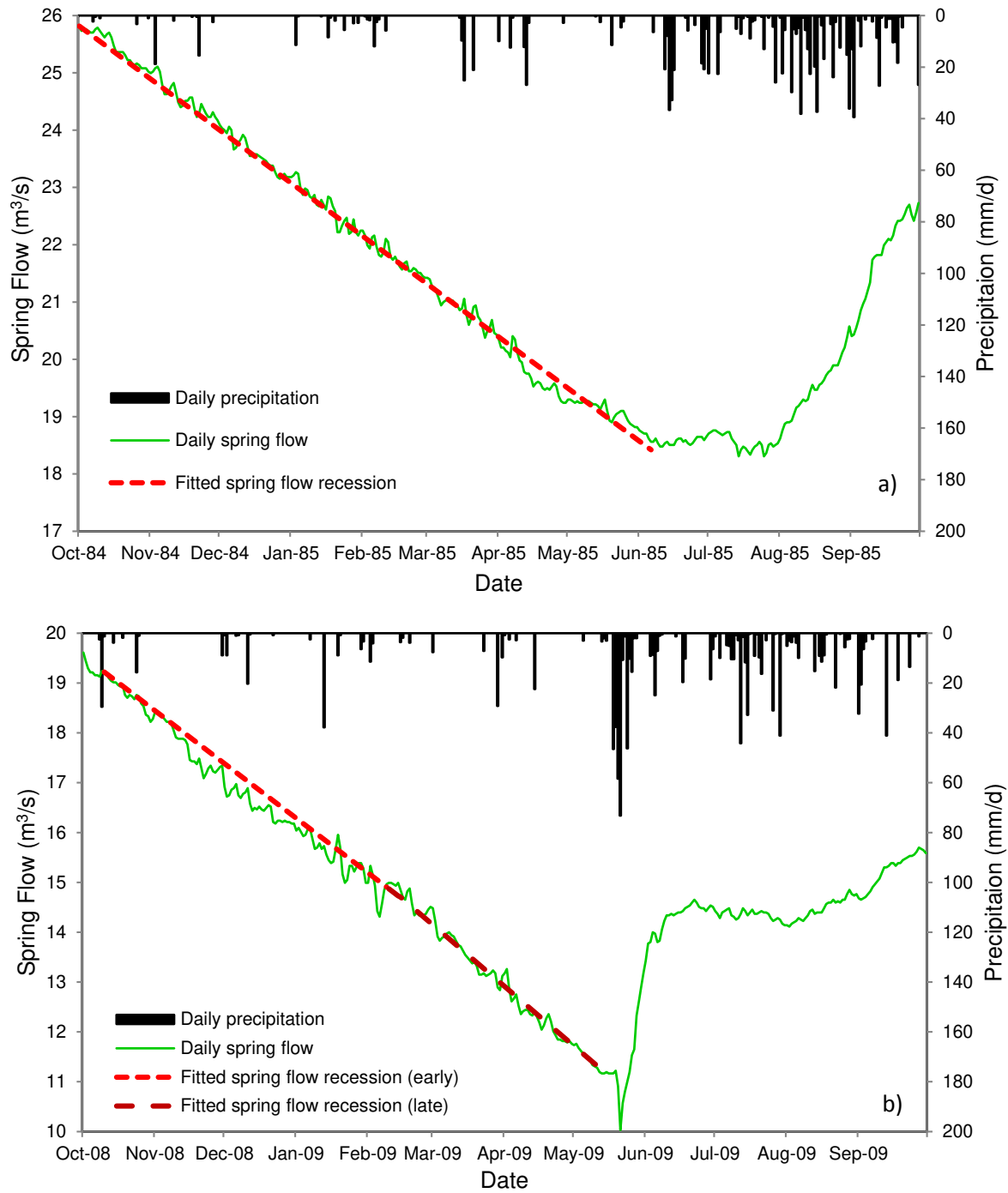
Figure 5.7. Precipitation, spring flow, and fitted spring flow recession for a recession event during a) 10/01/1984-06/06/1985 and b) 10/10/2008-05/11/2009.

The temporal variation of the recession slope from 1970 to 2010 is shown in Figure 5.8. The

spring flow recession slope (i.e., -dQ/dt) declined significantly for two periods: 1) from 1982 to

1989; and 2) from 1998 to 2002. The spring flow recession slope increased during the periods of 1989-1998 and post-2002. From equation (5.6), $-dQ/dt$ increases with decreasing springshed area A_1. The increasing trends of spring flow recession slope reflect the potential reduction trends of springshed.
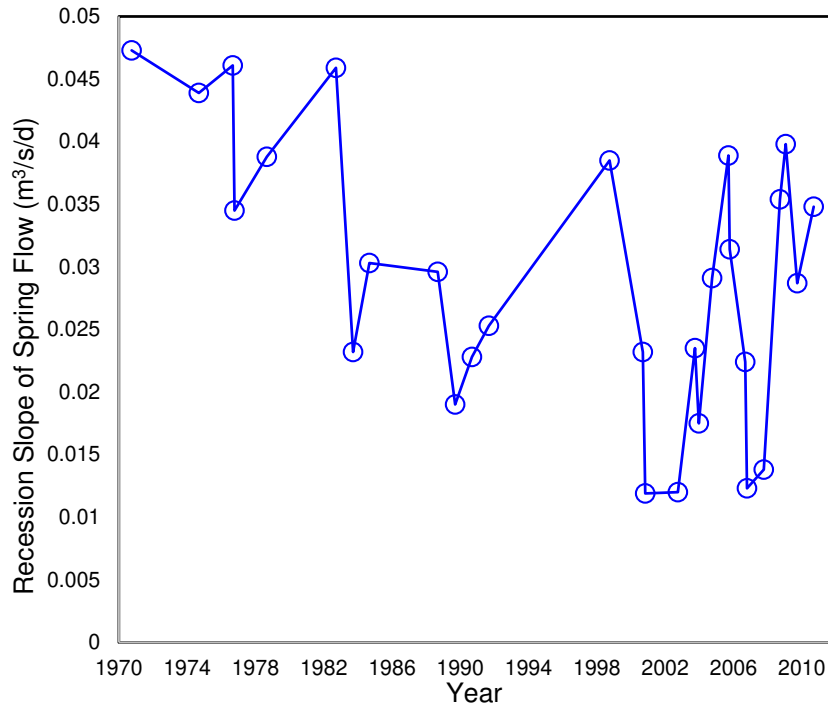
Figure 5.8. The recession slopes of spring flow during recession events.

5.4.3 *Effective springshed area and net recharge during recession events*

Considering the occurance of the recession events, the effective springshed area (A_1) during each recession event was calculated on October 31 from equation (5.6). The effective springshed area was stable during the period from 1970 to 1982 (Figure 5.9). The trends of A_1 increased for the periods of 1982-1989 and 1998-2002, the increasing trend of A_1 led to declined spring flow recession slope. However, the effective springshed area continuously declined post-2002; and this declining trend is partially contributed by the increasing trend of D according to equation (5.6). Generally, the springshed area has been declined since 1989 even though

93

fluctuation existed as a result of climatic variability. Figure 10 shows the net recharge on October 31 during each event as computed from equation (5.3). The estimated net recharge declined since the 1970s (Figure 5.10). Particularly, the net recharge dropped significantly from 1998 to 2000. After 2002, the net recharge increased, but was still lower than the level in the 1980s.
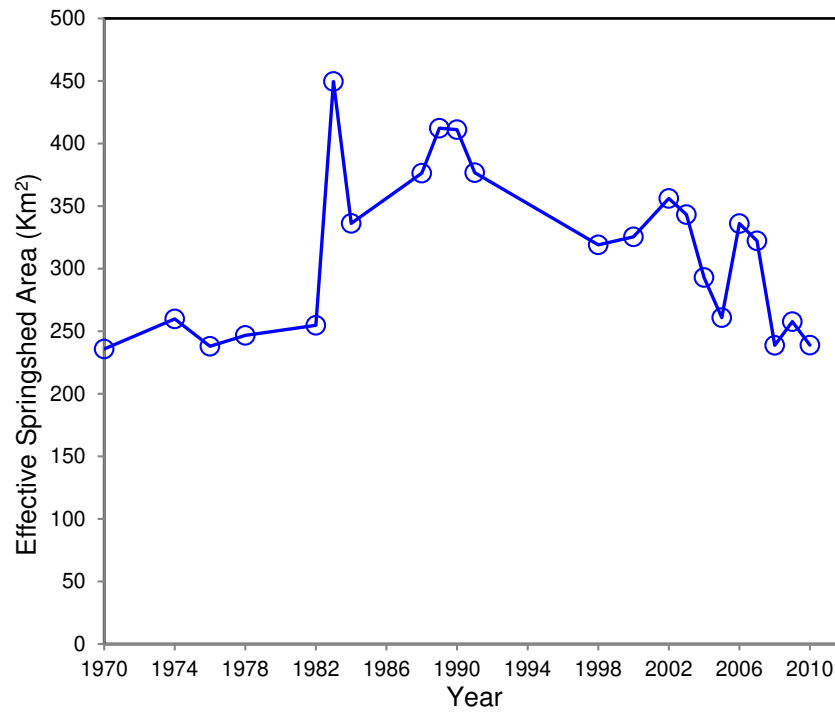
Figure 5.9. The estimated effective springshed area during recession events.
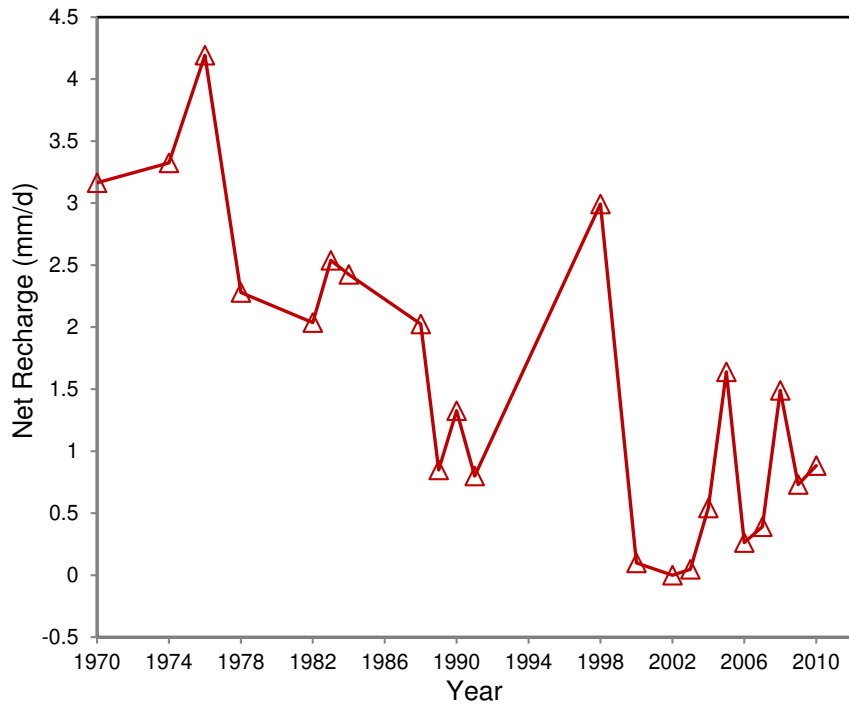
Figure 5.10. The estimated net recharge during recession events.

The declined trends of net recharge significantly contributed to the reduction of spring flow. The reductions of net recharge can be caused by changes in hydroclimatic conditions including rainfall and temperature, and groundwater withdrawals from UFA as a result of the rapid population growth in Marion Country [*Knowles et al.*, 2002].

5.5   Conclusions

In this study, the existing Torricelli model for spring recession was extended incorporating the impacts of net recharge and spring pool altitude. The groundwater head loss in the model was computed from the Darcy-Weisbach equation. The developed spring recession model was applied to Silver Springs for estimating the changes in effective springshed area and net recharge subsequent to 1970. Estimations of effective springshed area and net recharge were based on the observed recession slope changes for spring flow, groundwater head, and spring pool altitude. The

results show that 1) the effective springshed area continuously declined since 1987; and 2) the net recharge has also been declined since the 1970s, significantly dropped in 2002, then increased but remained lower than the levels observed before 1990. The spring flow of Silver Springs declined as a result of declined groundwater head and increased spring pool altitude. The groundwater head declined as a result of net recharge reduction. The spring pool altitude increased because of the growth of submerged aquatic vegetation such as water hyacinth and hydrilla due to the high nitrogen enrichment [*Nordlie*, 1990; *Phelps*, 2004], and the backwater effects from the Silver River [*SJRWMD*, 2012].

5.6 <u>References</u>

Amit, H., V. Lyakhovsky, A. Katz, A. Starinsky, and A. Burg (2002), Interpretation of spring recession curves, *Groundwater*, *40*(5), 543-551.

Atkinson, T. C. (1977), Diffuse flow and conduit flow in limestone terrain in the Mendip Hills, Somerset (Great Britain), *Journal of Hydrology*, *35*(1), 93-110.

Baedke, S. J., and N. C. Krothe (2001), Derivation of effective hydraulic parameters of a Karst Aquifer from discharge hydrograph analysis, *Water Resources Research*, *37*(1), 13-19.

Fiorillo, F. (2011), Tank-reservoir drainage as a simulation of the recession limb of karst spring hydrographs, *Hydrogeology Journal*, *19*(5), 1009-1019.

Fiorillo, F. (2014), The recession of spring hydrographs, focused on karst aquifers, *Water Resources Management*, *28*(7), 1781-1805.

Fiorillo, F., P. Revellino, and G. Ventafridda (2012), Karst aquifer draining during dry periods, *Journal of Cave and Karst Studies*, *74*(2), 148-156.

Goldscheider, N. (2012), A holistic approach to groundwater protection and ecosystem services in karst terrains, *AQUA mundi*, *3*, 117-124.

Huntoon, P.W. (1995), Is it appropriate to apply porous media groundwater circulation models to karstic aquifers? in: El-Kadi, A. I. (Eds.), *Groundwater Models for Resources Analysis and Management*, CRC Press, Florida, 339–358 pp..

King, W. A. (2004), Through the looking glass of silver springs: tourism and the politics of vision, *Americana*, *3*(1).

Knowles, L., A. M. O'Reilly, J. C. Adamski, and L. C. W. Authority (2002), Hydrogeology and simulated effects of ground-water withdrawals from the Floridan aquifer system in Lake

County and in the Ocala National Forest and vicinity, north-central Florida, *United States Geological Survey Water-Resources Investogations Report* 02-4207.

Knowles, L., Jr., B. Katz, and D. Toth (2010), Using multiple chemical indicators to characterize and determine the age of groundwater from selected vents of the Silver Springs Group, central Florida, USA, *Hydrogeology Journal*, *18*(8), 1825-1838.

Kresic, N. (2007), *Hydrogeology and groundwater modeling*, 2nd edition, CRC Press, Florida.

Martin, J. M. (2003), Quantification of the matrix hydraulic conductivity in the Santa Fe River sink/rise system with implications for the exchange of water between the matrix and conduits, University of Florida, 89pp.

Mangin, A. (1975), Contribution a`l'e´tude hydrodynamique des aquife`res karstiques. Institut des sciences de la Terre de l'universite´ de Dijon, Moulis, The`se de Doctorat e`s Sciences Naturelles.

National Oceanic and Atmospheric Administration (2010), Online meteorological data. [Accessed 11/09/2015] http://www.ncdc.noaa.gov/cdo-web/datasets/normal_mly/stations/GHCND:USC00086414/detail.

Nordlie, F.G. (1990), Rivers and springs. in: Myers, R.L. and Ewel, J.J. (Eds.), *Ecosystems of Florida*, chapter 12, University of Central Florida Press, Florida, 392-425 pp.

Osburn, W., D. Toth, and D. Boniol (2002), Springs of the St. Johns River Water Management District, *Water Management District St. Johns River Report SJ2002-5*.

Padilla, A., A. Pulido-Bosch, and A. Mangin (1994), Relative Importance of Baseflow and Quickflow from Hydrographs of Karst Spring, *Ground Water*, *32*(2), 267-277.

Phelps, G. G. (2004), Chemistry of ground water in the Silver Springs basin, Florida, with an emphasis on nitrate, *U.S. Geological Survey Scientific Investigations Report 2004-5144*, 54 pp.

Rosenau, J. C., G. L. Faulkner, C. W. Hendry Jr, and R. W. Hull (1977), Springs of Florida, Florida Department of Natural Resources, Bureau of Geology, *Bulletin No. 31*, 461 pp.

Samek, K. (2004), Unknown quantity: the bottled water industry and Florida's springs, *Journal of Land Use & Environmental Law*, 569-595.

Sepúlveda, N. (2009), Analysis of methods to estimate spring flows in a karst aquifer, *Groundwater*, *47*(3), 337-349.

St. Johns River Water management District (2012). Springs Protection Initiative: Minimum Flows and Levels for Silver Springs and Silver River, Government Board Meeting, November 2012.

St. Johns River Water management District (2013). Variability in Springsheds Delineated by Potentiometric Surfaces, Discussion Paper, May 2013. [Accessed 5/6/2015] http://www.silverspringsalliance.org/Resources/Documents/Variability%20in%20Springsheds%20Delineated%20by%20Potentiometric%20Surfaces.pdf.

Walsh, S. J., L. Knowles, B. G. Katz, and D. G. Strom (2009), Hydrology, water quality, and aquatic communities of selected springs in the St. Johns River Water Management District, Florida, *United States Geological Survey Scientific Investigations Report 2009-5046*.

CHAPTER 6: GENERAL CONCLUSION AND STUDY LIMITATIONS

6.1   Conclusions

Using the cumulative regression analysis in the dissertation overcomes the problem to identify the transition of recession from early stage to late recession for individual recession events and lower envelopes of recession slope curve with an ensemble of watersheds across the climate gradients. This cumulative regression analysis method was applied to the well-studied PMRW to identify the transition of recession from early to late recession, compared with the streamflow of the outlet when the flowing stream contracts to the perennial stream head. Twenty three recession events of PMRW were selected to perform the recession analysis. The average value of the transition of recession over the twenty-three recession events was 0.95 mm day^{-1} and the streamflow of the outlet when the flowing stream contracts to the perennial stream head was 0.92 mm day^{-1}. The correlation coefficient between these two characteristics of flow was 0.90, which indicated that two flows were similar with identical characteristics of flow. Since the transitions from early to late recession are linked with ephemeral and perennial streams, transition flows are hydrologic signatures related to stream types. The relationship between streamflow and flowing stream length and location provides valuable information for understanding stream ecosystem expansion and contraction [*Stanley et al.*, 1997] and spatial variability in stream chemistry [*McGuire et al.*, 2014]. Ephemeral streams are more dominant in arid regions than in humid regions. Therefore, the characteristics of transition flow across the climate gradients was also tested in 40 watersheds in contiguous United States and showed that climate, represented by climate aridity index, is a dominant control on the transition from early to late recession stages. The value of transition flow and long-term average base flow were 0.84 mm day^{-1} and 0.81 mm

day^{-1}, respectively for 40 watersheds with a correlation coefficient of 0.82. In reality, long term average base flow and the transition of base flow recession is basically the form of base flow at two temporal scales, i.e., the long-term time scale and the event scale during a recession period. The findings supported that the base flow characteristics at the long term scale and the event scale during a recession period, primarily controlled by climate. This may help the water manager to predict the long term base flow and climate situation after analyzing the transition flow of recession for ungaged watershed when long term data is not available.

In addition, the characteristics of early and late recession were applied on estimation of combined natural and human interference in heavy groundwater dependent agricultural watershed. A model was developed for incorporating the direct human (such as shallow and deep groundwater pumping) and natural interferences (such as evapotranspiration) with recession analysis. The estimated groundwater pumping rate was found consistent compared to the observed groundwater uses.

The novelty of the recession analysis also lies in the development of spring recession model to estimate the changes in effective springshed area and net recharge. The results showed that the effective springshed area had been gradually declined since 1987, the net recharge (recharge minus groundwater pumping and evapotranspiration) declined since the 1970s but significantly dropped in 2002 and then increased but remained lower than the levels observed before 1990. The spring flow of Silver Springs declined as a result of declined groundwater head and springshed area and increased spring pool altitude. The groundwater head declined as a result of net recharge reduction.

6.2   <u>Future Research</u>

As an extension to this research, projection of future climate (precipitation and potential evapotranspiration) from the general circulation models or regional circulation models can be combined with the characteristics of the transition of recession to project the climate change impact on base flow which will forecast the stream chemistry and stream ecosystem.

In addition, the spring recession model was only focused on the recession periods. Future research can quantify the human-induced and climate-induced changes in net recharge and spring flow at the monthly or annual scales. Human impacts include land cover change and groundwater pumping. The changes in precipitation and potential evapotranspiration can also affect the net recharge. A continuous simulation model, conceptual or physically-based continuous simulation model can be developed in future to simulate spring flow.

6.3   <u>References</u>

McGuire, L. A., J. D. Pelletier, and J. J. Roering (2014), Development of topographic asymmetry:

Insights from dated cinder cones in the western United States, *Journal of Geophysical Research: Earth Surface*, *119*(8), 1725-1750.

Stanley, E. H., S. G. Fisher, and N. B. Grimm (1997), Ecosystem expansion and contraction in

streams, *BioScience*, *47*(7), 427-435.

APPENDIX A: MATERIALS UNDER REVIEW

The contents of the chapter 2, 3, 4, 5 are submitted for review as follows:

- The content in chapter 2 has been submitted for publication as: Ghosh, D. K., Wang, D., and Zhu, T., "On the Transition of Base Flow Recession from Early Stage to Late Stage", Advances in Water Resources, accepted with minor revision, 2015

- The content in chapter 3 has been prepared for publication as Ghosh, D. K., and Wang, D., "Linking Long Term Climate to Transition of Base Flow Recession", Advances in Water Resources, in preparation, 2015

- The content in chapter 4 has been prepared for publication as Ghosh, D. K., and Wang, D., "Quantifying Shallow and Deep Groundwater Depletion in High Plain Aquifer by Streamflow Recession", Hydrological Processes, in preparation, 2015

- The content in chapter 5 has been submitted for publication as Ghosh, D. K., Wang, D., Bilskie, M. V, and Hagen, S. C., "Quantifying Changes of Springshed Area and Net recharge through Recession Analysis of Spring Flow", Hydrological Processes, To be submitted after moderate revision, 2015

APPENDIX B: TRANSITION OF RECESSION SLOPE CURVE FROM INDIVIDUAL RECESSION EVENT

Transition of recession slope curve, the slope and R^2 of the cumulative regression analysis for 23 recession events.
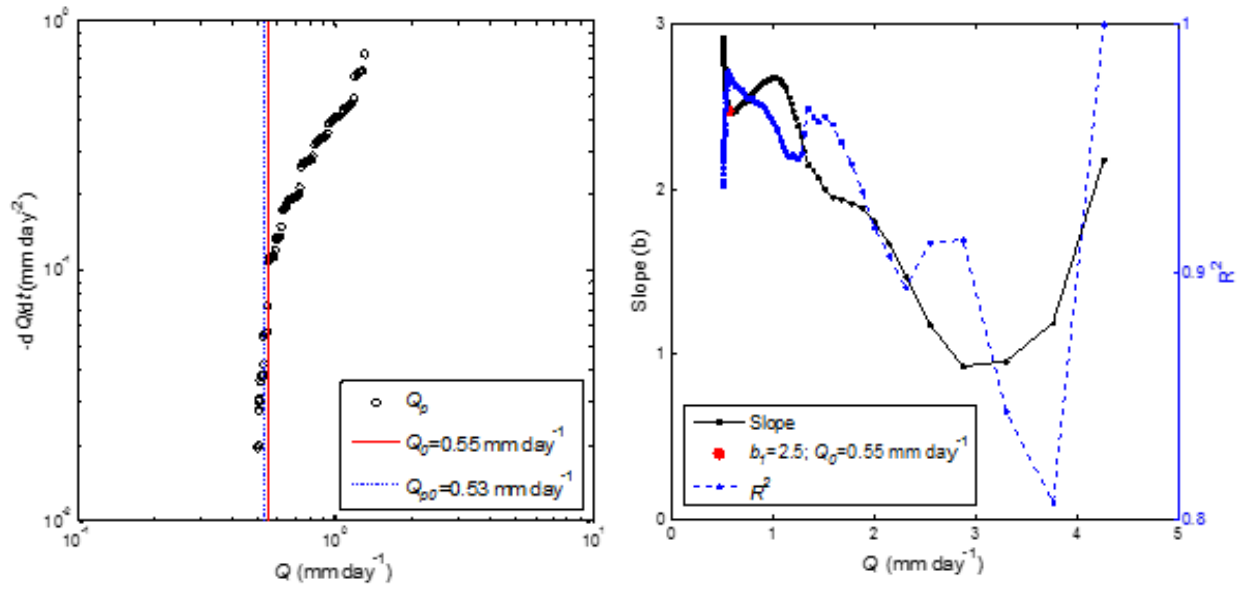
Figure B.1. 02 AM on 20 January, 1988
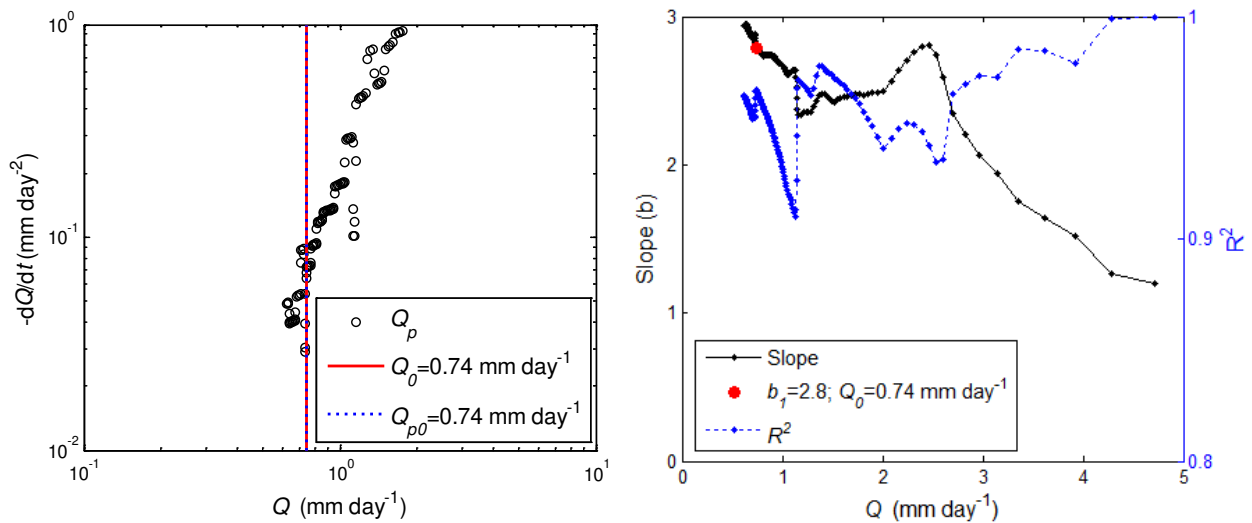
Figure B.2. 02 AM on 04 February, 1988
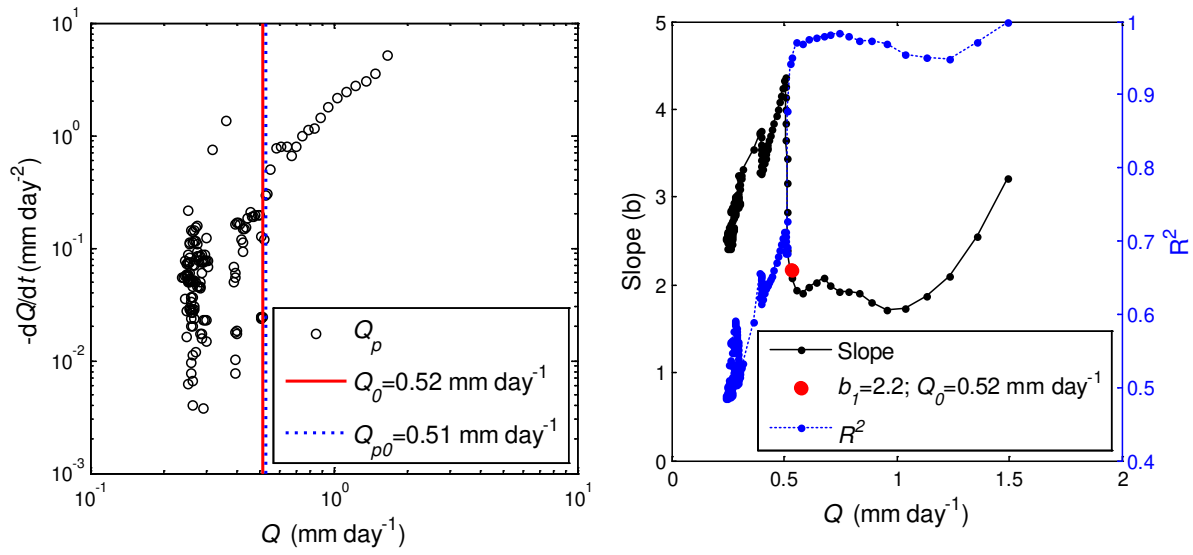
Figure B.3. 6 PM on 03 October, 1988
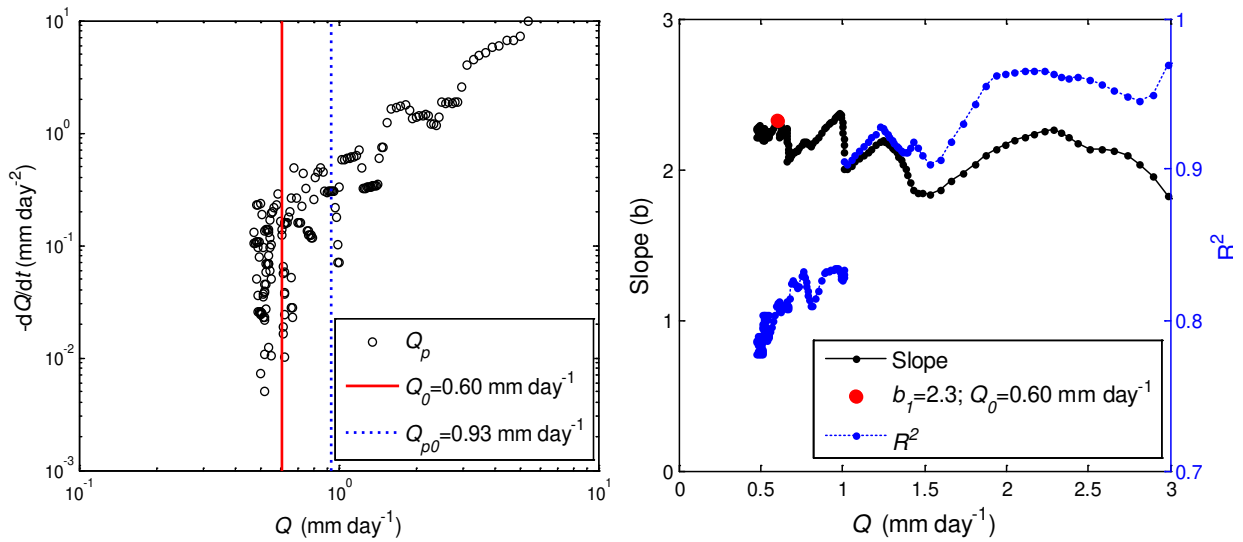
Figure B.4. 7 PM on 01 October, 1989
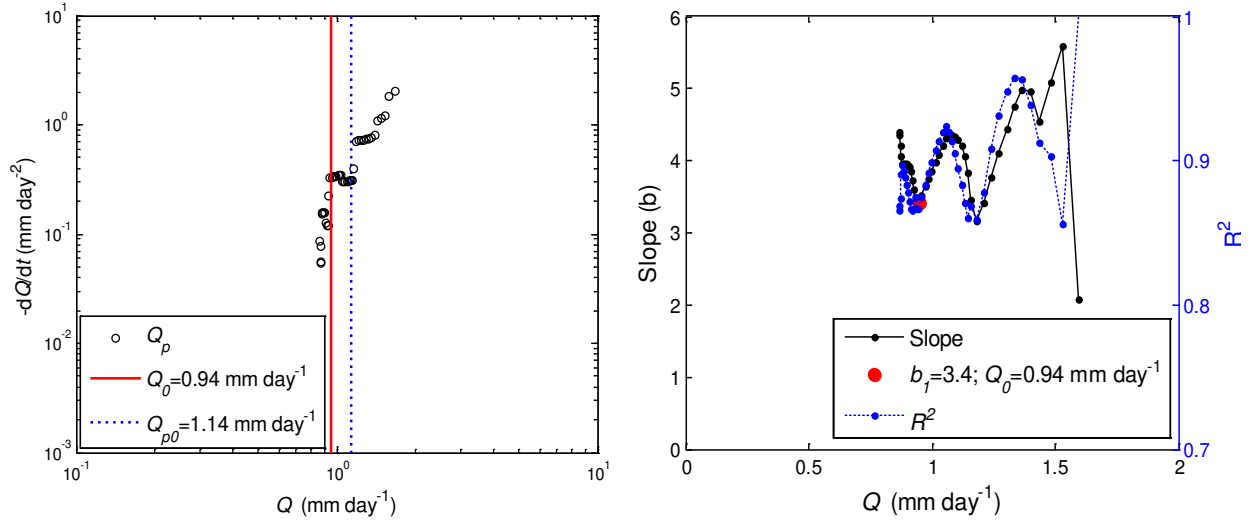
Figure B.5. 3 PM on 09 December, 1989
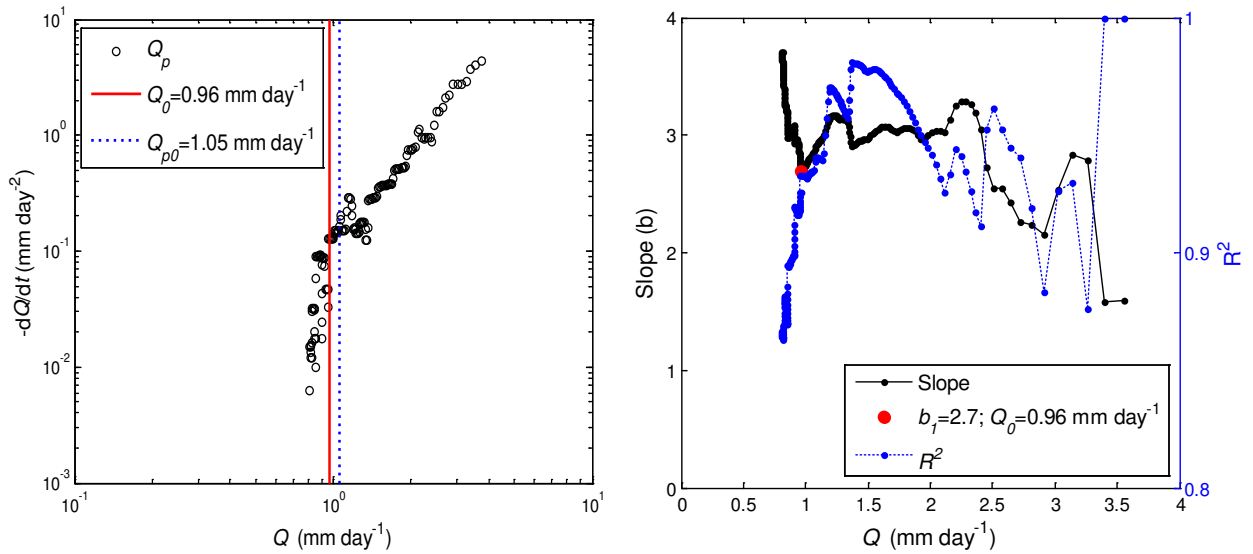
Figure B.6. 01 AM on 08 January, 1990
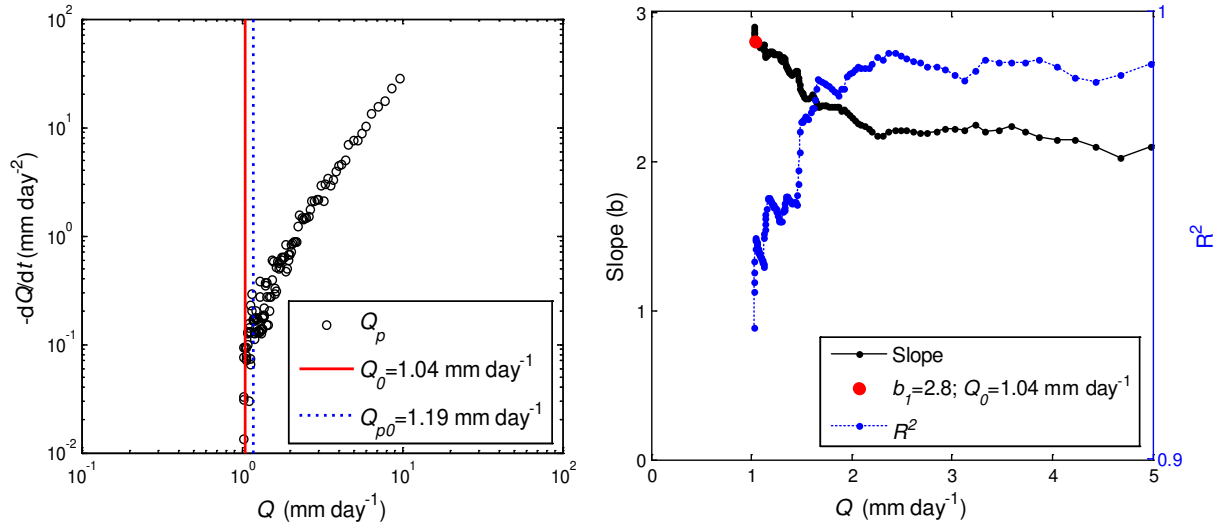
Figure B.7. 02 PM on 29 March, 1991
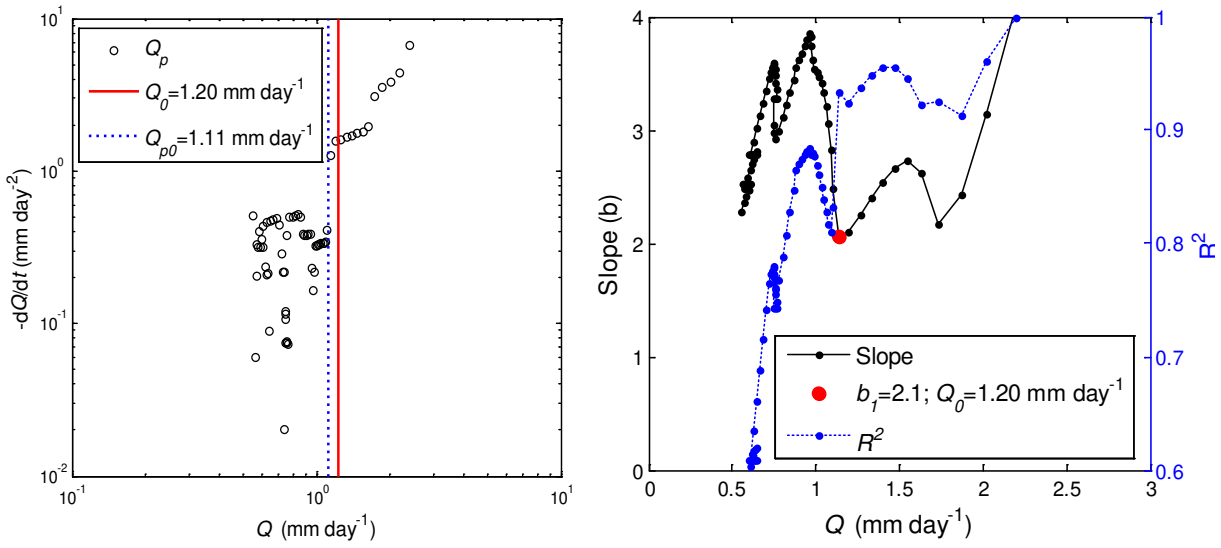
Figure B.8. 02 AM on 23 August, 1992
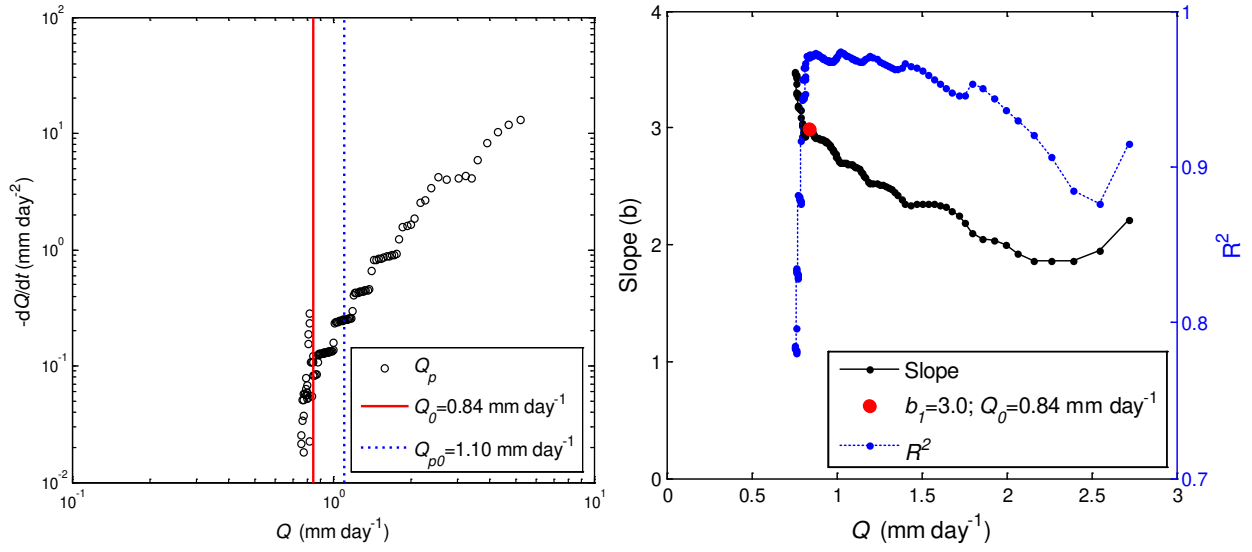
Figure B.9. 01 PM on 04 November, 1992
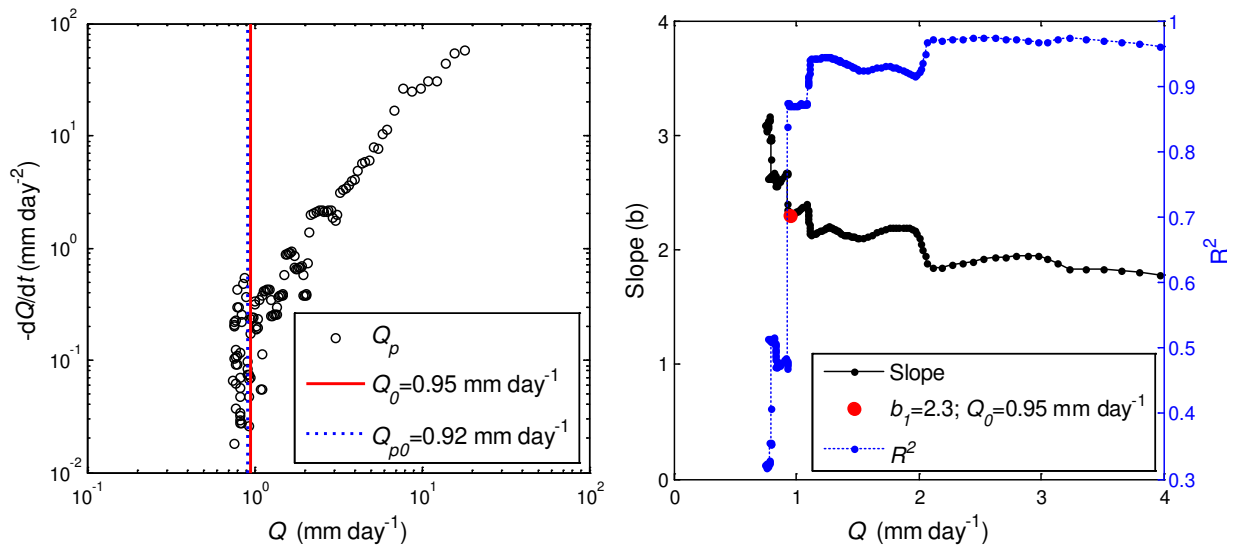
Figure B.10. 10 PM on 04 October, 1995

111
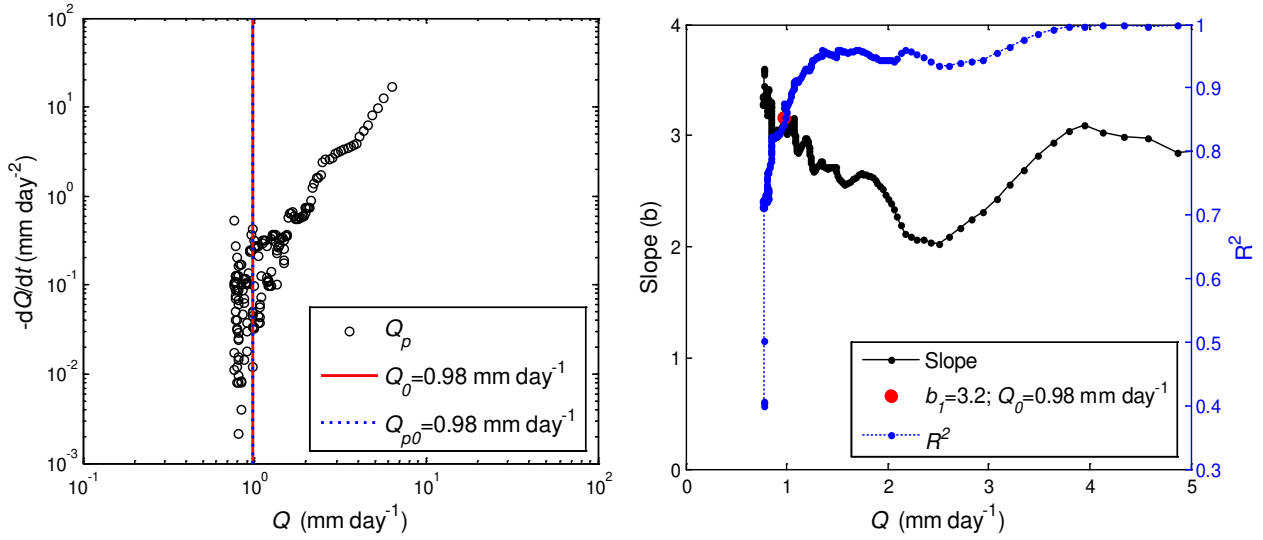
Figure B.11. 12 PM on 14 October, 1995
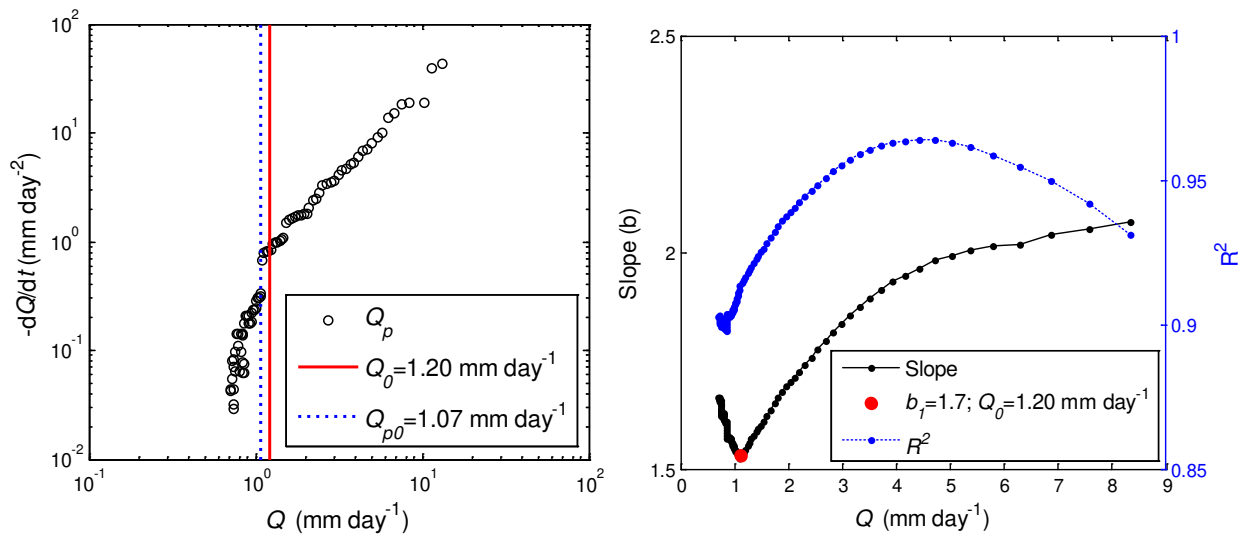
Figure B.12. 04 AM on 26 October, 1997
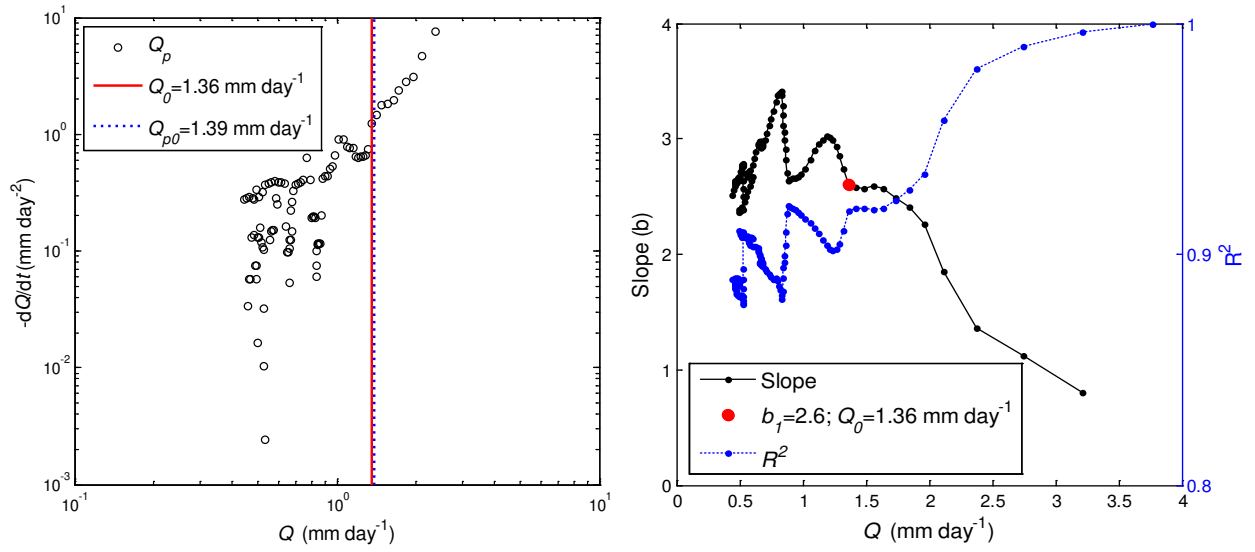
Figure B.13. 06 AM on 07 May, 1999
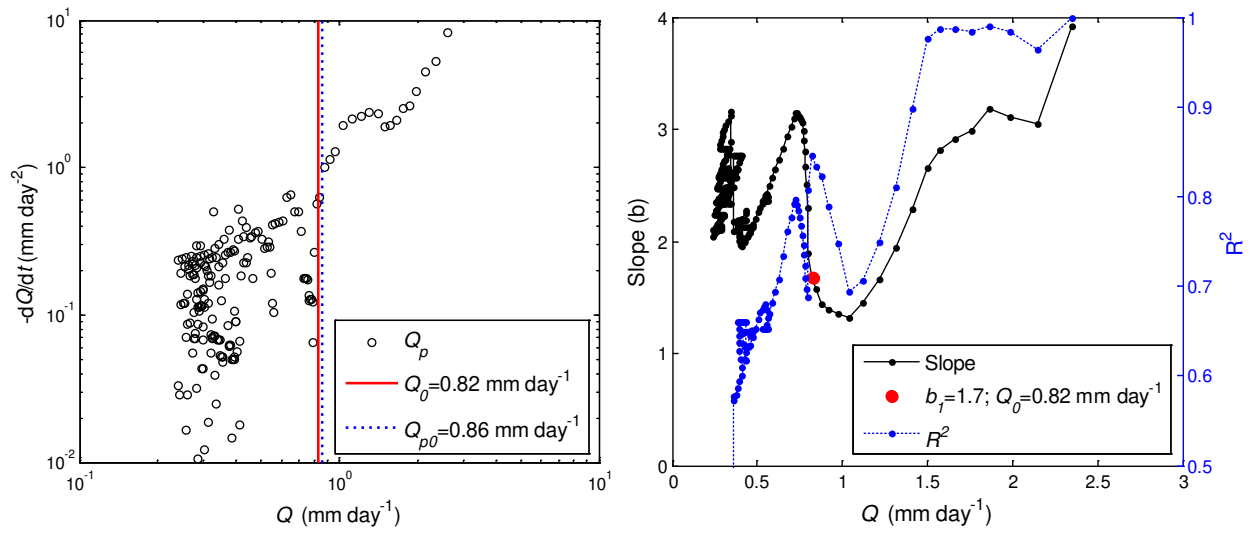
Figure B.14. 05 PM on 24 July, 1999

113
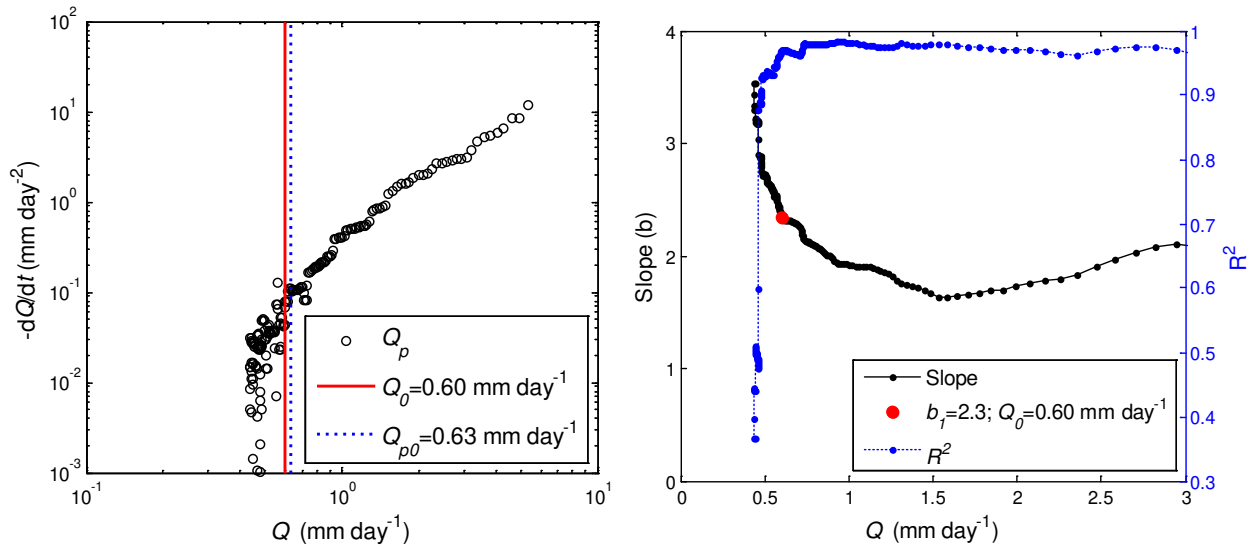
Figure B.15. 05 PM on 06 February July, 2002
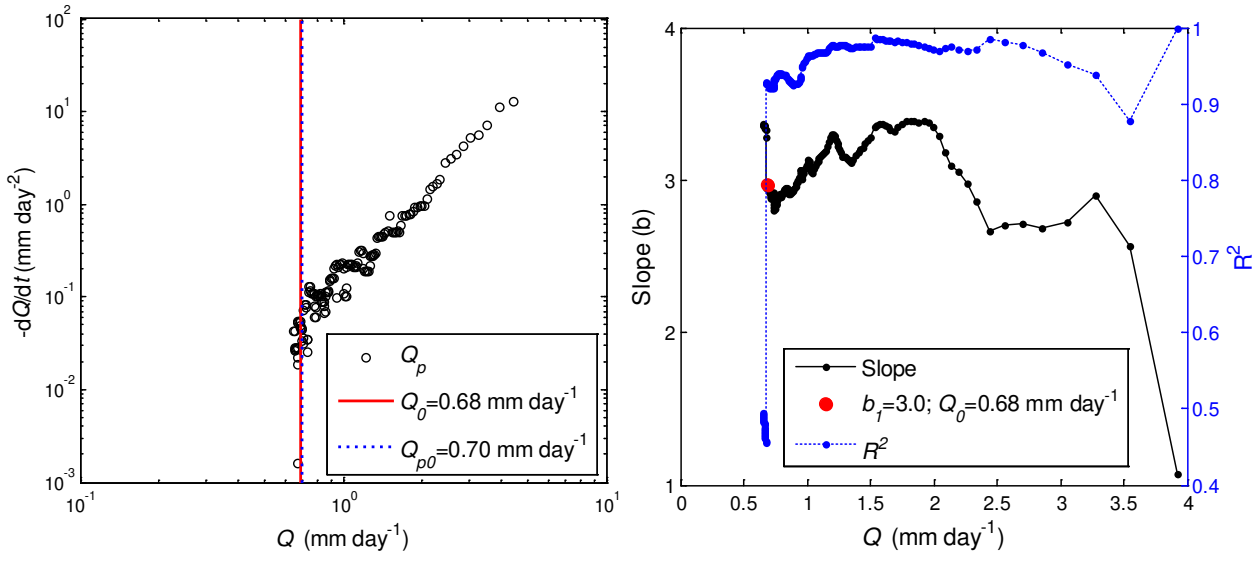
Figure B.16. 09 PM on 30 March, 2002

114
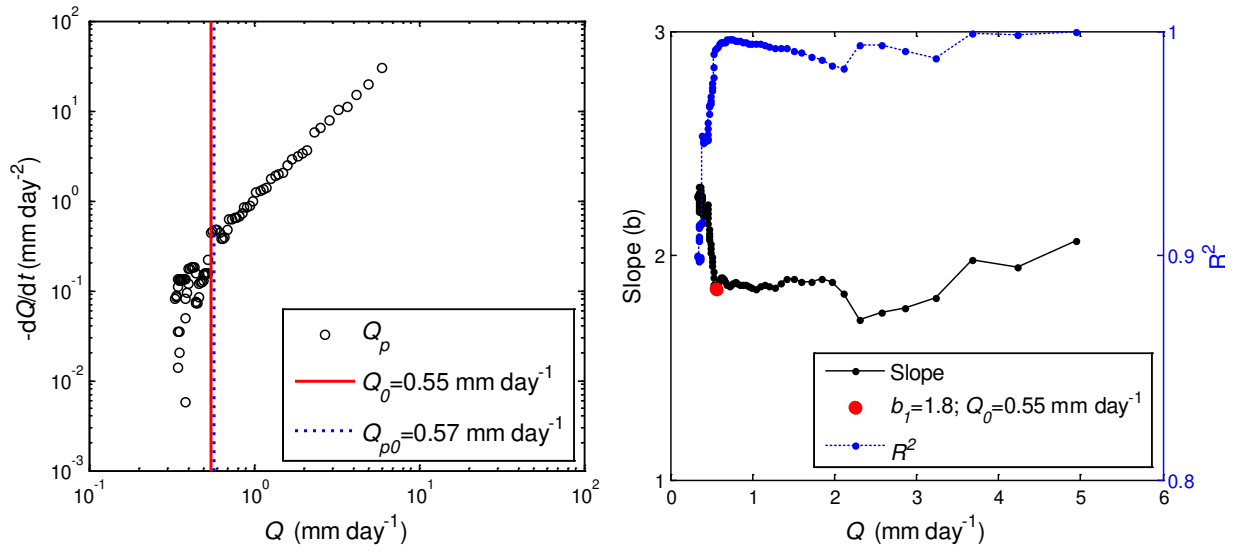
Figure B.17. 05 PM on 15 October, 2002
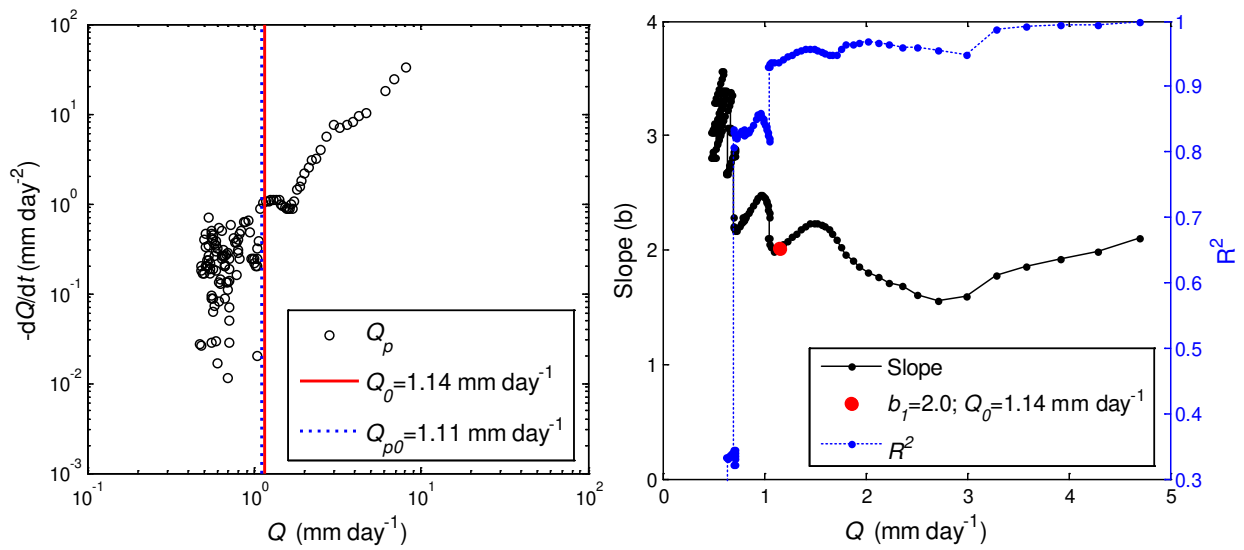
Figure B.18. 05 PM on 16 September, 2004

115
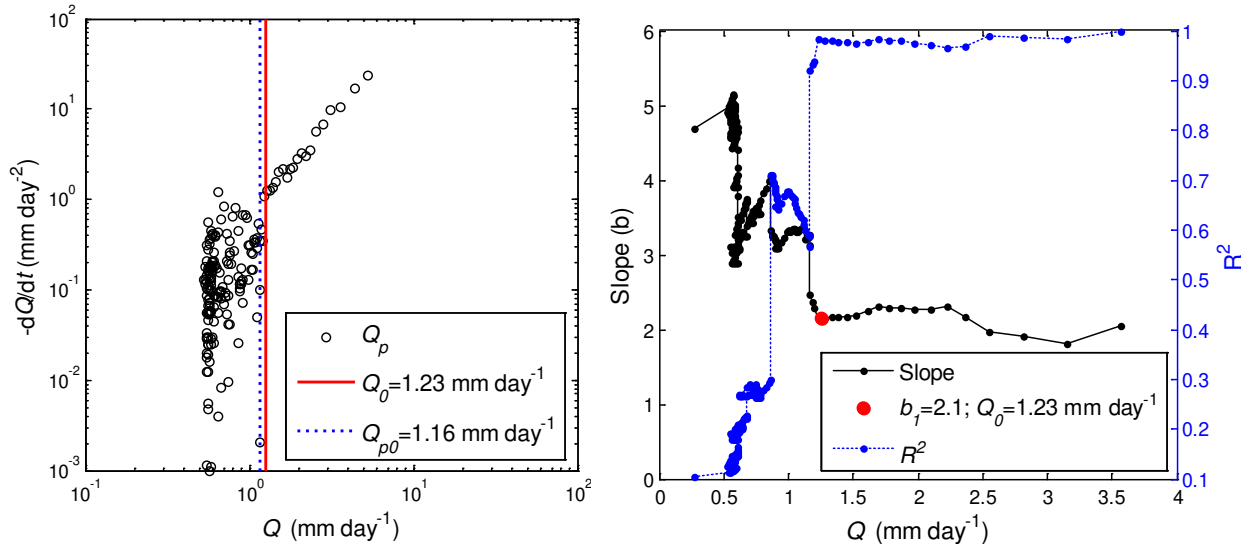
Figure B.19. 03 PM on 27 September, 2004
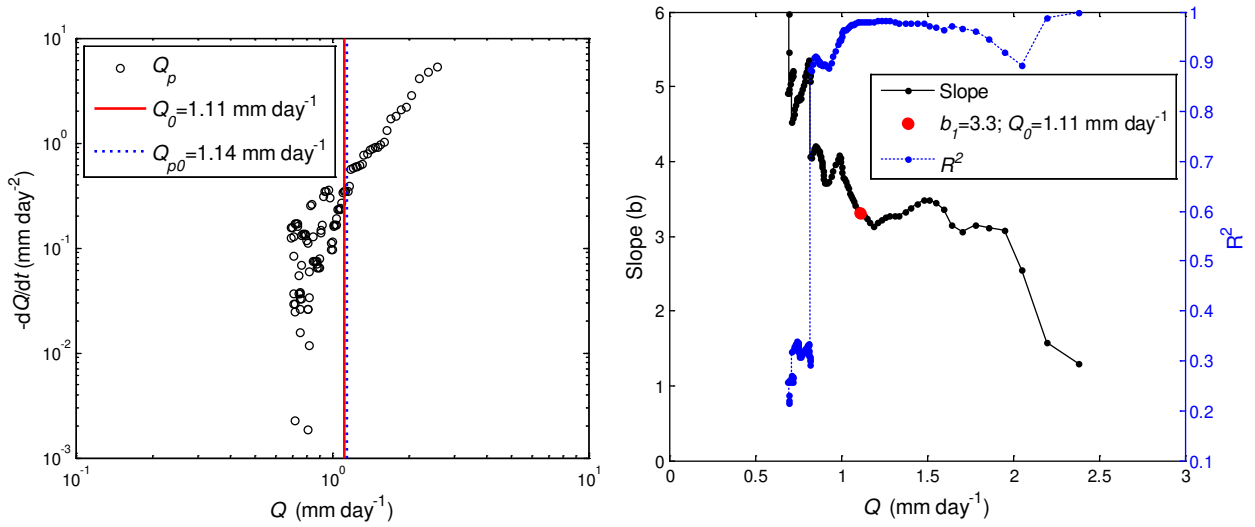
Figure B.20. 09 AM on 04 November, 2004
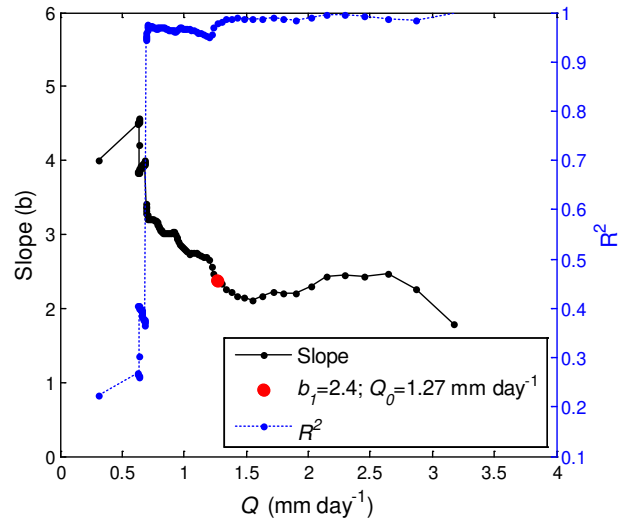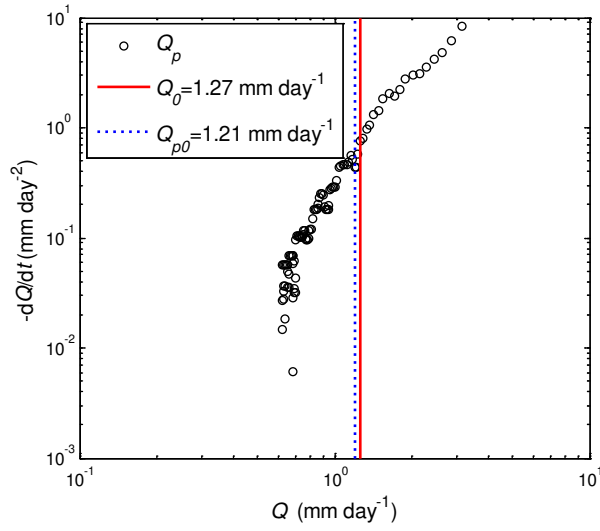
Figure B.21. 01 AM on 16 November, 2006
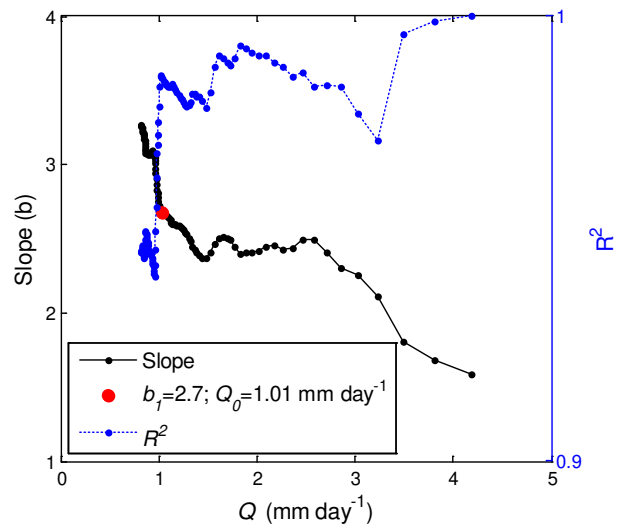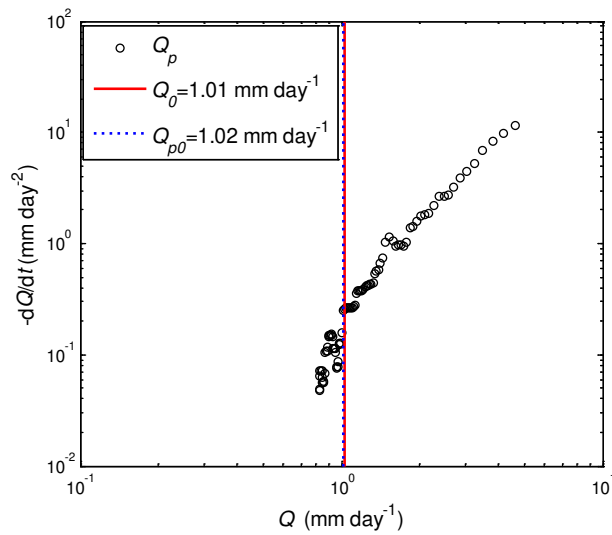
Figure B.22. 11 PM on 31 December, 2006
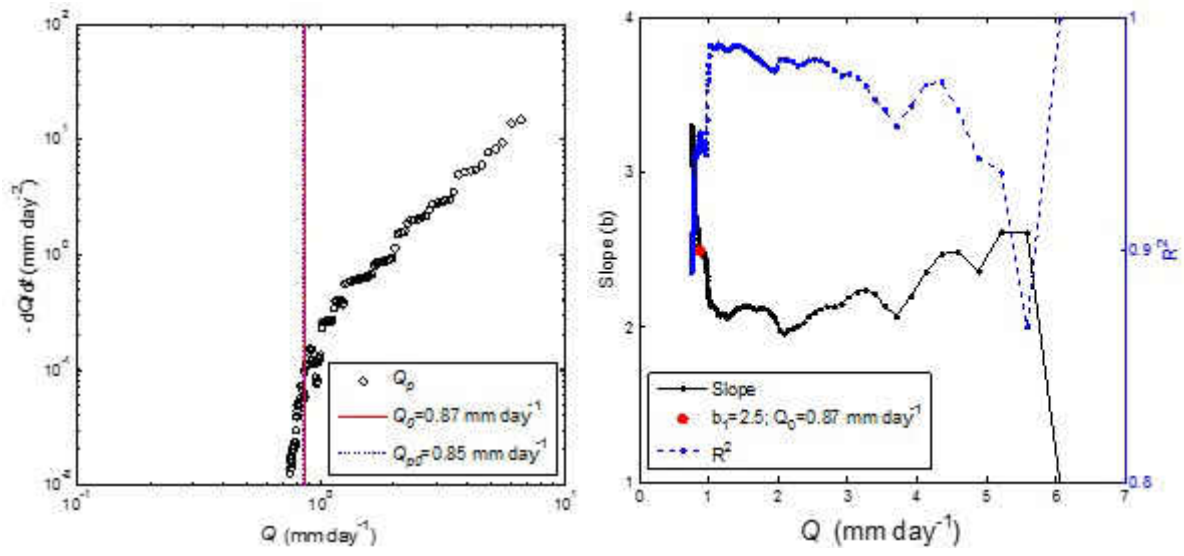
Figure B.23. 0 AM on 08 January, 2007

APPENDIX C: TRANSITION OF RECESSION SLOPE CURVE FROM LOWER ENVELOPE

Transition of recession slope curve (Q_0) obtained from lower envelop, long-term average base flow, the slope and R^2 of the cumulative regression analysis for 40 watersheds.
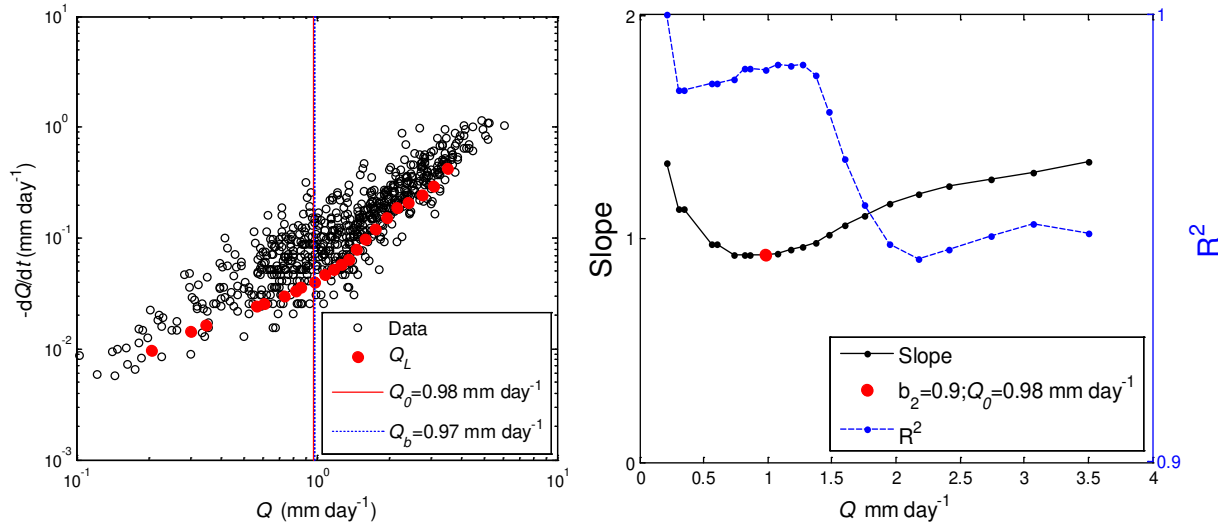
Figure C.1. Gage ID 01372500
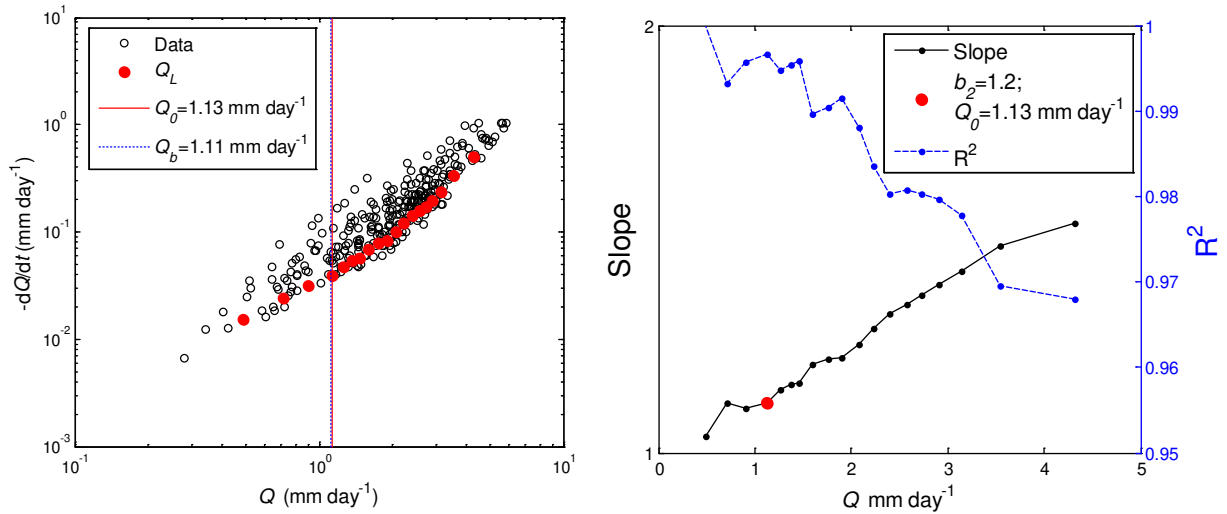
Figure C.2. Gage ID 01445500
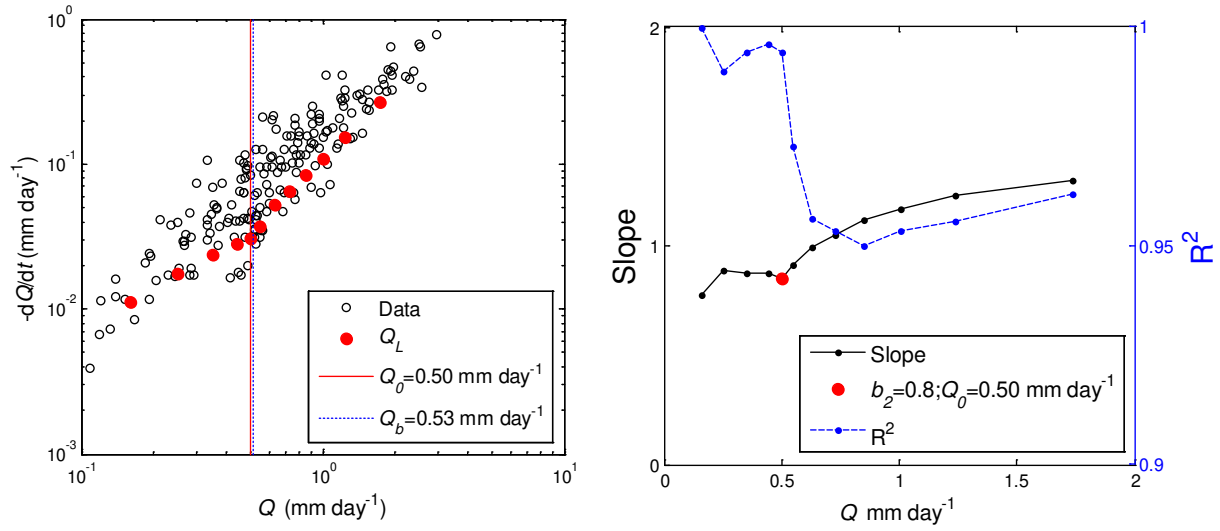
Figure C.3. Gage ID 01520000
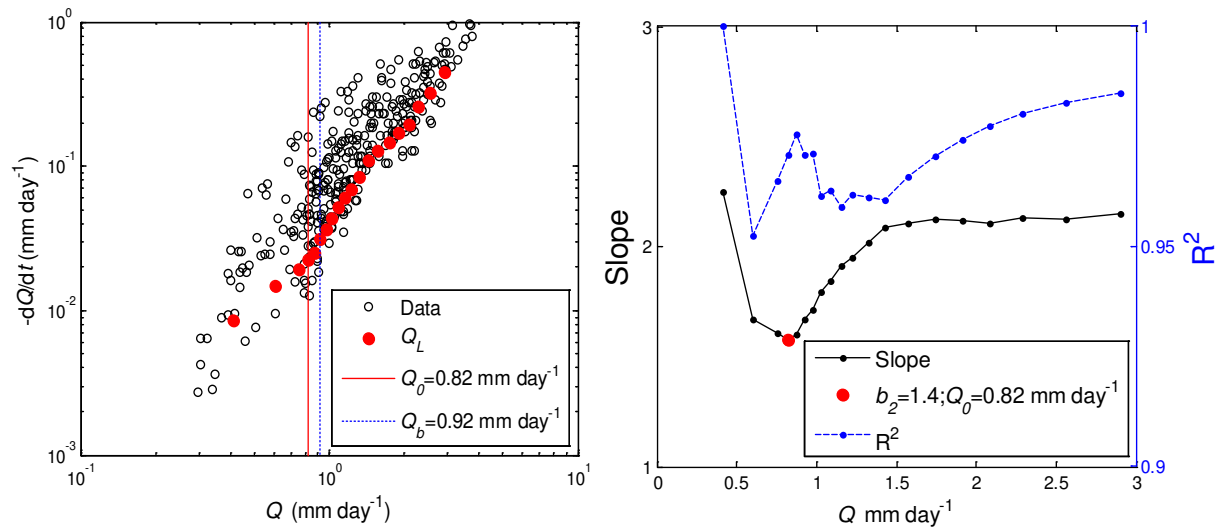
Figure C.4. Gage ID 01559000
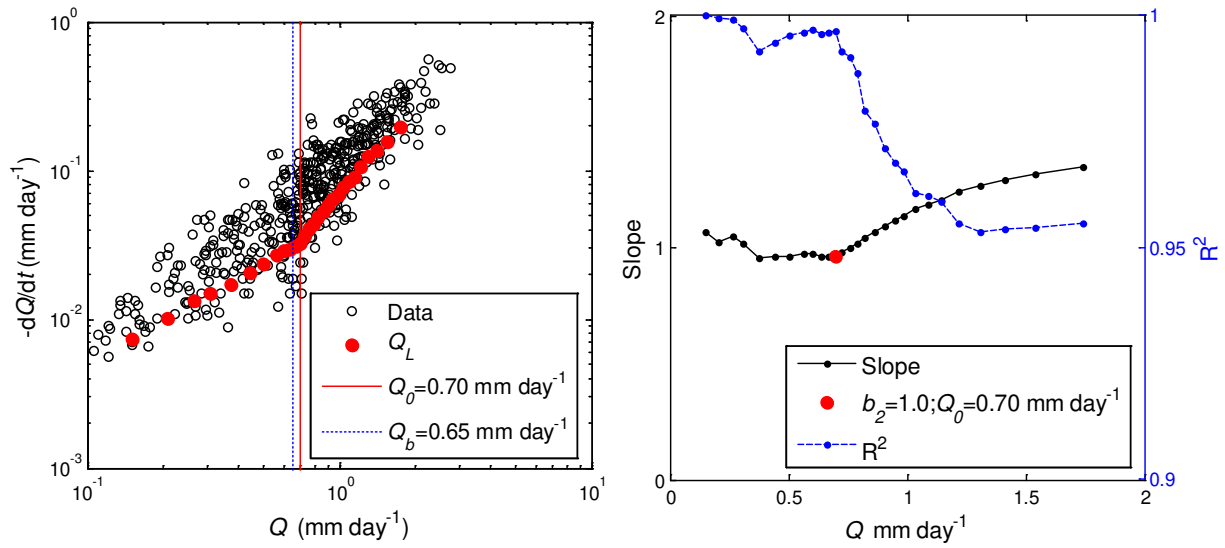
Figure C.5. Gage ID 01574000
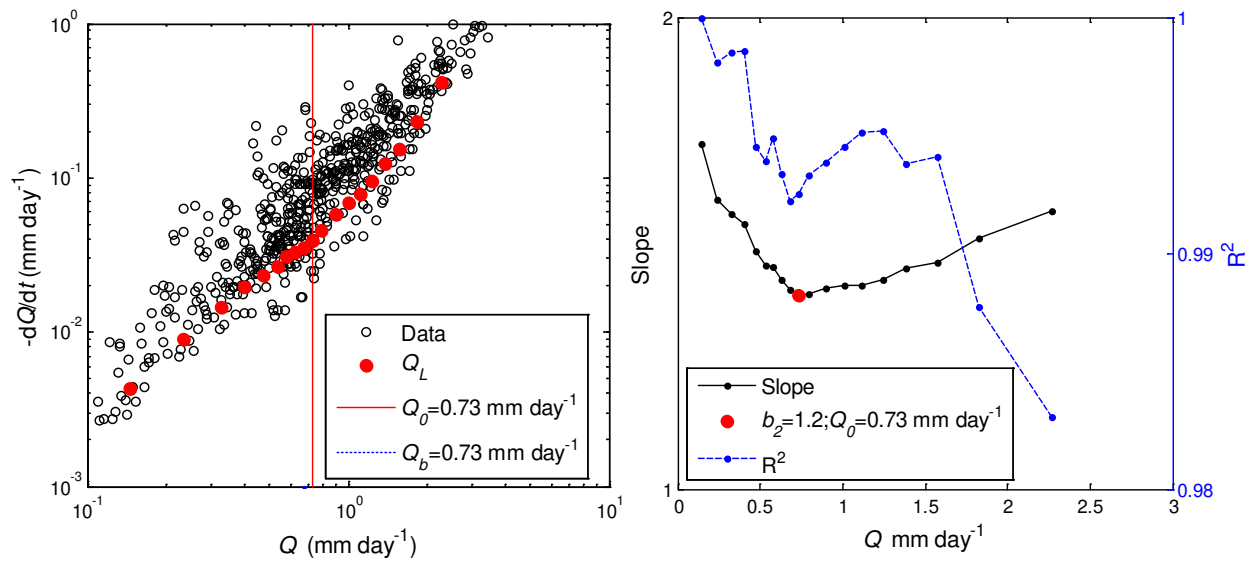
Figure C.6. Gage ID 01606500
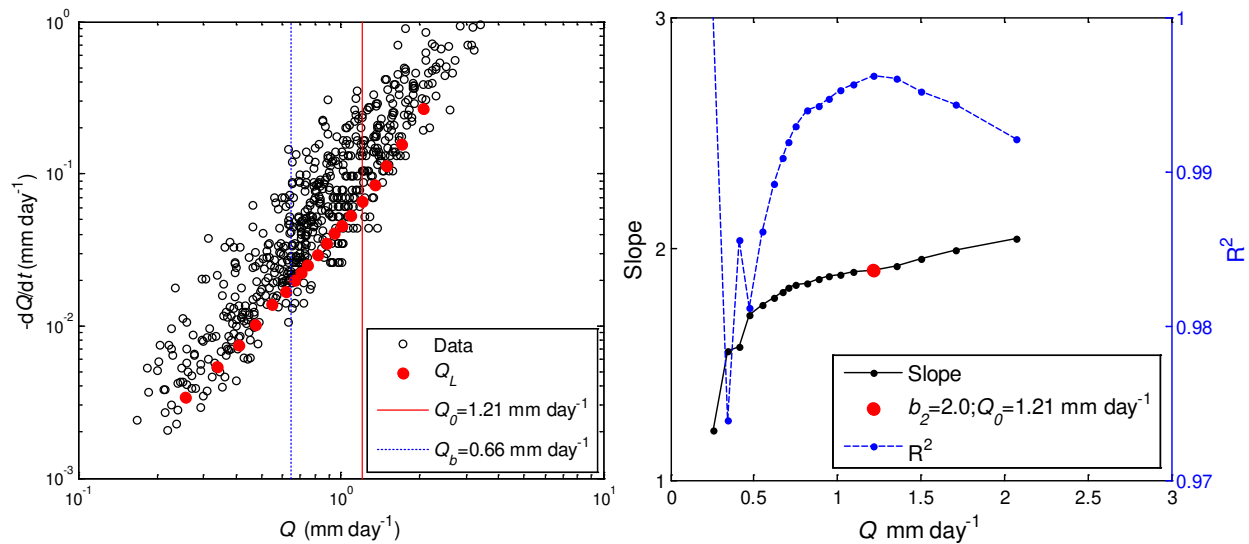
Figure C.7. Gage ID 01628500
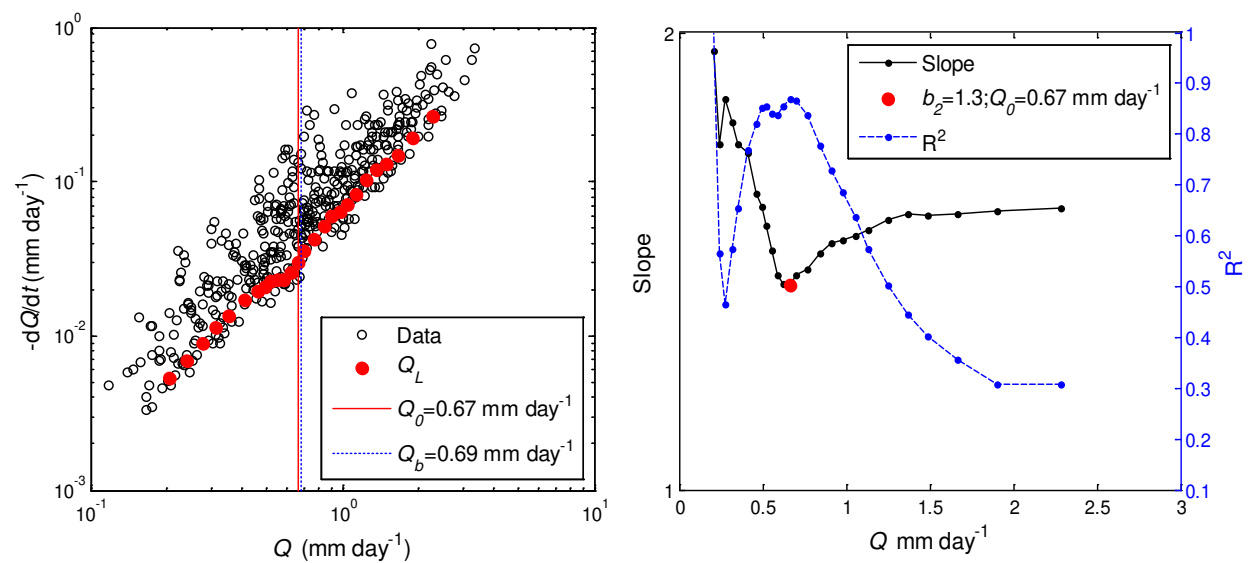
Figure C.8. Gage ID 01643000

123
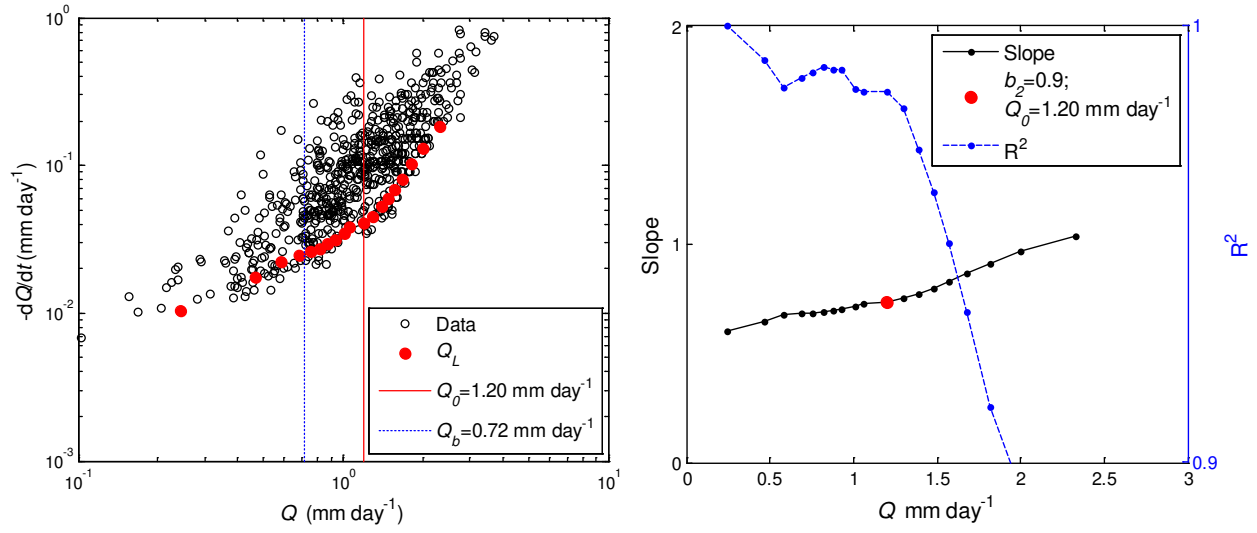
Figure C.9. 01664000
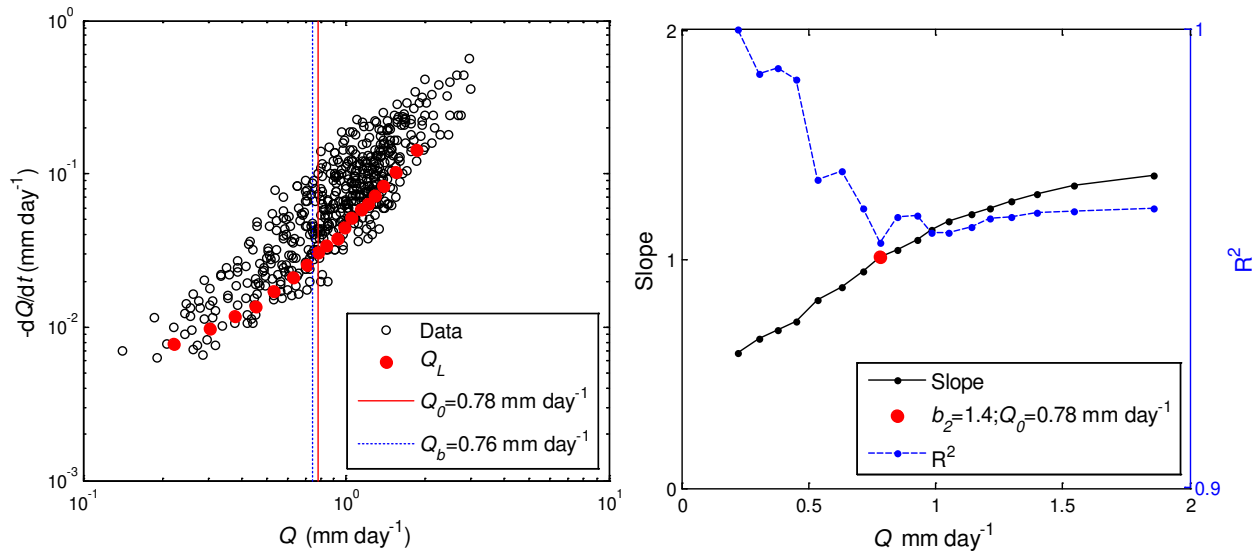
Figure C.10. Gage ID 01667500

124
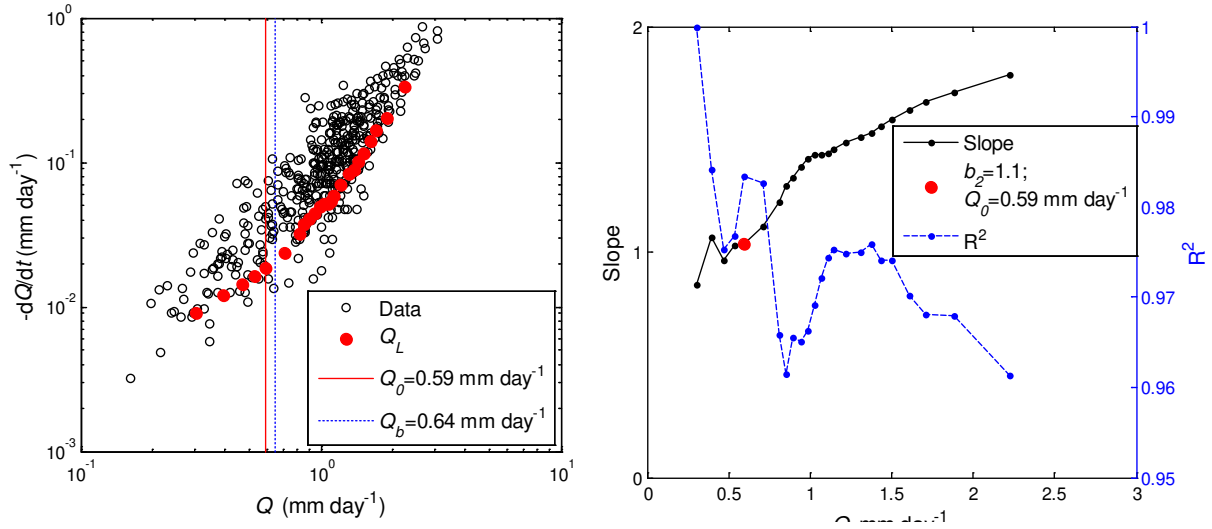
Figure C.11. Gage ID 01668000
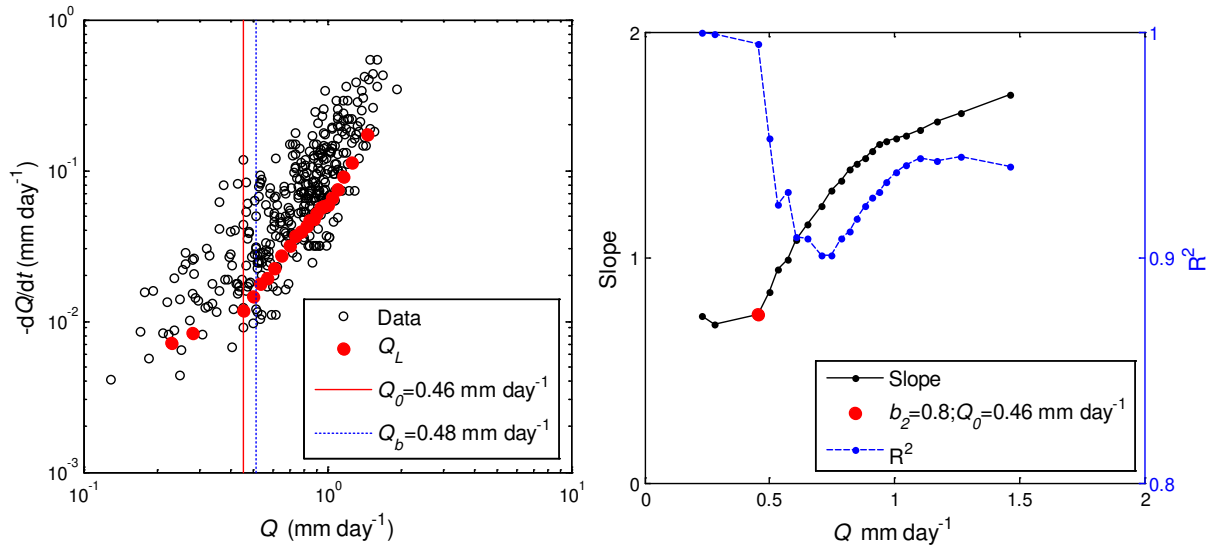
Figure C.12. Gage ID 01672500
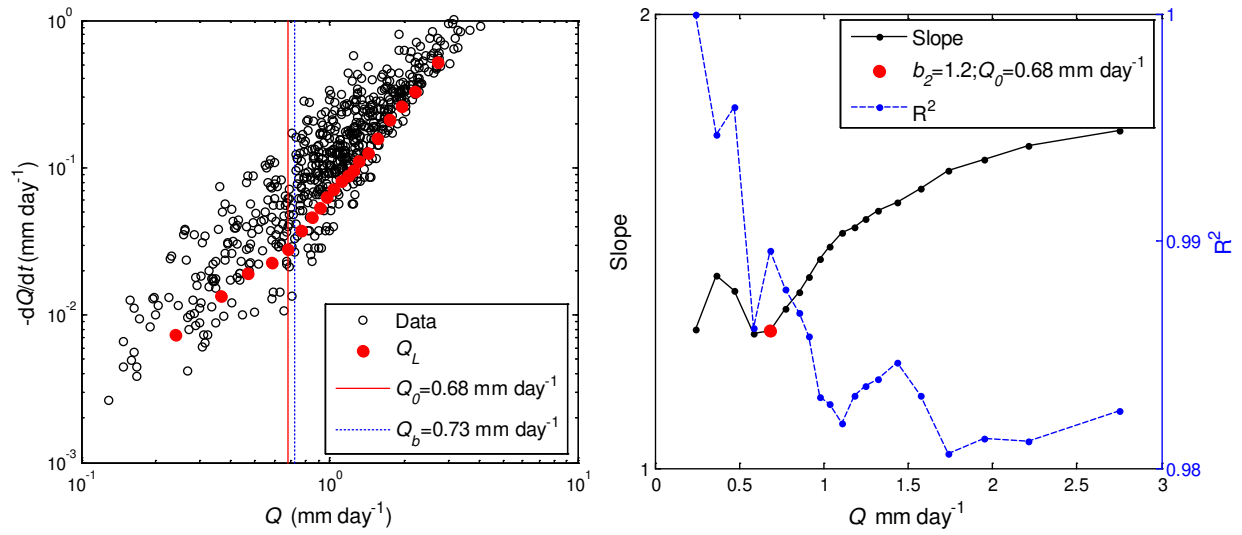
Figure C.13. Gage ID 02018000
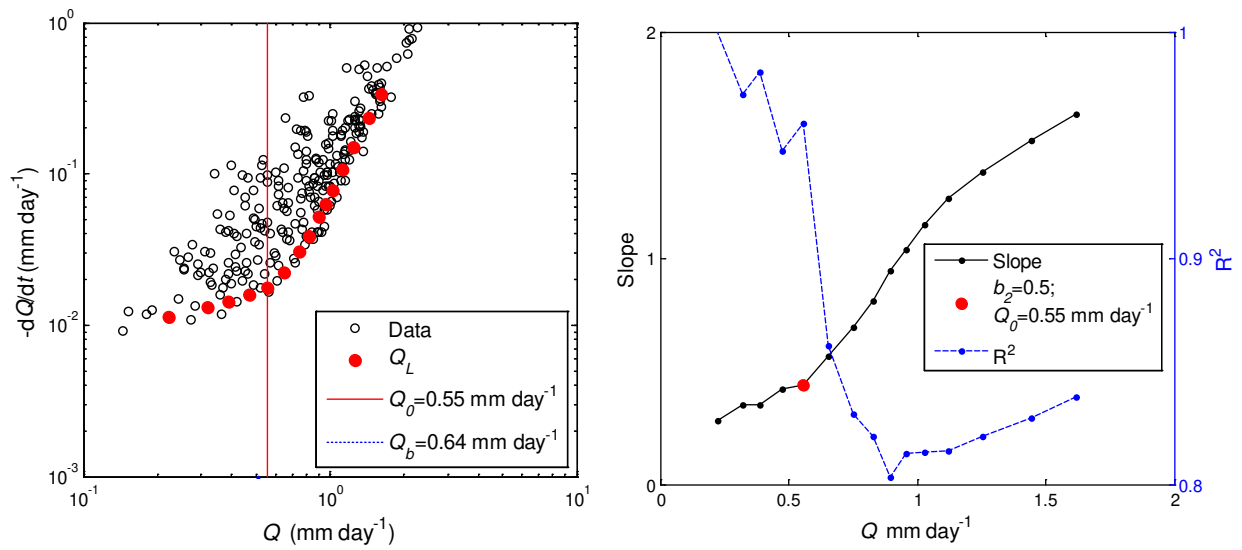
Figure C.14. Gage ID 02083500
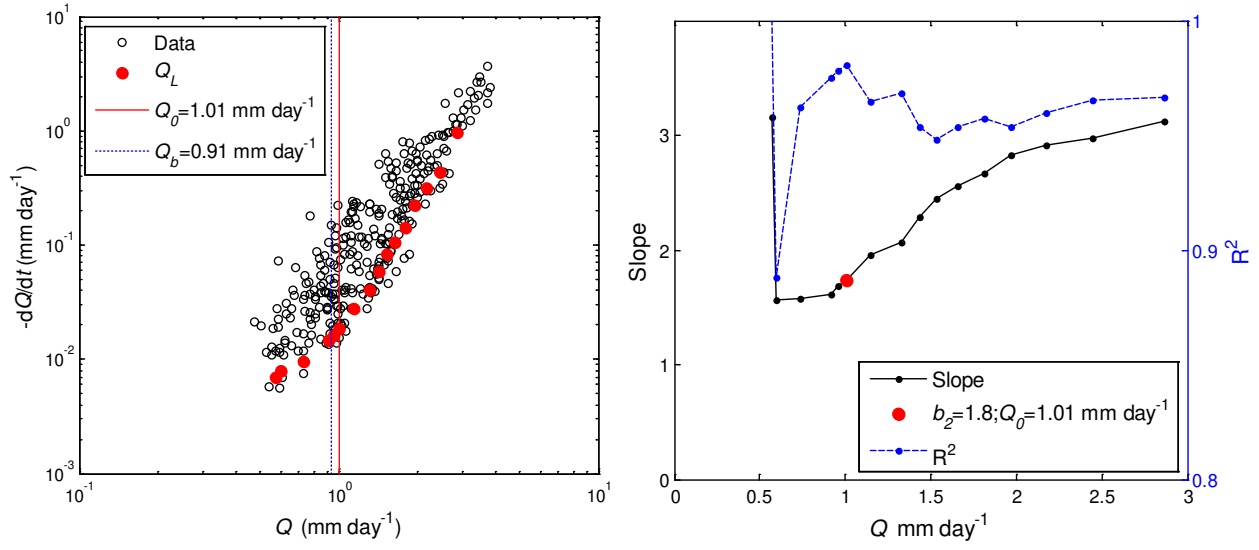
Figure C.15. Gage ID 02116500
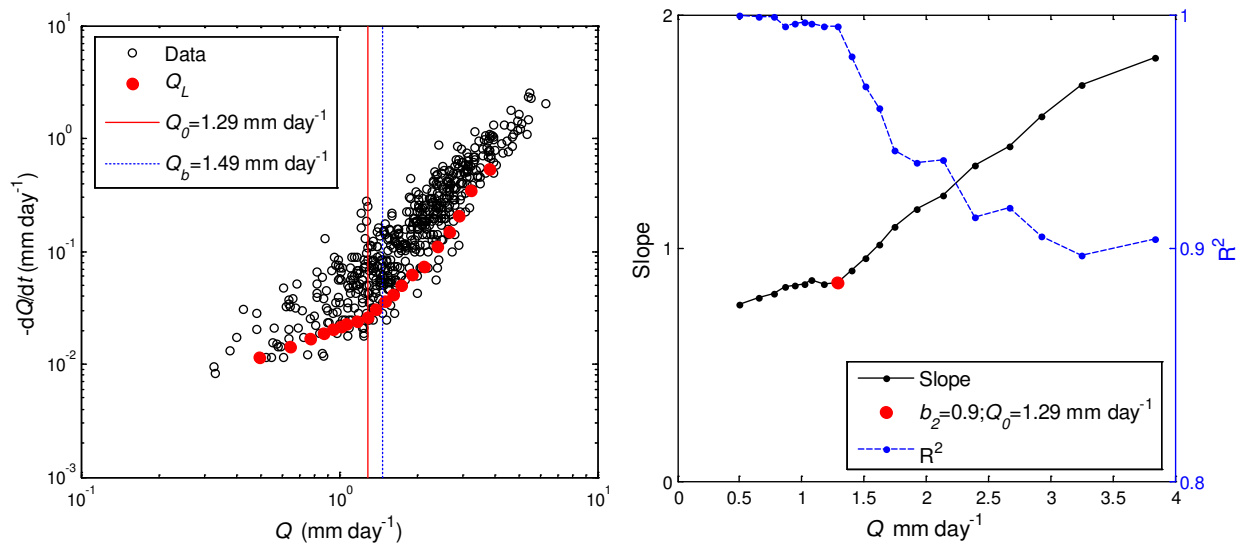
Figure C.16. Gage ID 02138500
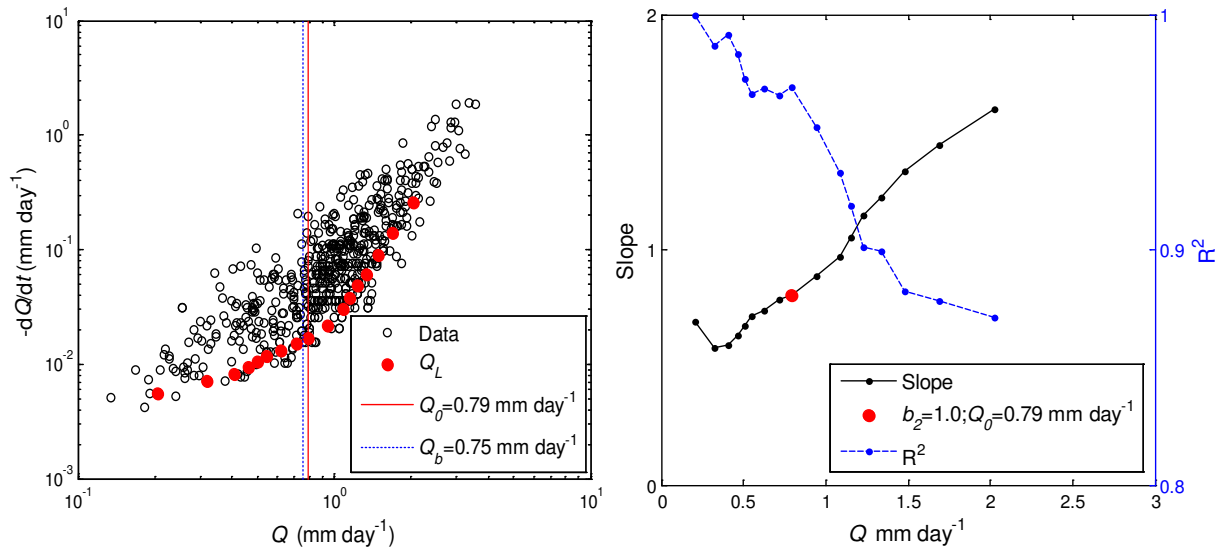
Figure C.17. 02347500
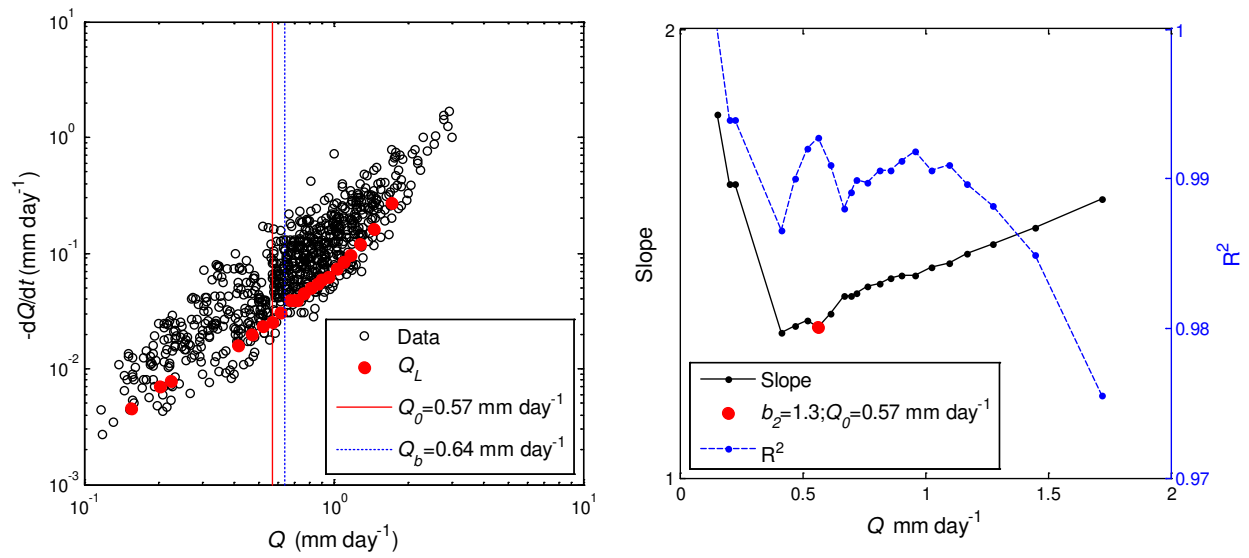
Figure B.18. Gage ID 02475500

128
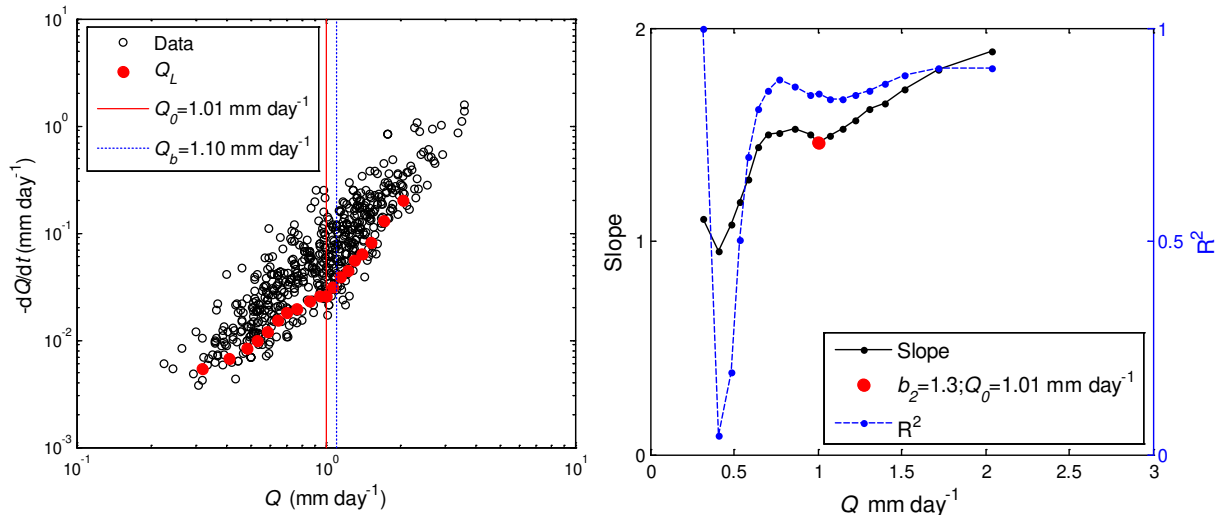
Figure B.19. Gage ID 02479300
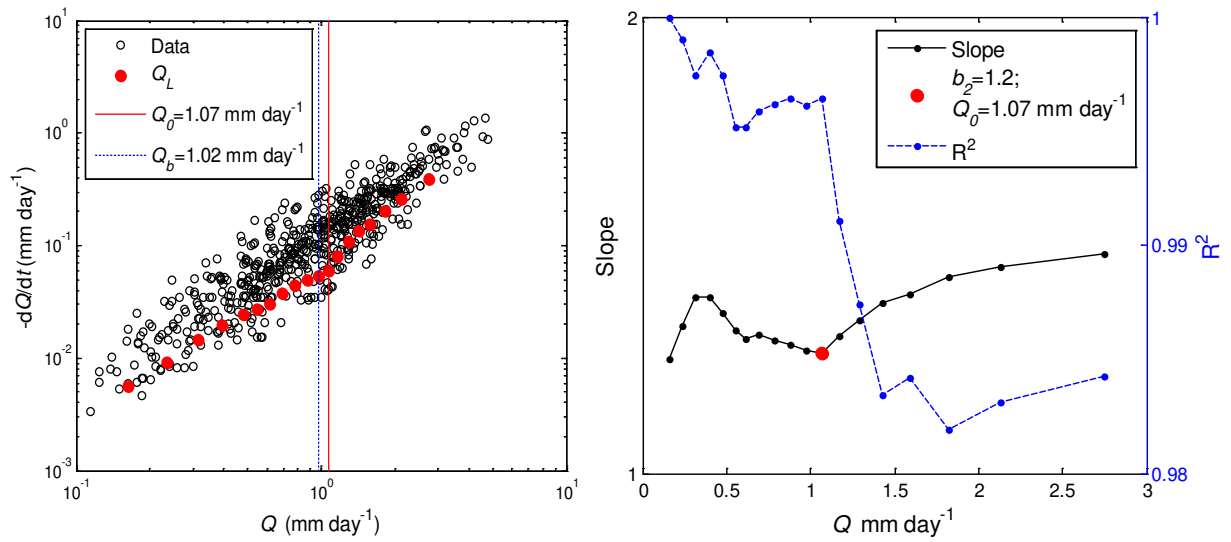
Figure B.20. Gage ID 03032500
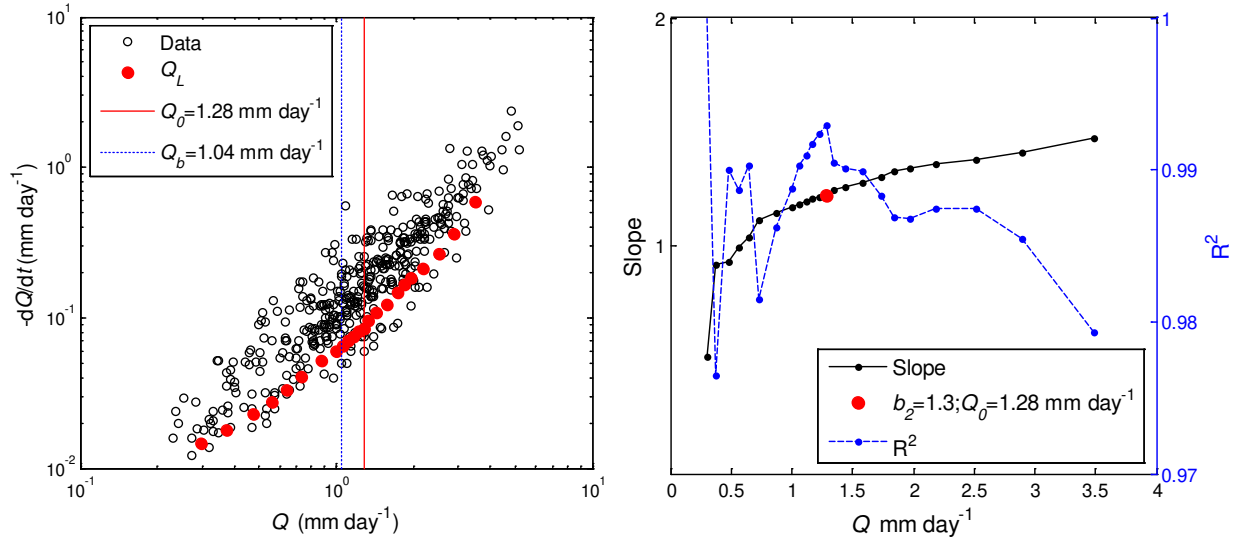
Figure B.21. Gage ID 03079000
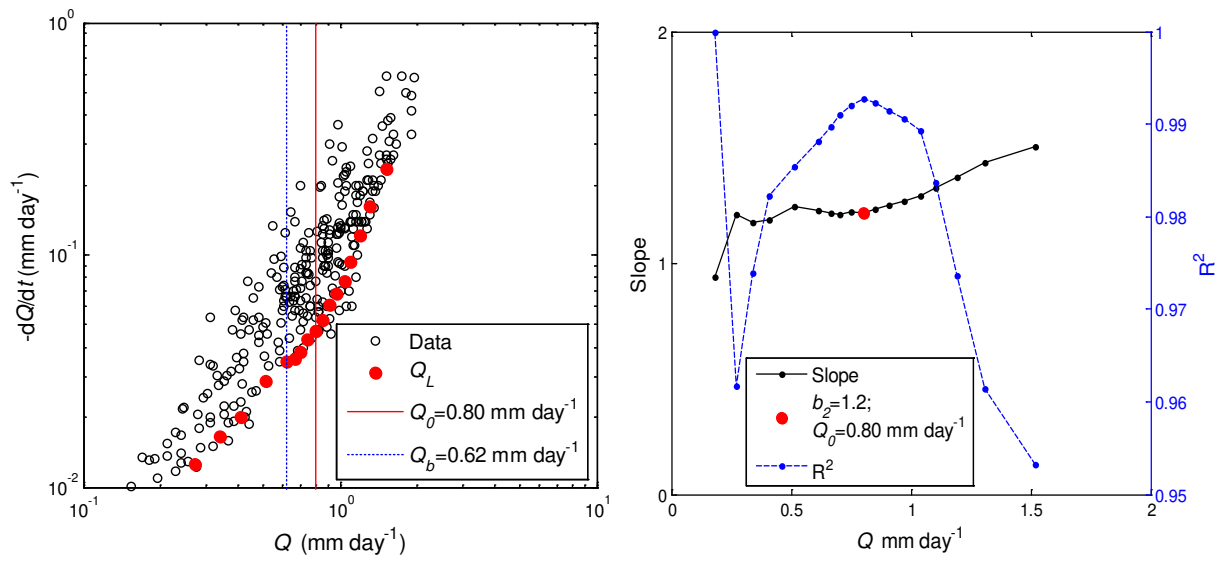
Figure B.22. Gage ID 03159500

130
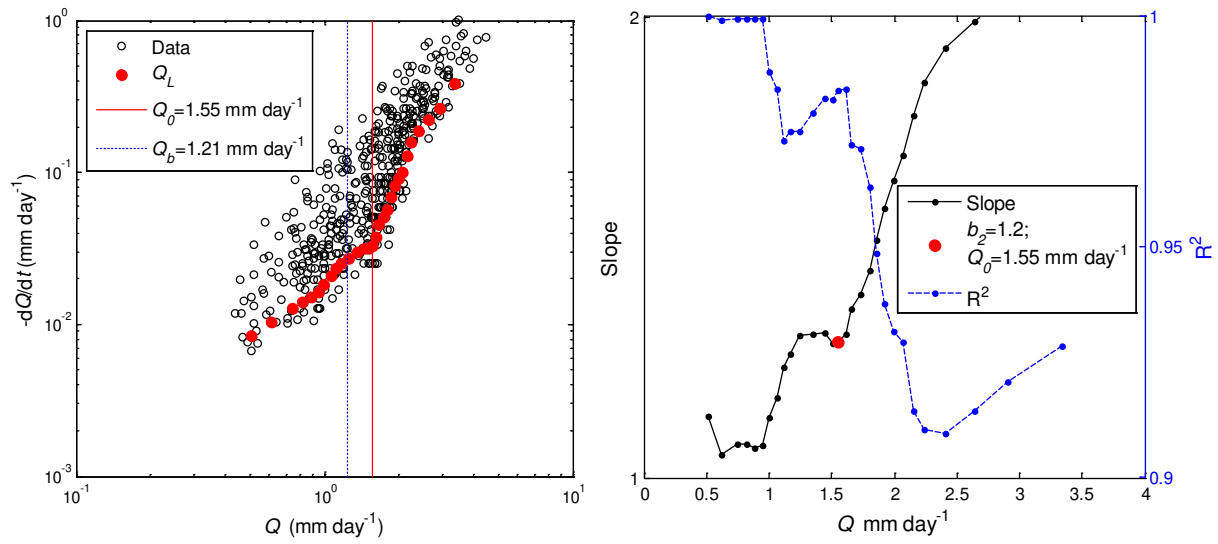
Figure B.23. Gage ID 03164000
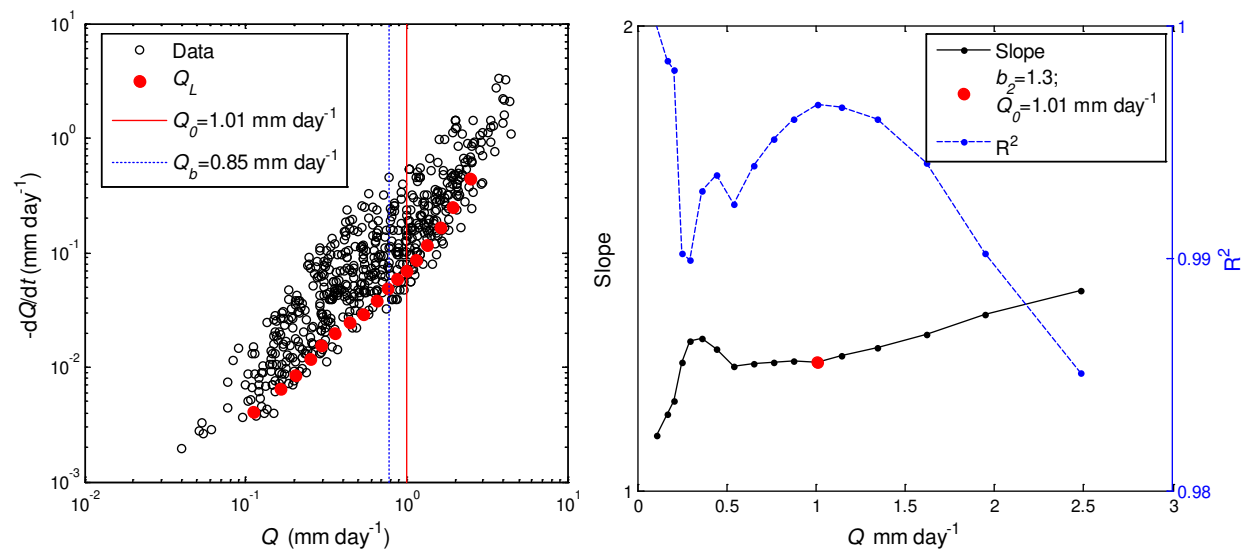
Figure B.24. Gage ID 03214000
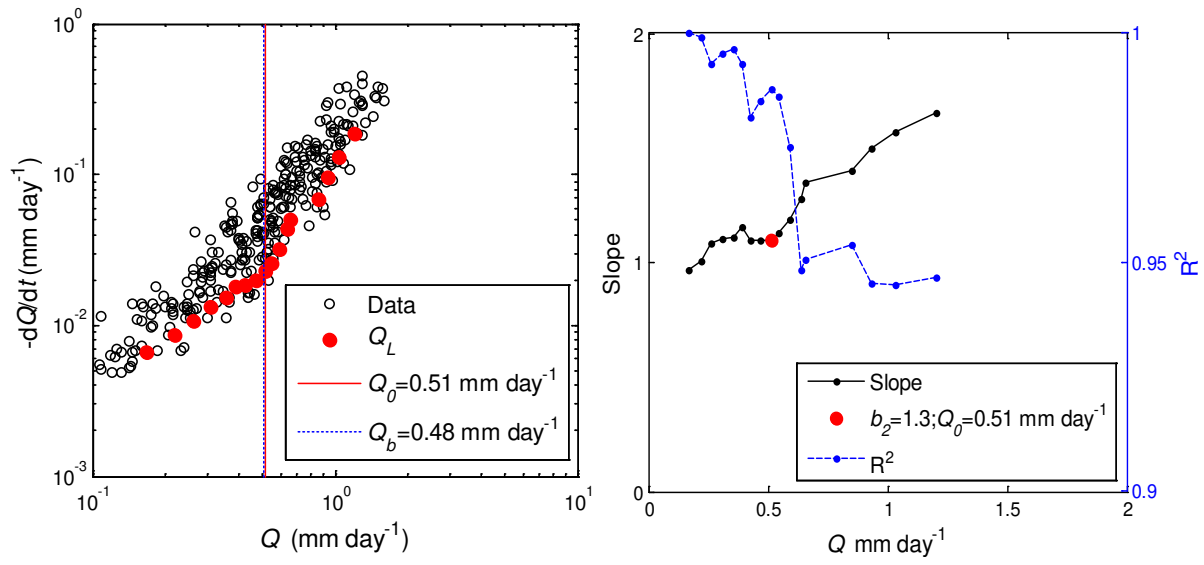
Figure B.25. Gage ID 03266000
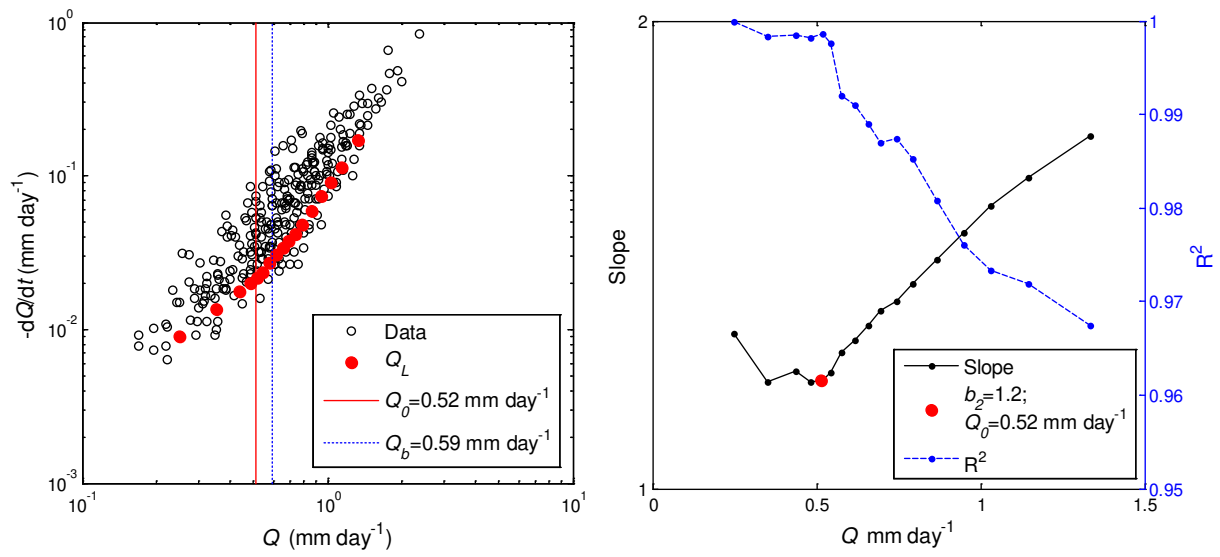
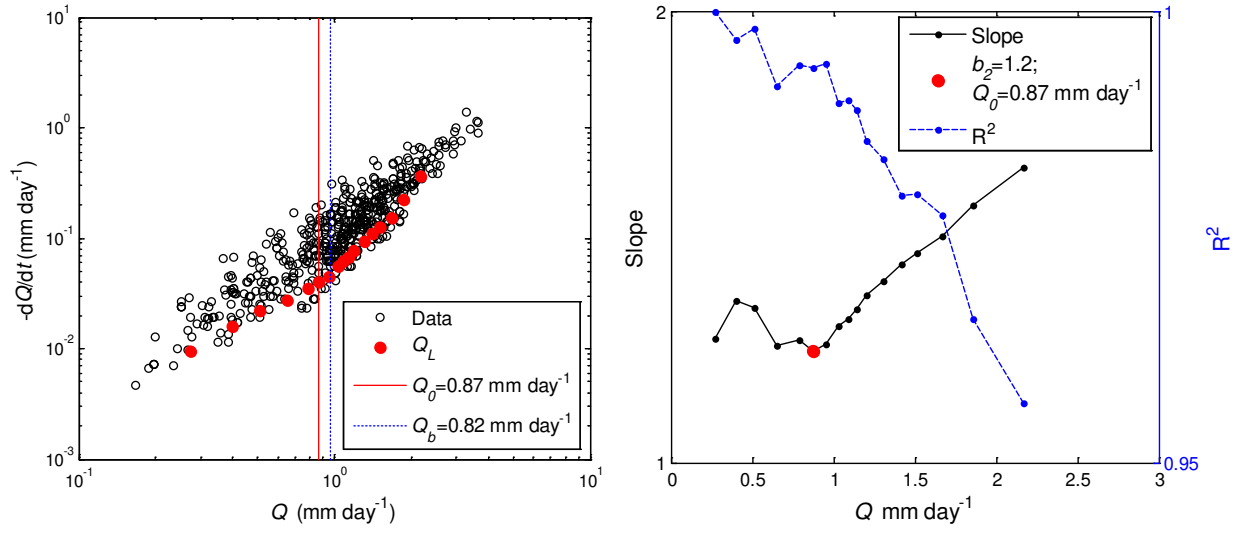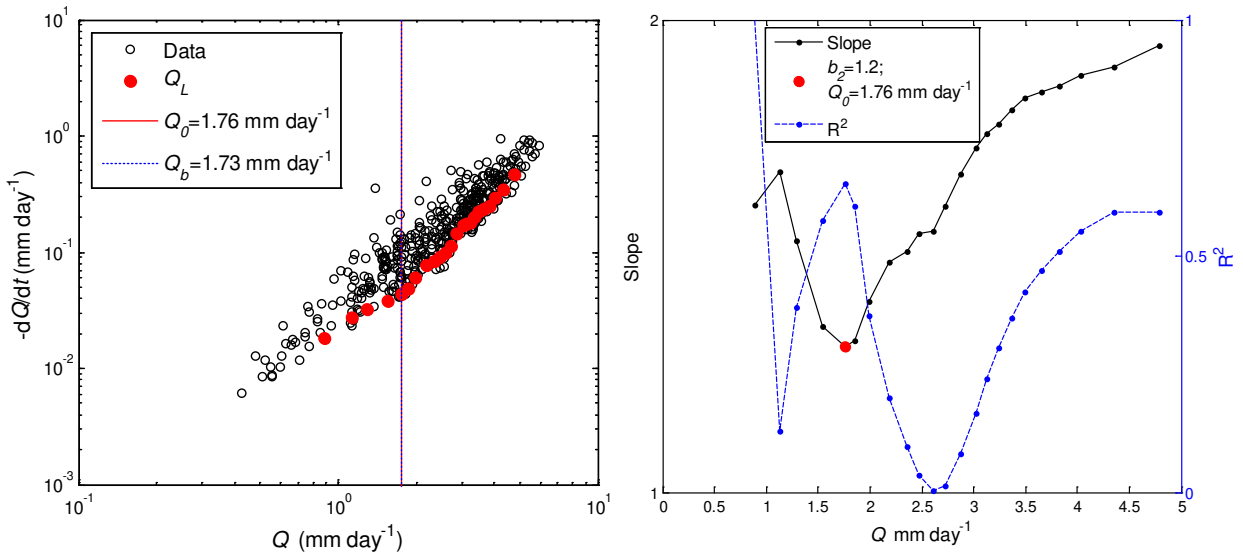Figure B.26. Gage ID 03274000
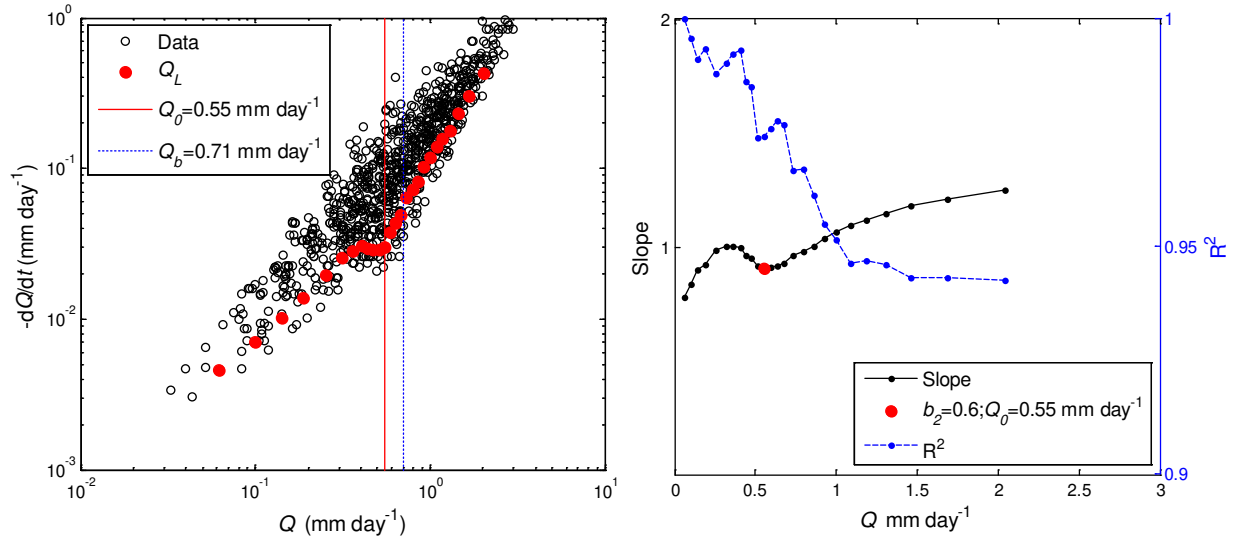
Figure B.27. Gage ID 03281500
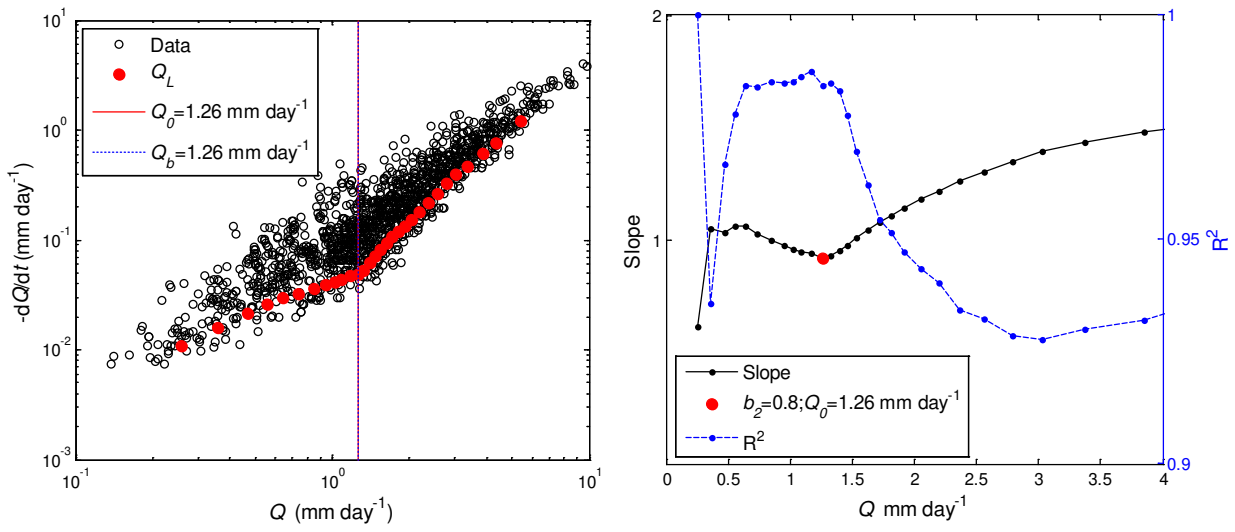
Figure B.28. Gage ID 03303000
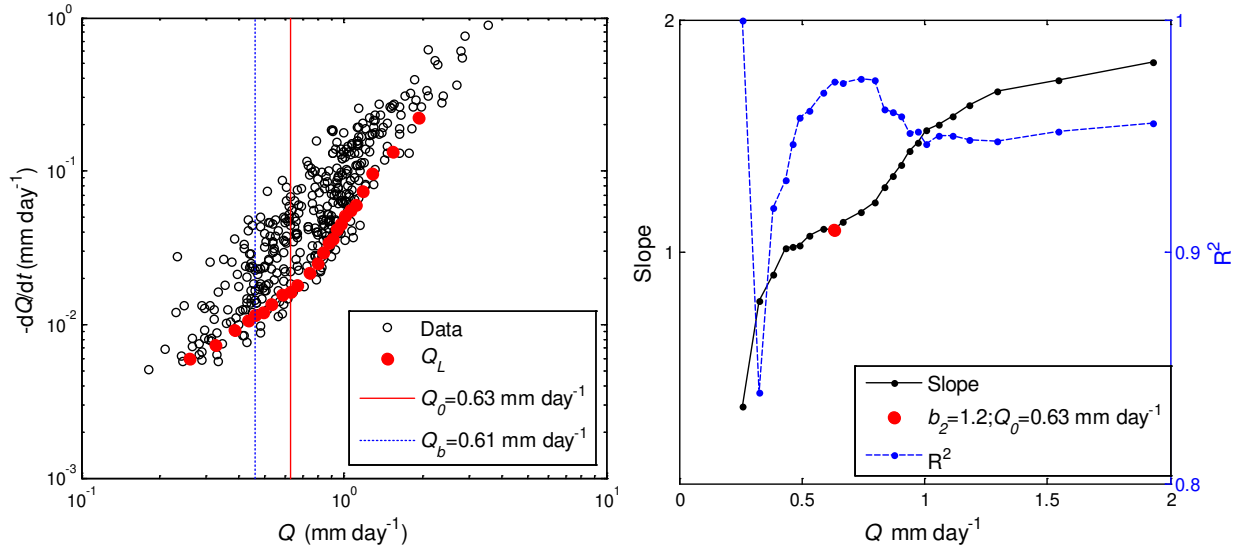
Figure B.29. Gage ID 03328500
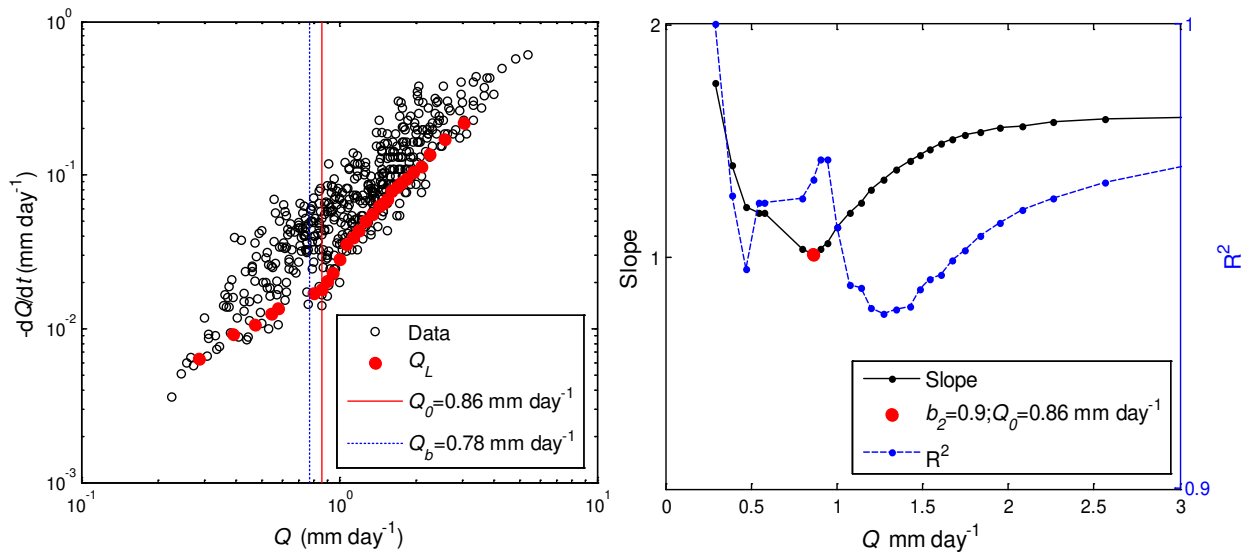
Figure B.30. Gage ID 03331500

134
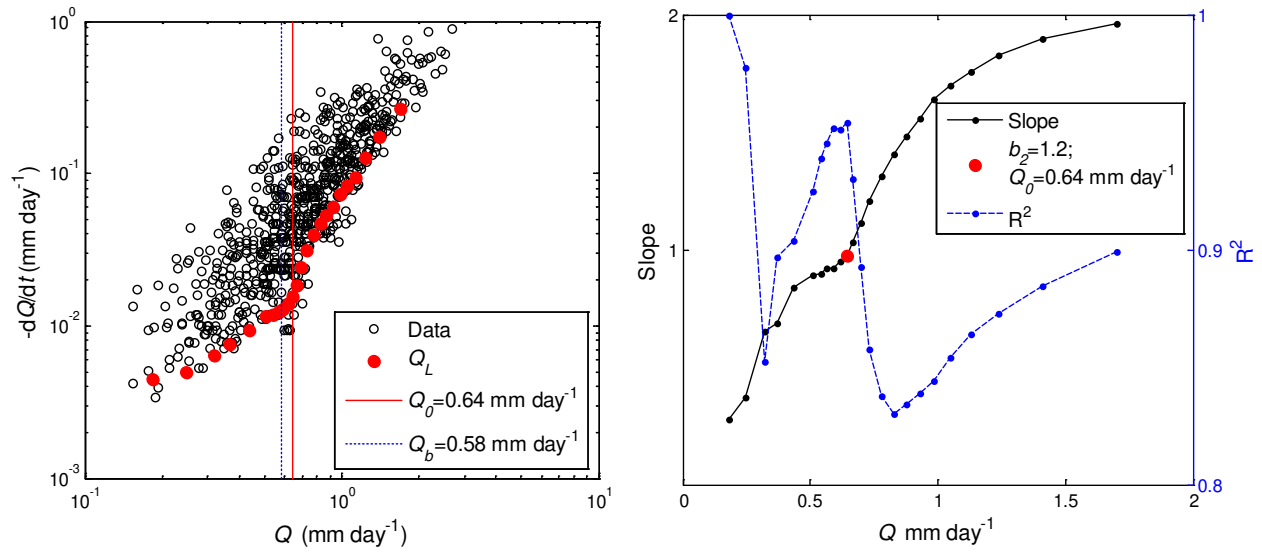
Figure B.31. Gage ID 03348000
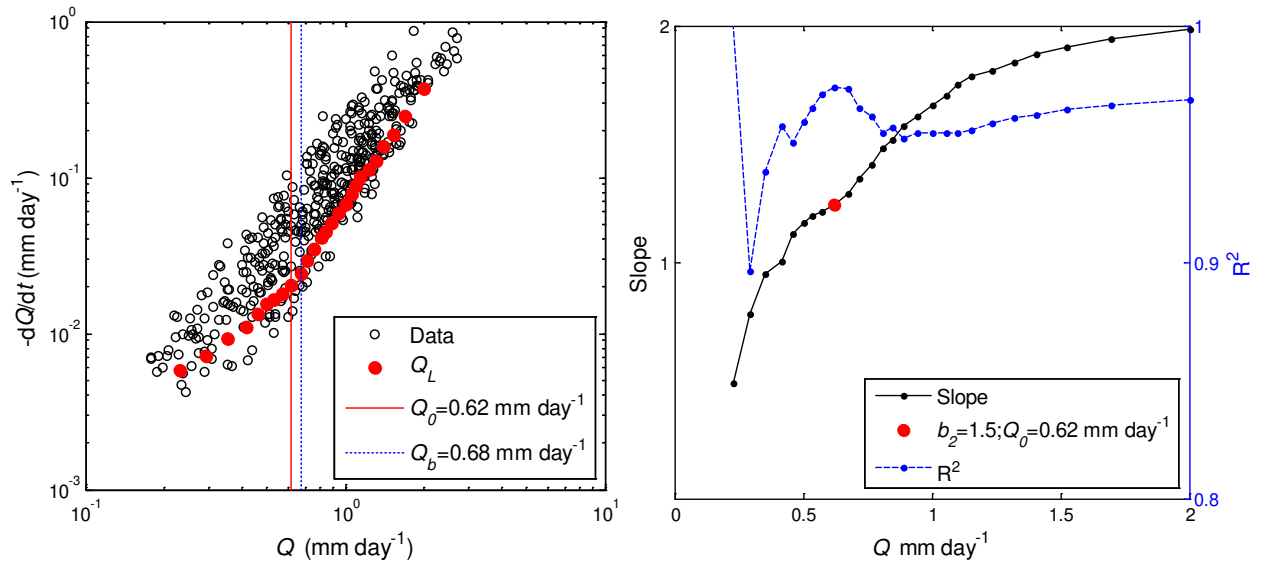
Figure B.32. Gage ID 03361500
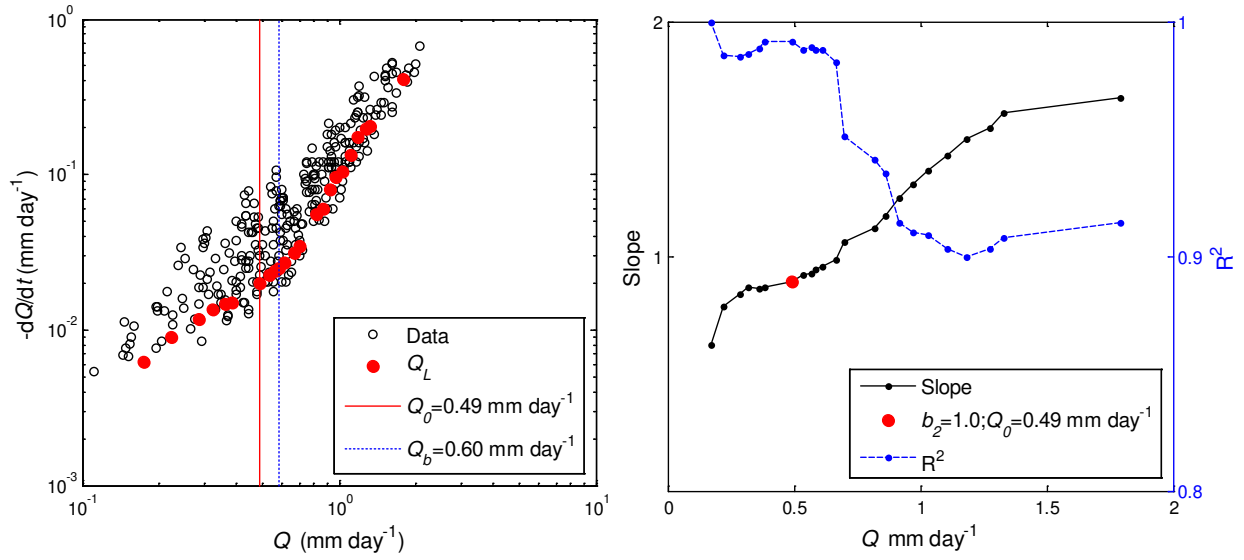
Figure B.33. Gage ID 03361650
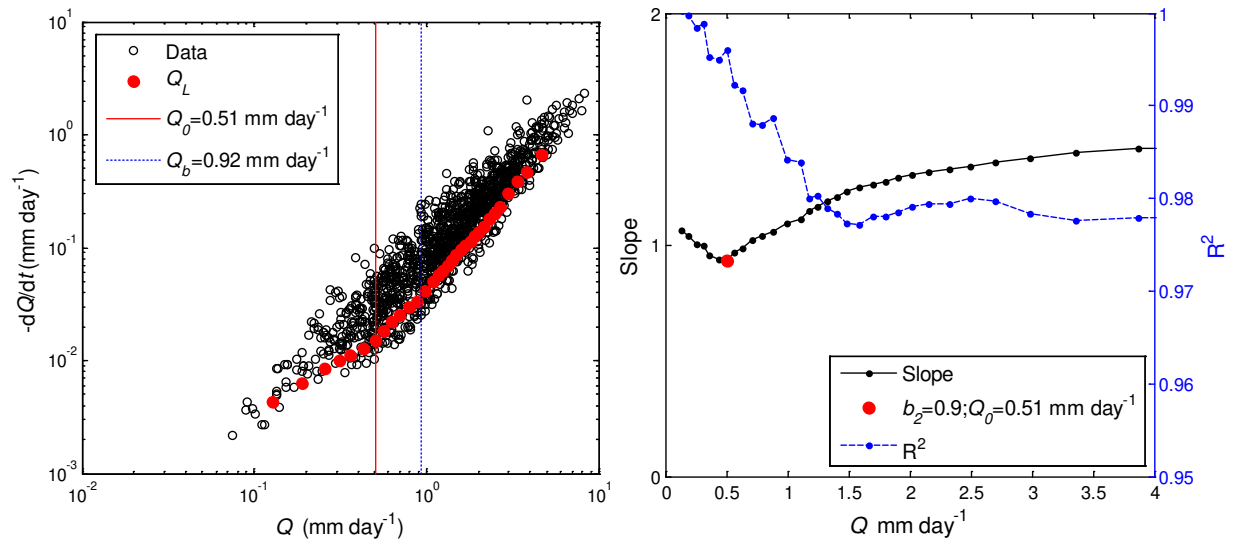
Figure B.34. Gage ID 03438000

136
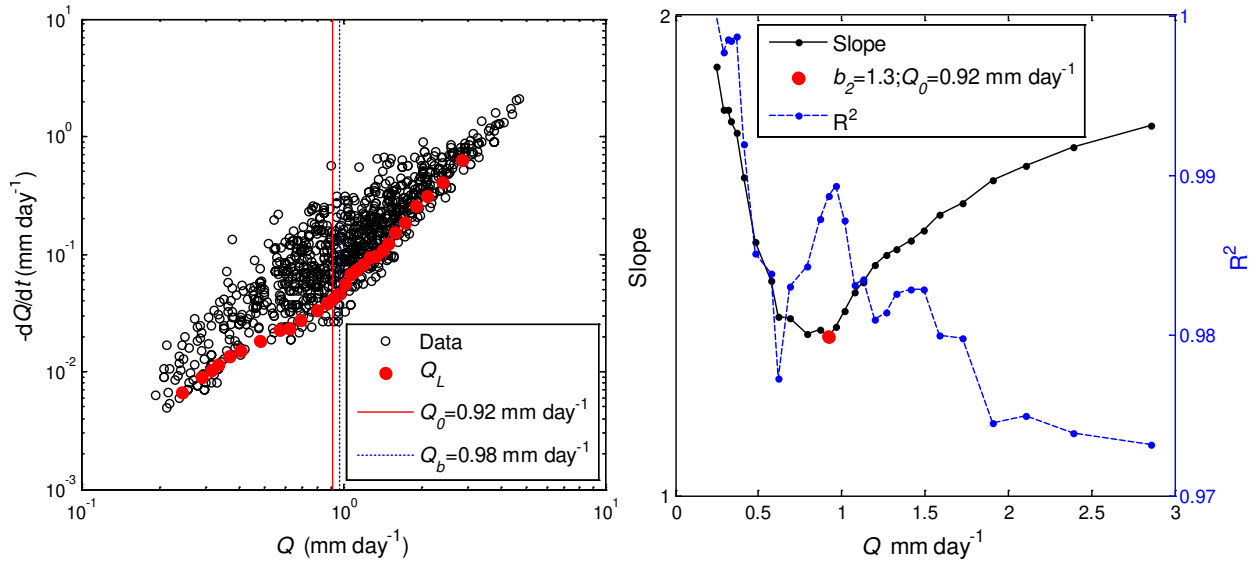
Figure B.35. Gage ID 03470000
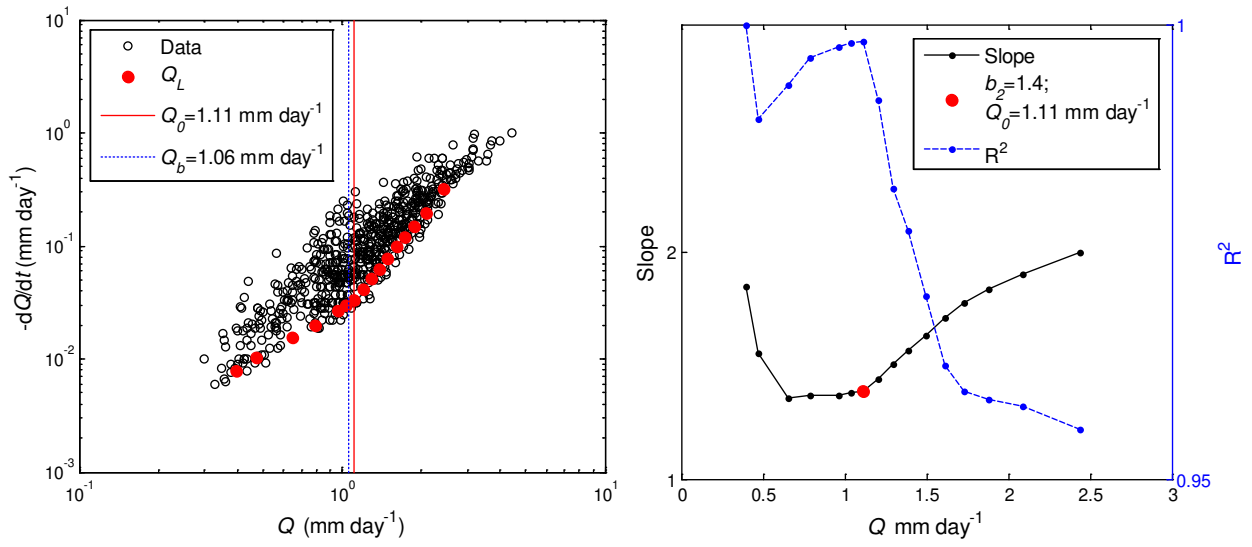
Figure B.36. Gage ID 03473000
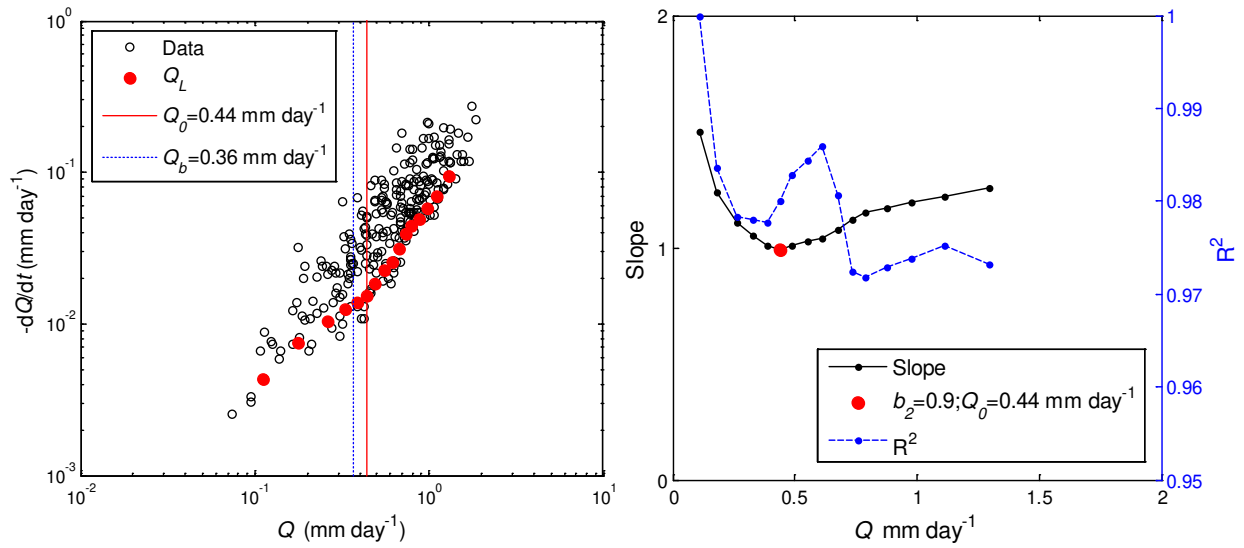
Figure B.37. Gage ID 03521500
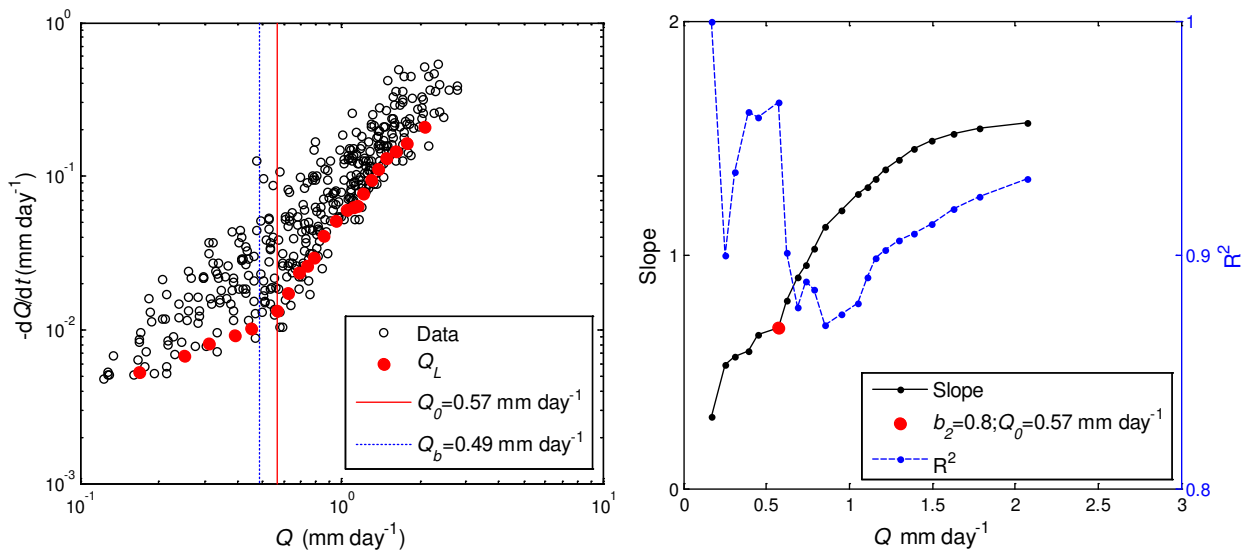

Figure B.38. Gage ID 03550000

138

Figure B.39. Gage ID 05472500

Figure B.40. Gage ID 05582000